

# World Journal of *Radiology*

*World J Radiol* 2021 September 28; 13(9): 258-313



**REVIEW**

- 258 Comprehensive literature review on the radiographic findings, imaging modalities, and the role of radiology in the COVID-19 pandemic

*Pal A, Ali A, Young TR, Oostenbrink J, Prabhakar A, Prabhakar A, Deacon N, Arnold A, Eltayeb A, Yap C, Young DM, Tang A, Lakshmanan S, Lim YY, Pokarowski M, Kakodkar P*

**MINIREVIEWS**

- 283 Role of cardiac magnetic resonance imaging in the diagnosis and management of COVID-19 related myocarditis: Clinical and imaging considerations

*Atri L, Morgan M, Harrell S, AlJaroudi W, Berman AE*

**SYSTEMATIC REVIEWS**

- 294 Review on radiological evolution of COVID-19 pneumonia using computed tomography

*Casartelli C, Perrone F, Balbi M, Alfieri V, Milanese G, Buti S, Silva M, Sverzellati N, Bersanelli M*

**CASE REPORT**

- 307 Neonatal infratentorial subdural hematoma contributing to obstructive hydrocephalus in the setting of therapeutic cooling: A case report

*Rousslang LK, Rooks EA, Meldrum JT, Hooten KG, Wood JR*

**ABOUT COVER**

Editorial Board Member of *World Journal of Radiology*, Alberto S Tagliafico, MD, Associate Professor, Department of Health Sciences, University of Genova, Italy. [alberto.tagliafico@unige.it](mailto:alberto.tagliafico@unige.it)

**AIMS AND SCOPE**

The primary aim of *World Journal of Radiology* (WJR, *World J Radiol*) is to provide scholars and readers from various fields of radiology with a platform to publish high-quality basic and clinical research articles and communicate their research findings online.

WJR mainly publishes articles reporting research results and findings obtained in the field of radiology and covering a wide range of topics including state of the art information on cardiopulmonary imaging, gastrointestinal imaging, genitourinary imaging, musculoskeletal imaging, neuroradiology/head and neck imaging, nuclear medicine and molecular imaging, pediatric imaging, vascular and interventional radiology, and women's imaging.

**INDEXING/ABSTRACTING**

The WJR is now abstracted and indexed in Emerging Sources Citation Index (Web of Science), PubMed, PubMed Central, China National Knowledge Infrastructure (CNKI), China Science and Technology Journal Database (CSTJ), and Superstar Journals Database. The 2021 edition of Journal Citation Reports® cites the 2020 Journal Citation Indicator (JCI) for WJR as 0.51.

**RESPONSIBLE EDITORS FOR THIS ISSUE**

Production Editor: *Ji-Hong Lin*; Production Department Director: *Yun-Jie Ma*; Editorial Office Director: *Jia-Ping Yan*.

**NAME OF JOURNAL**

*World Journal of Radiology*

**ISSN**

ISSN 1949-8470 (online)

**LAUNCH DATE**

January 31, 2009

**FREQUENCY**

Monthly

**EDITORS-IN-CHIEF**

Venkatesh Mani

**EDITORIAL BOARD MEMBERS**

<https://www.wjgnet.com/1949-8470/editorialboard.htm>

**PUBLICATION DATE**

September 28, 2021

**COPYRIGHT**

© 2021 Baishideng Publishing Group Inc

**INSTRUCTIONS TO AUTHORS**

<https://www.wjgnet.com/bpg/gerinfo/204>

**GUIDELINES FOR ETHICS DOCUMENTS**

<https://www.wjgnet.com/bpg/gerinfo/287>

**GUIDELINES FOR NON-NATIVE SPEAKERS OF ENGLISH**

<https://www.wjgnet.com/bpg/gerinfo/240>

**PUBLICATION ETHICS**

<https://www.wjgnet.com/bpg/gerinfo/288>

**PUBLICATION MISCONDUCT**

<https://www.wjgnet.com/bpg/gerinfo/208>

**ARTICLE PROCESSING CHARGE**

<https://www.wjgnet.com/bpg/gerinfo/242>

**STEPS FOR SUBMITTING MANUSCRIPTS**

<https://www.wjgnet.com/bpg/gerinfo/239>

**ONLINE SUBMISSION**

<https://www.f6publishing.com>



## Comprehensive literature review on the radiographic findings, imaging modalities, and the role of radiology in the COVID-19 pandemic

Aman Pal, Abulhassan Ali, Timothy R Young, Juan Oostenbrink, Akul Prabhakar, Amogh Prabhakar, Nina Deacon, Amar Arnold, Ahmed Eltayeb, Charles Yap, David M Young, Alan Tang, Subramanian Lakshmanan, Ying Yi Lim, Martha Pokarowski, Pramath Kakodkar

**ORCID number:** Aman Pal 0000-0001-7834-918X; Abulhassan Ali 0000-0001-7246-8444; Timothy R Young 0000-0001-8444-8571; Juan Oostenbrink 0000-0003-0103-4678; Akul Prabhakar 0000-0002-5451-8425; Amogh Prabhakar 0000-0001-9664-1520; Nina Deacon 0000-0002-8580-9081; Amar Arnold 0000-0002-8624-2996; Ahmed Eltayeb 0000-0002-3772-3179; Charles Yap 0000-0001-9477-6827; David M Young 0000-0001-6551-7527; Alan Tang 0000-0001-5744-3628; Subramanian Lakshmanan 0000-0002-2070-3657; Ying Yi Lim 0000-0003-1528-0191; Martha Pokarowski 0000-0001-6647-7029; Pramath Kakodkar 0000-0002-5288-1247.

**Author contributions:** Pal A, Ali A, Young TR, Oostenbrink J, Prabhakar A, Prabhakar A, Deacon N, Arnold A, Yap C, Young DM, Tang A, Lakshmanan S, and Kakodkar P performed acquisition and curation of the data; Pal A, Ali A, Young TR and Kakodkar P analyzed the data; Pal A, Ali A, Oostenbrink J, Prabhakar A, Prabhakar A, Deacon N, Arnold A, Eltayeb A, Eltayeb A, Yap C, Young DM, Tang A, and Kakodkar P performed interpretation of the data; Pal A, Ali A, Young TR, Oostenbrink J, Prabhakar A,

Aman Pal, Abulhassan Ali, Timothy R Young, Juan Oostenbrink, Akul Prabhakar, Amogh Prabhakar, Nina Deacon, Amar Arnold, Ahmed Eltayeb, Charles Yap, Subramanian Lakshmanan, Ying Yi Lim, Pramath Kakodkar, School of Medicine, National University of Ireland Galway, Galway H91 TK33, Galway, Ireland

David M Young, Department of Computer Science, Yale University, New Haven, CO 06520, United States

Alan Tang, Department of Health Science, Duke University, Durham, NC 27708, United States

Martha Pokarowski, The Hospital for Sick Kids, University of Toronto, Toronto M5S, Ontario, Canada

**Corresponding author:** Pramath Kakodkar, MD, Doctor, School of Medicine, National University of Ireland Galway, University Road, Galway H91 TK33, Galway, Ireland.  
[p.kakodkar1@nuigalway.ie](mailto:p.kakodkar1@nuigalway.ie)

### Abstract

Since the outbreak of the coronavirus disease 2019 (COVID-19) pandemic, over 103214008 cases have been reported, with more than 2231158 deaths as of January 31, 2021. Although the gold standard for diagnosis of this disease remains the reverse-transcription polymerase chain reaction of nasopharyngeal and oropharyngeal swabs, its false-negative rates have ignited the use of medical imaging as an important adjunct or alternative. Medical imaging assists in identifying the pathogenesis, the degree of pulmonary damage, and the characteristic features in each imaging modality. This literature review collates the characteristic radiographic findings of COVID-19 in various imaging modalities while keeping the preliminary focus on chest radiography, computed tomography (CT), and ultrasound scans. Given the higher sensitivity and greater proficiency in detecting characteristic findings during the early stages, CT scans are more reliable in diagnosis and serve as a practical method in following up the disease time course. As research rapidly expands, we have emphasized the CO-RADS classification system as a tool to aid in communicating the likelihood of COVID-19 suspicion among healthcare workers. Additionally, the utilization of other scoring



Prabhakar A, Deacon N, Arnold A, Eltayeb A, Yap C, Young DM, Tang A, Lakshmanan S, Lim YY, Pokarowski M, and Kakodkar P wrote the original draft; Pal A, Lim YY, Pokarowski M, and Kakodkar P performed the critical revision; All authors have read and approved the final manuscript.

#### Conflict-of-interest statement:

Authors declare no conflict of interest for this article.

**Open-Access:** This article is an open-access article that was selected by an in-house editor and fully peer-reviewed by external reviewers. It is distributed in accordance with the Creative Commons Attribution NonCommercial (CC BY-NC 4.0) license, which permits others to distribute, remix, adapt, build upon this work non-commercially, and license their derivative works on different terms, provided the original work is properly cited and the use is non-commercial. See: <http://creativecommons.org/licenses/by-nc/4.0/>

**Manuscript source:** Invited manuscript

**Specialty type:** Radiology, nuclear medicine and medical imaging

**Country/Territory of origin:** Ireland

#### Peer-review report's scientific quality classification

Grade A (Excellent): 0  
Grade B (Very good): 0  
Grade C (Good): 0  
Grade D (Fair): 0  
Grade E (Poor): 0

**Received:** February 6, 2021

**Peer-review started:** February 6, 2021

**First decision:** March 17, 2021

**Revised:** March 28, 2021

**Accepted:** August 4, 2021

**Article in press:** August 4, 2021

**Published online:** September 28, 2021

**P-Reviewer:** Kashyap MK

**S-Editor:** Liu M

**L-Editor:** Filipodia

**P-Editor:** Liu JH

systems such as MuLBSTA, Radiological Assessment of Lung Edema, and Brixia in this pandemic are reviewed as they integrate the radiographic findings into an objective scoring system to risk stratify the patients and predict the severity of disease. Furthermore, current progress in the utilization of artificial intelligence *via* radiomics is evaluated. Lastly, the lesson from the first wave and preparation for the second wave from the point of view of radiology are summarized.

**Key Words:** Coronavirus; COVID-19; Computed tomography; Ultrasound; MuLBSTA Scoring system; Radiological Assessment of Lung Edema classification; Brixia score

©The Author(s) 2021. Published by Baishideng Publishing Group Inc. All rights reserved.

**Core Tip:** Since there is a rapid expansion and knowledge regarding the radiological findings in coronavirus disease 2019 (COVID-19), it is important to condense and collate the most important findings into a one-stop guide. We tried to undertake the same and provide digital images with markings that would be helpful for anyone interested in understanding the typical radiological features alongside the evidence-based findings of COVID-19 pneumonia. Additionally, we highlight and provide evidence-based findings regarding the predominantly utilized clinical scoring systems that integrate radiology.

**Citation:** Pal A, Ali A, Young TR, Oostenbrink J, Prabhakar A, Prabhakar A, Deacon N, Arnold A, Eltayeb A, Yap C, Young DM, Tang A, Lakshmanan S, Lim YY, Pokarowski M, Kakodkar P. Comprehensive literature review on the radiographic findings, imaging modalities, and the role of radiology in the COVID-19 pandemic. *World J Radiol* 2021; 13(9): 258-282

**URL:** <https://www.wjgnet.com/1949-8470/full/v13/i9/258.htm>

**DOI:** <https://dx.doi.org/10.4329/wjr.v13.i9.258>

## INTRODUCTION

The current standard for the definitive diagnosis of coronavirus disease 2019 (COVID-19) is reverse-transcription polymerase chain reaction (RT-PCR) from the upper respiratory tract *via* nasopharyngeal and oropharyngeal swabs[1]. The diagnostic accuracy of real-time RT-PCR is as high as 95%[2]. However, the limitations of RT-PCR lies in its much lower diagnostic accuracy; it has high specificity but variable sensitivity ranging from 60%-70% to 95%-97%, respectively[3-5].

Medical imaging plays a key role in assisting the clinical decisions made towards the diagnosis, management, and follow-up of COVID-19 patients. This review presents the current literature related to the characteristics and key findings of COVID-19 in common radiological imaging modalities such as chest x-rays (CXRs), computed tomography (CT), and lung ultrasonography (LUS). To objectively stratify the severity of COVID-19, CXRs and CT scans are used in conjunction with various classifications systems such as CO-RADS, MuLBSTA, and the Radiological Assessment of Lung Edema (RALE) to facilitate the appropriate evaluation and treatment for infected cases. These are also explored within this review. Other imaging modalities such as magnetic resonance imaging (MRI), positron emission tomography (PET), and echocardiography are less commonly used but can be ordered to assess certain complications and treatment responses. Prior to reviewing these topics, the fundamental basics of COVID-19 pathophysiology are highlighted in the following section.

### Pathophysiology of COVID-19

Aerosolization of respiratory droplets containing the severe acute respiratory syndrome coronavirus-2 (SARS-CoV-2) is the primary mode of transmission of COVID-19. The SARS-CoV-2 virion can further inoculate the mucous membranes *via* the facial T-zone (eyes, nose, and mouth). The current suggested model of pathogenesis for SARS-CoV-2 infection is composed of three phases: Viral replication, hyperactive immune system, and pulmonary destruction[6]. These phases are discussed in the following subsections.



### Viral replication

Viral particles manifest their infectivity through replication within the host cell in the following five steps: Attachment, penetration, biosynthesis, maturation, and release [7]. SARS-CoV-2 binds with high affinity to angiotensin-converting enzyme 2 (ACE2) receptors and transmembrane protease serine 2 (TMPRSS2) receptors. Interestingly the ACE2 receptors are predominantly expressed with high density within the type II pneumocytes of the lung [8]. These receptors are also found in the heart (pericytes), ileum (enterocytes), kidney (podocytes), and bladder (urothelial cells) [8]. Once SARS-CoV-2 attaches to host receptors (ACE2 and TMPRSS2), the virion fuses with the membrane and enters the cell *via* endocytosis. Subsequently, inside the cell, the viral RNA enters the nucleus and alters the replication machinery to biosynthesize viral proteins. Upon maturation of the new viral particles, they are released to infect and continue their vicious cycle in other nearby cells [7].

### Hyperactive immune system

Immune hyperactivity is a result of the stress-induced apoptosis of the affected cells and the viral RNA being recognized as a foreign genome by Toll-like receptors [9]. This leads to a cytokine storm (release of tumor necrosis factor, interleukin 6 [IL-6], IL-1 $\beta$ ,

C-C motif chemokine ligand 2), which is stimulated by macrophages and dendritic cells and causes the infiltration of several inflammatory mediators in the alveolar-capillary interface [9]. Since there is a high density of ACE2 receptors along the peripheries of the lung parenchyma, the majority of damage early on is seen at these sites as a characteristic pulmonary ground-glass opacity (GGO) detected by a CT scan.

### Pulmonary destruction

Although the purpose of inflammatory mediators is to fight against the virus until development of the adaptive immune system, their excessive infiltration damages this membrane, causing a build-up of fluid within the alveolar sacs and lung injury that further reduces ventilation [10]. The migration of fluid into the alveolar sacs is governed by the imbalance in Starling forces;  $F = k ([P_c - P_a] - s [\pi_c - \pi_a])$  [11]. The diffuse alveolar damage caused by the viral particles results in an increased capillary wall permeability (high  $k$  value), thereby increasing the force at which fluid migrates from the capillaries to the alveolar space. Figure 1 summarizes the findings of Gralinski *et al* [12] as an illustration of the progressive development within an infected alveolus, both pathologically and radiologically [12]. The normal alveolar wall is comprised of type I and II pneumocytes, while the alveolar macrophages and surfactant reside in the alveolar space. In an acute setting of infection, the pneumocytes secrete inflammatory cytokines and exhibit cytopathic effects, while surfactant levels decrease. As the disease progresses, ventilation is impeded as pulmonary edema and airway debris coincide within the alveolar spaces, alongside the formation of hyaline membrane. Radiologically, the initial features of localized pulmonary edema is seen as GGOs (highly attenuated patches on CXR/CT) and as the severity of tissue damage increases, the pulmonary edema becomes more diffuse and is seen as wide areas of consolidation on the chest imaging modalities [13].

The radiodensities vary between each material and can be quantified using the Hounsfield scale, measured as Hounsfield units. Air, lung, ground glass, water, consolidation, and metal have radiodensities of -1000, -900, -800 to -100, 0, 30, and > 100, respectively [14]. The varying radiodensity of ground glass is associated with the severity of tissue damage and pulmonary edema as a more severe alveolar damage would elicit a higher radiodensity due to a greater fluid accumulation. Extreme tissue damage with complete alveolar consolidation presents as increased attenuation with anomalous opacities on chest imaging.

## CHEST RADIOGRAPHY AND CT IMAGING

The role of imaging during the COVID-19 pandemic has yet to be fully explored. CXR and chest CT scans are not an official primary component of diagnosis but rather a supporting feature for diagnosis specifically to determine severity and the appropriate treatment response required. The high rate of false-negative results and fear of viral spread during sample transfers in RT-PCRs show the need for a systematic approach in the diagnosis of COVID-19 through a combination of clinical signs and radiological findings on CXR and CT, which are important in determining the severity of disease and guiding treatment responses [15]. It is important to note that chest CTs have the additional advantage of detecting changes of COVID-19 pneumonia in asymptomatic

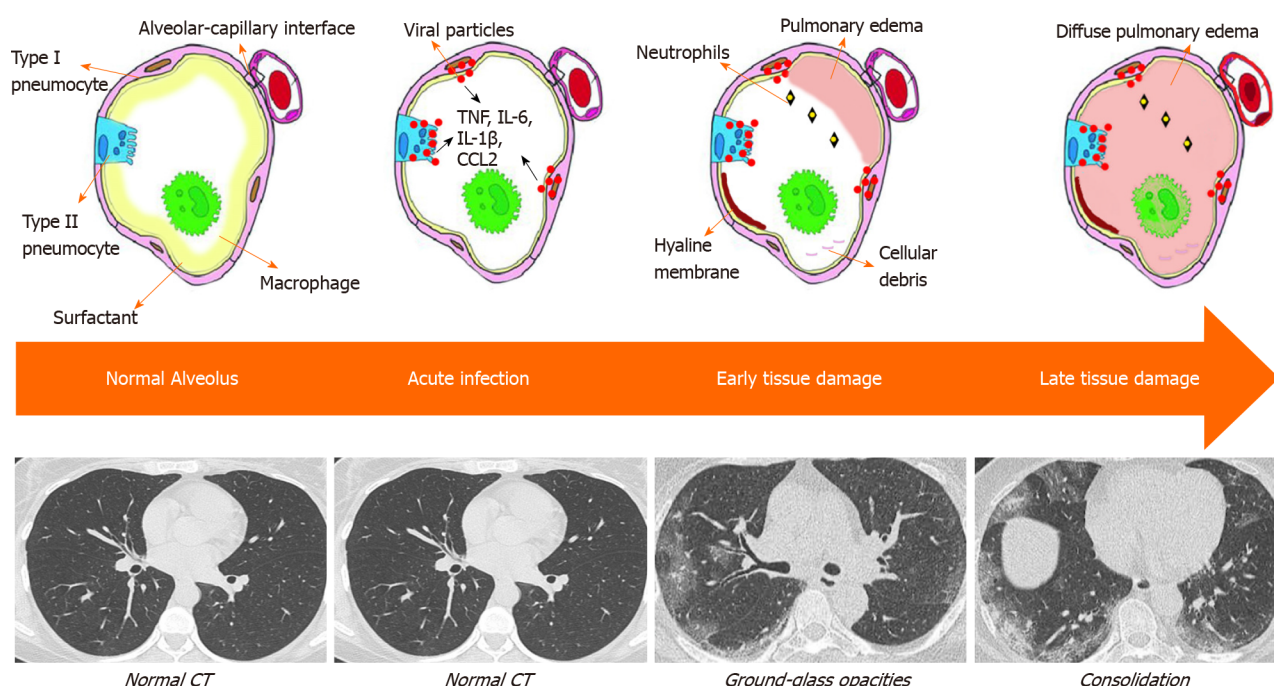


**Figure 1** Model of infected lung through pathological and radiological perspectives.

patients[16].

## CLASSICAL FINDINGS IN CHEST RADIOGRAPHY

Admitted in-patients presenting with COVID-19 provide a large repository of radiological images due to the ease of evaluations *via* solitary portable CXR. Findings of COVID-19 on CXR include hazy opacification, which is the radiographic equivalent to GGO found on a chest CT scan. These hazy opacifications have a predilection for the basal lung and its peripheries. These opacifications may be unilateral or bilateral. In severe cases, the middle to upper fields of the lung may become affected. In the penultimate disease stage (days 10-12), the areas of opacity coalesce and become denser. This presents as patchy consolidates similar to the pattern of acute respiratory distress syndrome (ARDS)[13]. The compilation of diagnostic factors such as signs, symptoms, oxygen saturation, and CXR appearance can offer a faster and inexpensive method for severity assessment. Most notable CXR findings included bilateral chest involvement 76.8% (95% confidence interval [CI]: 62.5%-87%), consolidation 75.5% (95%CI: 50.5%-91%), GGO 71% (95%CI: 40%-90%), and unilateral chest involvement in 16.5% (95%CI: 8.5%-29.5%)[17]. Some less common CXR findings include reticular interstitial thickening in 39.9% ( $n = 107/268$ ), nodules 9.3% ( $n = 25/268$ ), and pneumothorax, or pleural effusion (1%-3%)[18]. These findings could be a consequence of COVID-19 or pre-existing comorbidities, or just coincidental. Figure 2 shows a collection of chest radiographs with abnormal findings with a background of a positive SARS-CoV-2 PCR test. Examples of bilateral patchiness (Figure 2A), unilateral GGO (Figure 2B), pneumothorax (Figure 2C), and linear patchiness (Figure 2D) are modified from Singh *et al*[15], Martini *et al*[19], Rampa *et al*[20], and Kaufman *et al*[21]. Examples of nodular (Figure 2E) and reticular consolidations (Figure 2F) are modified from Yasin *et al*[22].

One large study ( $n = 1198$ ) showed that the sensitivity and specificity of CXR for detecting features of COVID-19 pneumonia were 56% (95%CI: 51%-60%) and 60% (95%CI: 54%-65%), respectively[23]. In comparison, the chest CT provides an increase in sensitivity by 29% (95%CI: 19%-38%) in comparison to CXR[23]. This variable explains the limited usage of CXR in the screening, diagnosis, or follow-up of COVID-19 patients.



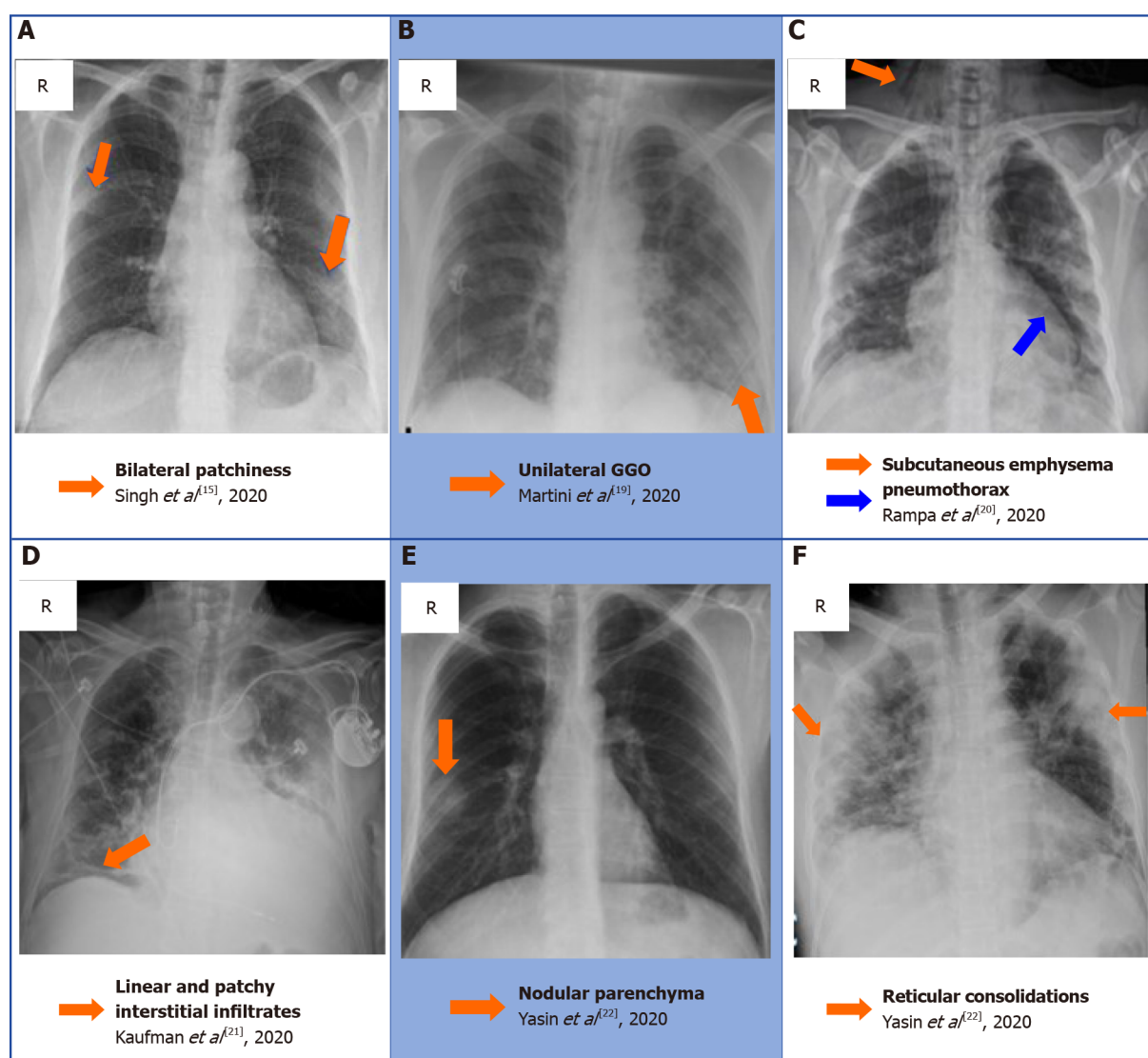


**Figure 2** A collection of chest radiographs that displays some of the common and rare findings of coronavirus disease 2019 pneumonia [15,19-22]. A: Bilateral patchiness; B: Unilateral ground glass opacification; C: Subcutaneous emphysema secondary to a pneumothorax; D: Linear and patchy interstitial infiltrate in the right basal zone; E: Nodular appearance of the right lobe parenchyma; F: reticular appearance of the consolidation bilaterally. A: Citation: Singh B, Kaur P, Reid RJ, Shamoon F, Bikina M. COVID-19 and Influenza Co-Infection: Report of Three Cases. *Cureus* 2020; 12: e9852. Copyright ©The Author(s) 2020. Published by Cureus; B: Citation: Martini K, Blüthgen C, Walter JE, Messerli M, Nguyen-Kim TD, Frauenfelder T. Accuracy of Conventional and Machine Learning Enhanced Chest Radiography for the Assessment of COVID-19 Pneumonia: Intra-Individual Comparison with CT. *Journal of Clinical Medicine* 2020;9: 3576 Copyright ©The Author(s) 2020. Published by MDPI, Basel, Switzerland; C: Citation: Rampa L, Miceli A, Casilli F, Biraghi T, Barbara B, Donatelli F. Lung complication in COVID-19 convalescence: A spontaneous pneumothorax and pneumatocele case report. *Journal of Respiratory Diseases and Medicine* 2020; 2. Copyright ©The Author(s) 2020. Published by Open-access article; D: Citation: Kaufman A, Naidu S, Ramachandran S, Kaufman D, Fayad Z, Mani V. Review of radiographic findings in COVID-19. *World Journal of Radiology* 2020; 12: 142-55. Copyright ©The Author(s) 2020. Published by Baishideng Publishing Group Inc; E and F: Citation: Yasin R, Gouda W. Chest X-ray findings monitoring COVID-19 disease course and severity. *The Egyptian Journal of Radiology and Nuclear Medicine* 2020; 51: 193. Copyright ©The Author(s) 2020. Published by BMJ.

## CLASSICAL CT FINDINGS OF COVID-19 PNEUMONIA

While CXR is a practical method of screening, a recent meta-analysis showed that chest CTs are superior in the screening and assessment of COVID-19 pneumonia due to its increased sensitivity of 91.9% (95%CI: 89.8%-93.7%)[2]. CT is proficient in detecting early signs of COVID-19 pneumonia in comparison to CXR. This is evident by the detection of early-stage GGOs and consolidative opacities, which are often not visible on CXR or may appear normal with minimal interstitial markings[24]. In similar patients where CXR detects minimal interstitial markings, subtle opacities, or occult signs, CT would display identifiable GGO. Figure 3 shows a summary of the meta-analysis of classical and ancillary CT imaging findings by Bao *et al*[25].

Ancillary late-stage CT finding of COVID-19 pneumonia includes crazy-paving, which is defined by the Fleischner Society as diffuse GGO with superimposed

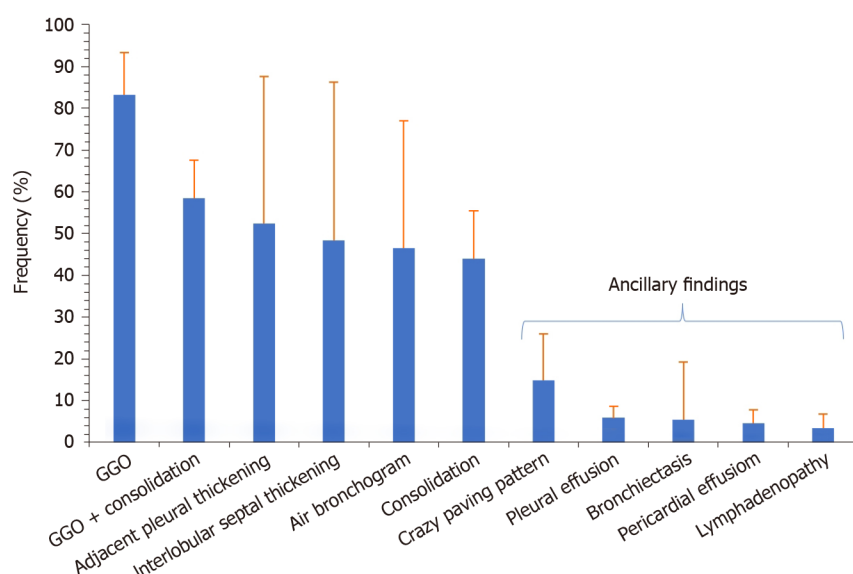


**Figure 3 Summary of the frequency distribution of classical and ancillary computed tomography imaging findings in coronavirus disease 2019 pneumonia.** The whiskers indicate the 95% confidence interval. GGO: Ground-glass opacity.

thickened intralobular lines and interlobular septa. The discovery of crazy-paving on a CT image is radiographic evidence of progressive COVID-19[26]. Additionally, diffuse patchy consolidation with reticular configuration becomes more predominant later in the disease course. Other classical chest CT findings that rule-in COVID-19 are lateralization of GGO early in the disease course, with multifocal, bilateral, and basilar lobe predominance, peripheral GGO with a rounded or oval morphology[18]. **Figure 4** shows a collection of some notable classical chest CT findings in the axial plane of COVID-19 patients. Examples of classical findings such as GGOs (**Figure 4A**), air bronchograms (**Figure 4B**), bronchial thickening (**Figure 4E**), and pleural adhesions (**Figure 4F**) are all modified from Fu *et al*[27]. Additionally, examples of GGO superimposed with consolidation (**Figure 4D**) and crazy paving sign (**Figure 4C**) are modified from Gillespie *et al*[26] and Ali *et al*[28].

Additionally, **Figure 5** shows the common lobes wherein classical CT findings of COVID-19 are distributed based on the findings of a meta-analysis by Bao *et al*[25]. Although the exact mechanism is unidentified, the increased incidence of findings in the lower lobes may be related to the anatomical structure of the trachea and bronchi, alongside the gravitational force that allows the virion particles to settle at the base more readily. Furthermore, since the right main bronchus bifurcates at a smaller angle and is wider than the left main bronchus, the virion particles can travel more easily towards the right lower lobe.

## NON-CLASSICAL CT FINDINGS OF COVID-19 PNEUMONIA

Less commonly reported imaging findings that may help to rule-in COVID-19 is subsegmental vascular engorgement[29]. Furthermore, another uncommon but positive feature that rules in COVID-19 is the atoll sign on CT, also referred to as the reverse halo sign[18]. This is defined as a focal rounded area of GGO which is surrounded by a complete or nearly complete ring of denser consolidation which is observed on CT[30]. Other causes of the reverse-halo sign may be chronic lung injury, and notably, may raise the concern of pulmonary infarction. Interestingly, one meta-analysis indicates that these non-classical CT findings might be more common than previously predicted. **Figure 6** shows the summary of results from a meta-analysis conducted by Ojha *et al*[31] to tabulate the incidence of non-classical CT findings in COVID-19 patients.

**Figure 7** displays a collection of chest CTs in the axial plane that are examples of the ancillary findings in COVID-19. Examples of vascular enlargement (**Figure 7A**) are modified from Kwee *et al*[32]. Examples of subpleural curvilinear opacities (**Figure 7B**) and reverse halo sign (**Figure 7F**) are modified from Kong *et al*[33]. Additionally, examples of reticular pattern (**Figure 7C**), pulmonary nodules (**Figure 7D**), and

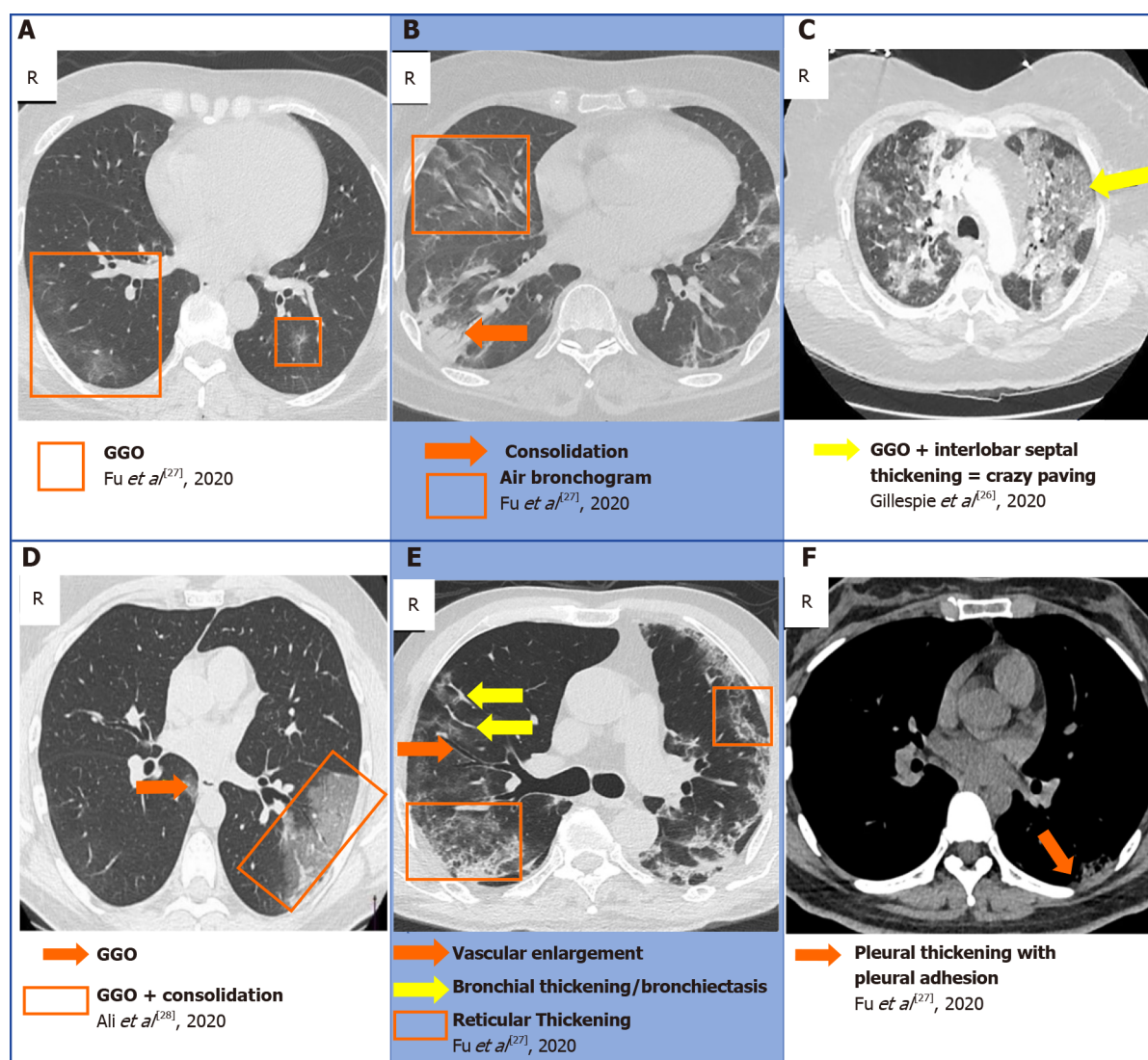


**Figure 4** A collection of chest computed tomography that displays some of the classical findings of coronavirus disease 2019 pneumonia[26-28]. A: Ground-glass opacity (GGO); B: Consolidation and air bronchogram; C: Crazy paving; D: GGO superimposed with consolidation; E: Bronchiectasis, reticular thickening, with vascular enlargement; F: Pleural adhesion. A, B, E and F: Citation: Fu Z, Tang N, Chen Y, Ma L, Wei Y, Lu Y, Ye K, Liu H, Tang F, Huang G, Yang Y, Xu F. CT features of COVID-19 patients with two consecutive negative RT-PCR tests after treatment. *Science Report* 2020; 10: 11548. Copyright ©The Author(s) 2020. Published by Springer Nature; C: Citation: Gillespie M, Flannery P, Schumann JA, Dincher N, Mills R, Can A. Crazy-Paving: A Computed Tomographic Finding of Coronavirus Disease 2019. *Clinical Practice and Cases in Emergency Medicine* 2020; 4: 461-463. Copyright ©The Author(s) 2020. Published by UC Irvine; D: Citation: Ali TF, Tawab MA, ElHariri MA. CT chest of COVID-19 patients: what should a radiologist know? *Egyptian Journal of Radiology and Nuclear Medicine* 2020; 51: 120. Copyright ©The Author(s) 2020. Published by Springer Nature.

bilateral hilar lymphadenopathy (Figure 7E) are modified from Meirelles *et al*[34], Zhang *et al*[35], Mughal *et al*[36], respectively.

Negative features that rule-out COVID-19 include lobar consolidation, which is more commonly seen in bacterial pneumonia rather than COVID-19 pneumonia, along with lack of GGO. Moreover, in early disease, there is a notable absence of features such as pleural effusion, mediastinal lymphadenopathy, lung cavitation and discrete pulmonary nodules such as the tree-in-bud sign in centrilobular nodules[24]. Ultimately, CT has an extremely high sensitivity of 94% in the detection of COVID-19; however, due to multiple pathologies which may be causative for the features seen in CT; CT has a particularly poor, and varying specificity of 25%-80%[37].

## NON-COVID-19 CAUSES OF GGO

There are many causative pathologies unrelated to COVID-19, which may present as GGO on imaging, and this is the reason for the low specificity of CT imaging (25.1%, [95% CI: 21.0%-29.5%]) in diagnosing COVID-19 pneumonia[2]. Acute causes have

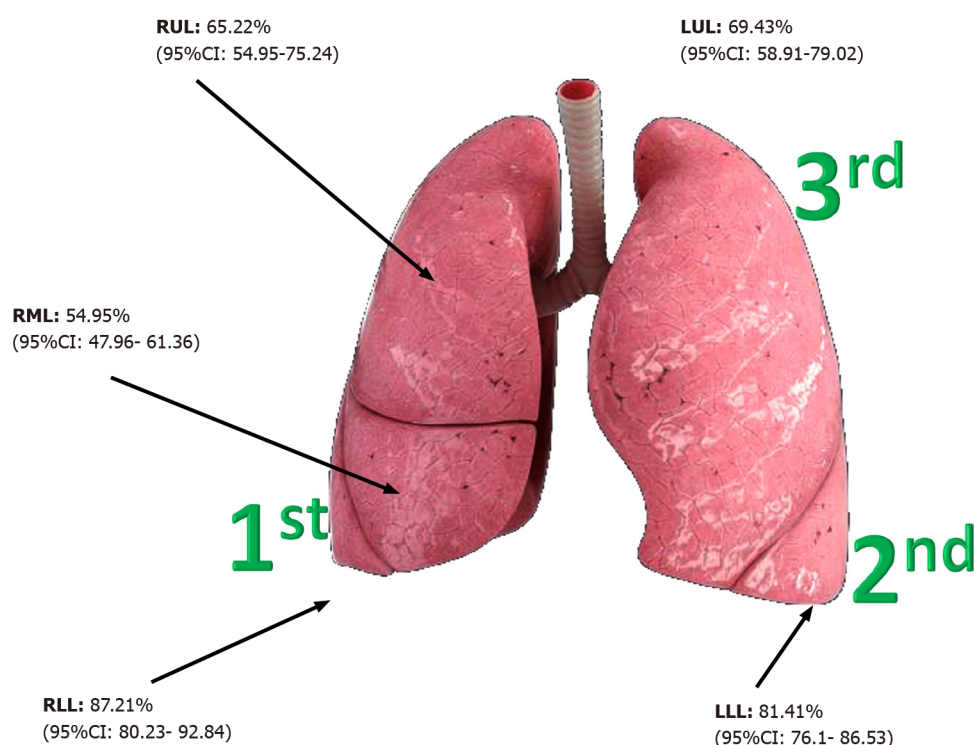


**Figure 5** Summary of the frequency distribution of lesions in the lung lobes on computed tomography imaging of coronavirus disease 2019 patients. CI: Confidence interval; LLL: Left lower lobe; LUL: Left upper lobe (LUL); RLL: Right lower lobe; RML: Right middle lobe; RUL: Right upper lobe.

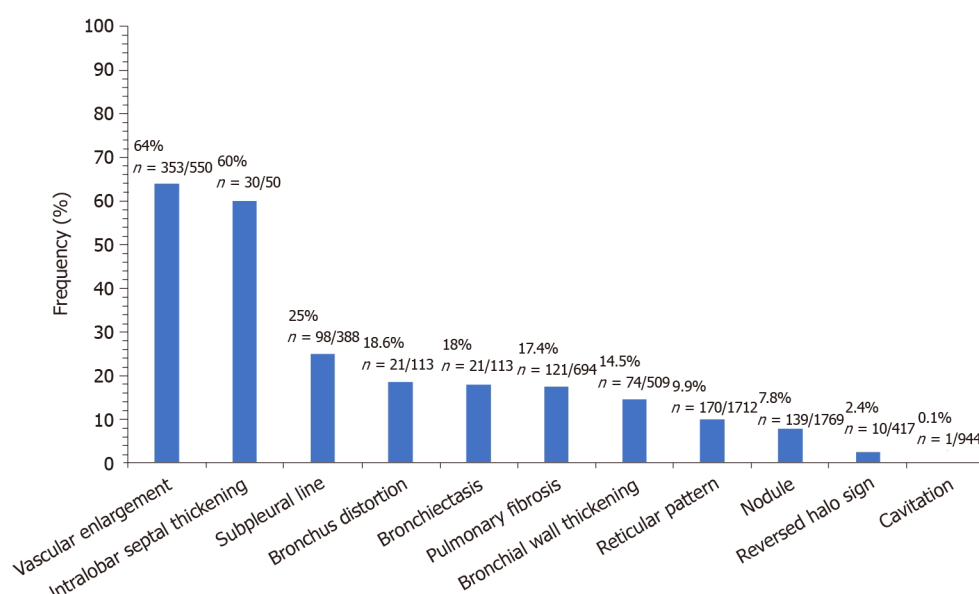


**Figure 6** Summary of the frequency distribution of classical and ancillary computed tomography imaging findings in coronavirus disease 2019 pneumonia. The whiskers indicate the 95% confidence interval. The data are adapted from the meta-analysis conducted by Ojha *et al*[31].

abrupt signs on imaging arising in less than 4 wk. This may be pneumonia caused by a myriad of viruses such as influenza A or B, herpes simplex virus type 1, and cytomegalovirus[10]. In addition, acute eosinophilic pneumonia (AEP) may present as bilateral patchy GGO areas with interlobular septal thickening[38]. Drug toxicity due to cytotoxic drugs such as cyclophosphamide or bleomycin may manifest as scattered or diffuse areas of GGO[39]. Additional presentations may be due to chronic diseases lasting greater than 4 wk. Chronic eosinophilic pneumonia may also give rise to similar signs as AEP. Moreover, early lung cancer such as lung adenocarcinoma may be detected early by the appearance of GGO, improving surgical outcomes[40]. Ultimately, the varying causes of GGO on imaging demonstrates why CT alone is not



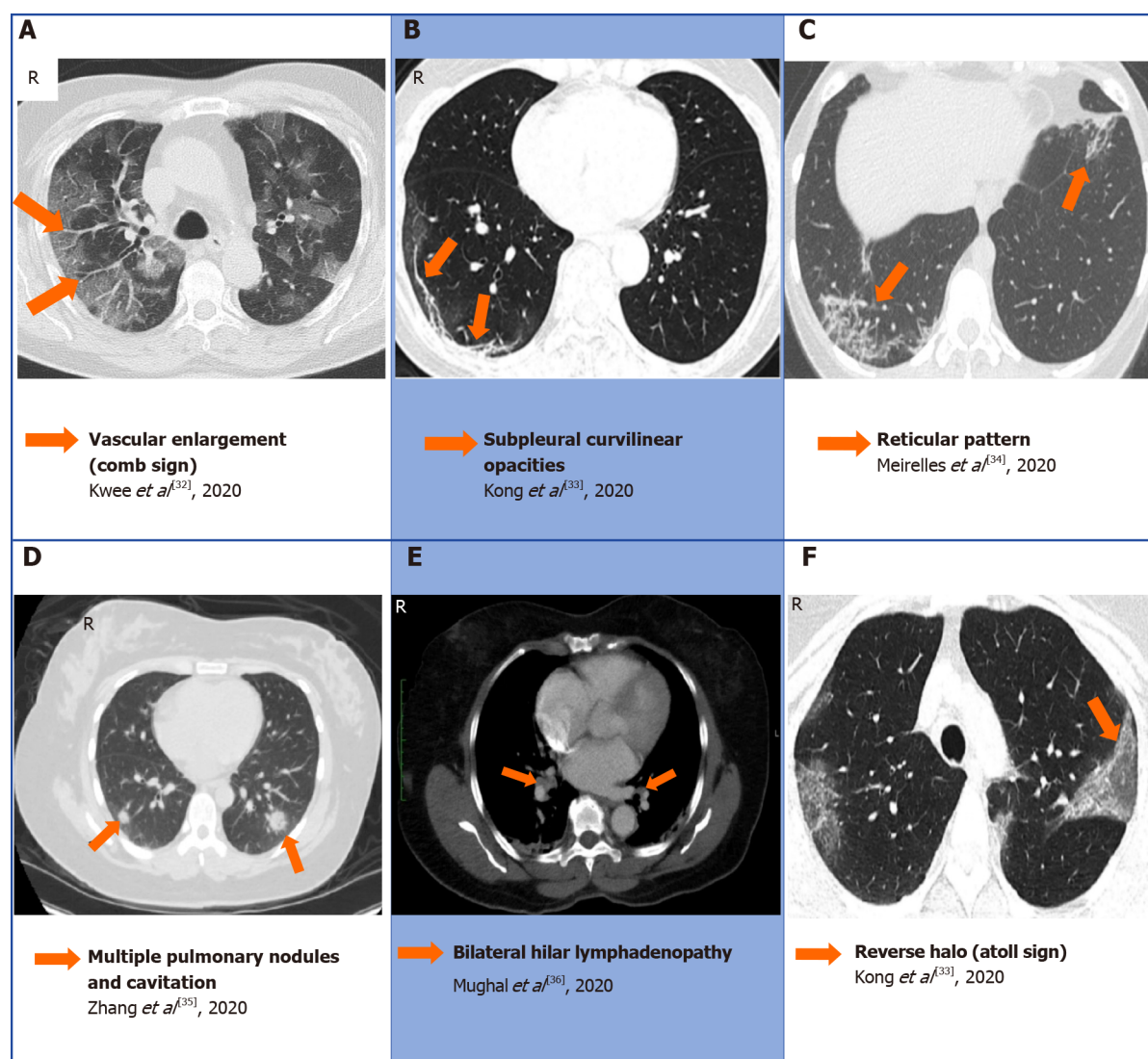


**Figure 7** A collection of chest computed tomography that displays some of the atypical findings of coronavirus disease 2019 pneumonia [32-36]. A: Comb sign in the right lobe characterized by vascular enlargement; B: Curvilinear opacities in the subpleural area; C: Reticular pattern bilaterally; D: Multiple nodules and cavitation; E: Bilateral hilar lymphadenopathy; F: Atoll sign also known as reverse halo. A: Citation: Kwee TC, Kwee RM. Chest CT in COVID-19: What the radiologist needs to know. *Radiographics* 2020; 40: 1848-1865. Copyright ©The Author(s) 2021. Published by Radiographics; B and F: Citation: Kong W, Agarwal PP. Chest imaging appearance of COVID-19 infection. *Radiology: Cardiothoracic Imaging* 2020; 2: e200028. Copyright ©The Author(s) 2020. Published by the Radiological Society of North America, Inc; C: Citation: Meirelles GSP. COVID-19: A brief update for radiologists. *Radiologia Brasileira* 2020; 53: 320-328. Copyright ©The Author(s) 2020. Published by Radiology brasil; D: Citation: Zhang Q, Douglas A, Abideen ZU, Khanal S, Tzamas S. Novel coronavirus (2019-nCoV) in disguise. *Cureus* 2020; 12: e7521. Copyright ©The Author(s) 2020. Published by Cureus; E: Citation: Mughal MS, Rehman R, Osman R, Kan N, Mirza H, Eng MH. Hilar lymphadenopathy, a novel finding in the setting of coronavirus disease (COVID-19): A case report. *Journal of Medical Case Reports* 2020; 14: 124. Copyright ©The Author(s) 2020. Published by BMC.

enough to accurately diagnose a patient with COVID-19 without clinical context, medication history, and RT-PCR/serology COVID-19 testing.

## TIME COURSE: LAGGING OF COVID-19 FEATURES ON RADIOLOGICAL IMAGING

Although the preliminary imaging modality for patients presenting with COVID-19 is a solitary portable anteroposterior chest radiograph, many patients will have an early negative CXR/CT result. This can be due to a lack of macroscopic lung involvement at the time of presentation or minute findings on CXR/CT. During the early stages of disease (0-3 d), the viral particles take over host cell machinery, replicating and inducing a cytokine storm in the form of an acute infection. Gu *et al.*[41] reported that nearly 13% of CT scans depict a normal finding in this early phase, while 63.2% of the cases exhibit a classical GGO appearance. A proposed hypothesis suggests that the



SARS-CoV-2 virion has not accumulated at an adequate density to induce pulmonary parenchymal damage. Therefore, the chest CT appears as a minimally hazy opacification with normal-appearing underlying vessels and bronchial structures. As the disease course progresses to the intermediate stage (4-7 d), there will be diffuse alveolar damage and GGO evolves into consolidation. The majority of the structures on chest CT will appear obscured in comparison to the primary GGO feature seen in the early stages. In the final stage (8-14 d), fibrotic lesions are significantly increased due to scarring of the lung tissue secondary to the resolution of organizing pneumonia [42]. Consolidation is also markedly enhanced in over 78% of the cases; however, the fibrotic lesions help distinguish the case presentation of late-stage from intermediate-stage disease in the majority of patients. Figure 8 summarizes the frequencies of typical CT findings (GGO, consolidation, fibrosis) based on the temporal stages of disease according to data from Gu *et al*[41].

## ULTRASOUND IMAGING

### LUS

LUS is an established imaging test for detecting various lung abnormalities, and in the context of COVID-19, may help clinicians with the diagnosis and evaluation of disease severity. Furthermore, it is useful for prognostic stratification and assessing the development of disease, and has assisted with the management of associated respiratory complications[43-46]. In comparison to CXR or CT, bedside LUS is faster, non-invasive, and radiation-free[47,48]. Point-of-care ultrasound (POCUS) machines are portable, allowing clinicians to assess patients at their bedside. This mitigates the need for patient mobilization to the radiology unit, thereby decreasing the risk of exposure to other patients[49,50]. POCUS is also economical, easy to learn, repeatable, and can obtain results of high reproducibility[51,52]. Moreover, POCUS offers an alternative imaging modality to triage patients' COVID risk levels and to streamline the pathway to warrant a requisition for second-level imaging or interventional management[51]. Heightened transmission of COVID-19 in healthcare workers has highlighted the importance of LUS in providing the option of concomitant execution of clinical examination and lung imaging at the bedside by the same physician[53,54].

## CLASSICAL ULTRASOUND SIGNS: A AND B LINES

A- and B-lines are ultrasonographic artifacts that can be seen during the ultrasonography of an aerated lung. A-lines are typically horizontal artifacts that represent a normal lung surface[55]. B-lines are vertical, comet tail-like artifact indicating subpleural interstitial edema, likely representing reverberations generated by thickened interlobular septa and other subpleural structures[56]. In a normal lung ultrasound, the A-lines are horizontal to pleura and typical B-line patterns include a single cone-shaped line, single thin or thick line, or subpleural consolidation without air bronchogram[57].

## ULTRASONOGRAPHIC PATTERNS IN COVID-19

Clear ultrasonographic patterns can be found in patients with COVID-19. Large numbers of B-lines, irregularity of the pleural line, and small clusters of subpleural pulmonary consolidations also frequently occur in the posterior and inferior areas[54, 58]. Poggiali *et al*[44] concluded a strong correlation between LUS findings and concurrent CT scans in patients ( $n = 12$ ) with COVID-19. These results also revealed diffuse B patterns and bilateral lung involvement with GGO in all of these patients [58]. Additionally, both imaging modalities also detected organizing pneumonia in four patients[59]. A summary of results from Norbedo *et al*[59] and McDermott *et al* [60] showed typical LUS findings in pediatric and adult patients with COVID-19. The literature review conducted by Norbedo *et al*[59] in pediatric patients ( $n = 18$ ) with COVID-19 revealed LUS findings of B-line vertical artifacts, pleural irregularities, and small subpleural consolidations, as well as white patchy lung areas. A similar review conducted by Norbedo *et al*[59] on adult patients ( $n = 43$ ) with COVID-19 revealed consistent LUS findings; irregular B-lines (focal), multifocal and confluent; thickening of pleural line with pleural line subpleural consolidations; and a variety of patterns

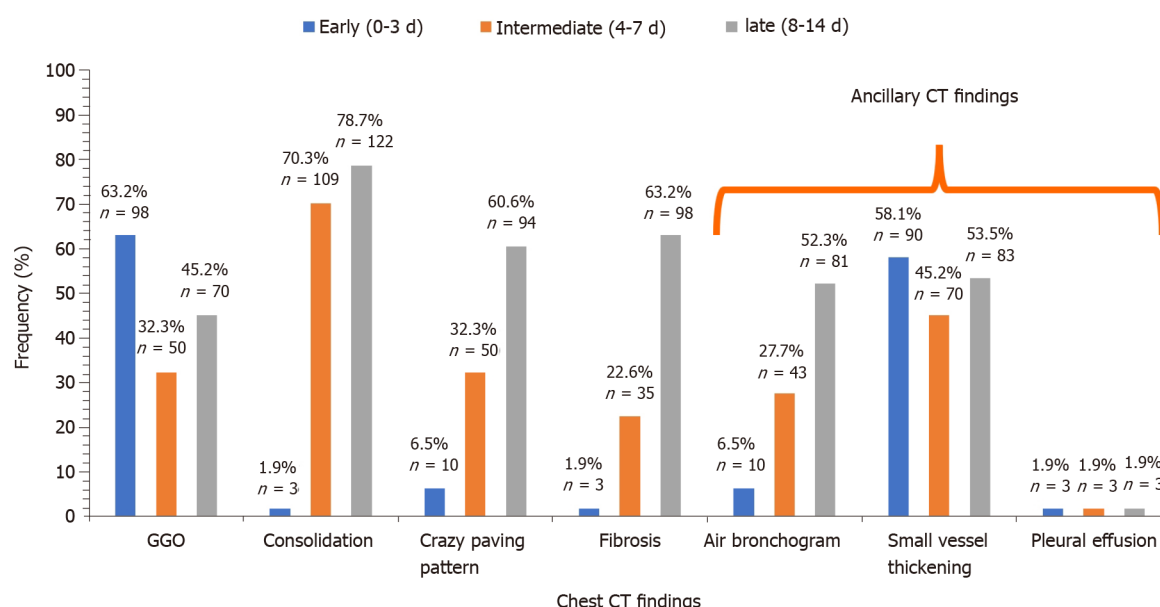


**Figure 8 Summarizes the frequencies of chest classical and ancillary computed tomography findings at different stages of disease progression (early [ $n = 155$ ], intermediate [ $n = 155$ ], and late [ $n = 155$ ]). Data acquired from Gu *et al*[41].**

including multifocal small, non-translobar, and translobar with occasional mobile air bronchograms. The authors also concluded that pleural effusion in COVID-19 patients is uncommon[59].

LUS is able to detect dynamic changes associated with COVID-19. The main early-stage ultrasound finding was focal B-lines, which becomes multifocal and confluent as the disease progresses with further development of consolidations. During convalescence, B-lines and consolidations gradually disappear and are replaced by A-lines[57,61,62].

Interestingly, one study showed that LUS findings in patients with COVID-19 pneumonia exhibited typical patterns consistent with COVID-19 in 38.5% of cases ( $n = 52$ ) and atypical patterns in 61.5% of cases ( $n = 83$ )[63]. The ability of LUS to diagnose COVID-19 can be inferred from its sensitivity of 76.9%, specificity of 77.1%, positive predictive value of 57.7%, and negative predictive value of 89.2%[63]. Additionally, when comparing LUS to chest CT, the results suggest a sensitivity and specificity of 65% and 72.7%, respectively[63]. Figure 9 shows a simplified flowchart for triaging patients presenting with respiratory symptoms during the COVID-19 pandemic in the emergency department as suggested by Schmid *et al*[63].

## 12-ZONE SCORING SYSTEM

In clinical practice, there are various scoring systems to quantify the extent of lung involvement, and in the context of COVID-19, we observed the most prominent one to be the 12-zone scoring system, used as a tool to assess regional and global lung aeration in ARDS as well as COVID-19 pneumonitis[61,64-66]. A total of 12 areas in the right and left lung are examined, namely the anterosuperior, anteroinferior, laterosuperior, lateroinferior, posterosuperior, and posteroinferior lung regions on each side of the lung. Scoring of each area is performed in accordance with the most severe lung ultrasound finding detected in the corresponding intercostal spaces and is given a score from 0-3, tallying up to a maximum of 36. Figure 10 outlines the assessed zone and the criteria for each of the values. The Australasian College of Emergency Medicine proposed a severity classification of patients based on this score as normal (0), mild (1-5), moderate ( $> 5-15$ ), and severe ( $\geq 15$ )[65].

One study by Speidel *et al*[67] showed that the lung ultrasound scoring system (LUSS) had promising diagnostic efficacy with an odds ratio (OR) of 1.30, a 95%CI between 1.09 to 1.54 ( $P = 0.003$ ), and an area under the curve (AUC) of 0.85 (95%CI: 0.71 to 0.99)[67]. Utilization of a cutoff of 8 of 36 points in participants ( $n = 10/11$ ) with a primary diagnosis of COVID-19 were correctly predicted with a sensitivity of 91% (95%CI: 59% to 100%)[67]. In the cohort without a primary diagnosis of COVID-19

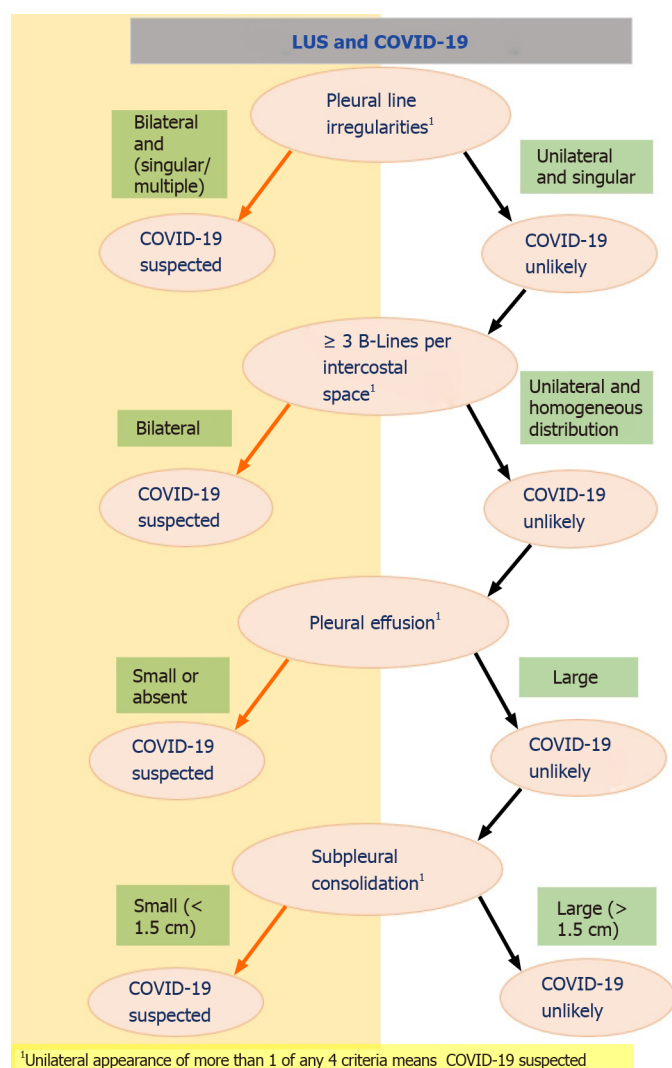


**Figure 9** Shows a simplified flowchart guiding the triage in patients presenting with respiratory symptoms during the coronavirus disease 2019 pandemic using lung ultrasonography in the emergency department. <sup>1</sup>Unilateral appearance of more than 1 of any 4 criteria means coronavirus disease 2019 suspected. COVID-19: Coronavirus disease 2019; LUS: Lung ultrasonography.

(others,  $n = 38$ ), COVID-19 was correctly ruled out in 29 of these 38 patients (specificity = 76%, 95%CI: 60% to 89%)[67]. LUSS, therefore, is a promising screening tool in hospitalized patients suspected of COVID-19. A summary of the results by Speidel *et al* [67] are shown in Figure 11 of typical LUS findings (B-line, and subpleural consolidations) and LUSS scores at varying lung zones in patients with and without a primary diagnosis of COVID-19.

LUS appears to have a promising role in screening clinically suspected or diagnosed COVID-19, only when it is implemented as an adjunct with other diagnostic modalities. An amalgamation of LUS findings with clinical history, physical examination, and knowledge of pretest probability will supplement increasing efficacy. POCUS may facilitate the physician in undertaking the appropriate management pathway or rule in an alternative diagnosis. The practicality of utilization of LUS will remain dependent on resource availability, personnel expertise, and flexibility of LUS configuration for each situation.

## DISADVANTAGES OF LUS

LUS has been criticized for its low specificity in the diagnosis of COVID-19. This is because described features including confluent B-lines, consolidations, and irregular pleural lines simply refer to the lung surface density state and are not pathognomonic for COVID-19[68]. Additionally, LUS cannot detect deep lesions as the aerated parenchyma blocks the transmission of ultrasonography. In order for the lesion to

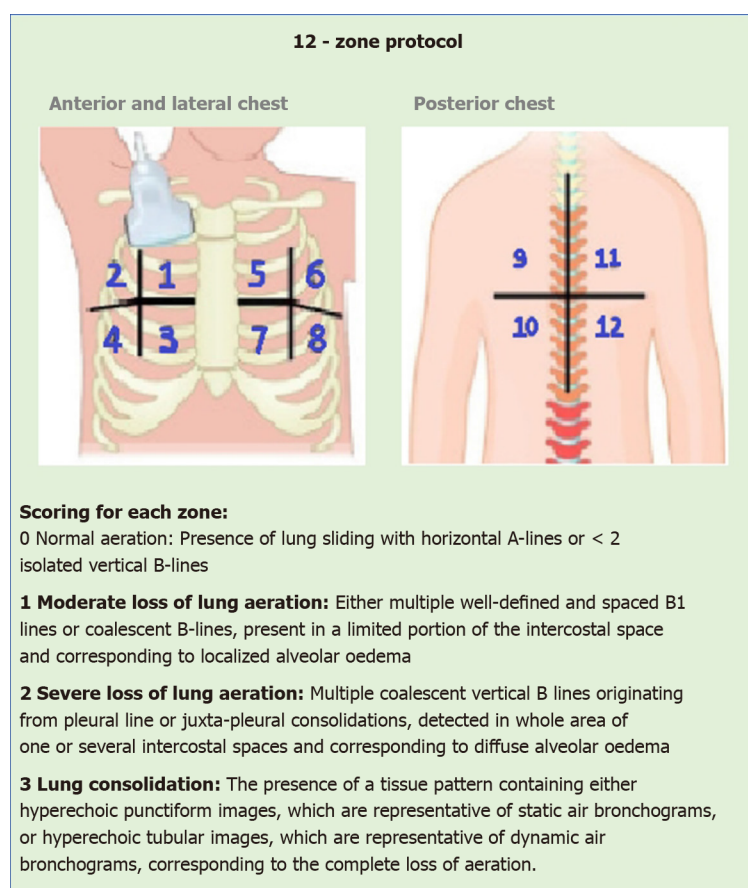


**Figure 10** Schematic diagram describing the 12-zone assessed using the lung ultrasonography 12-zone scoring method. The criteria for each score value (0-3) is described and tabulated.

detected, it must extend to the pleural surface. Furthermore, LUS does not exclude COVID-19 in subjects with no pulmonary complications, and therefore cannot be used as a diagnostic tool by itself to stratify patients who may or may not be infected with COVID-19[47].

## ROLE OF MRI, PET, AND ECHO IMAGING

There is no documented role of pulmonary MRI in the diagnosis of COVID-19 pneumonia. Cardiac MRIs may be helpful in the future to detect complications such as myocarditis and cardiomyopathy. Fluorodeoxyglucose PET (FDG-PET) scans are not used in emergencies, but some studies explain its utilization in describing the subtleties of typical pulmonary findings in COVID-19 pneumonia. The FDG-PET avidity corresponds to the GGOs in CTs, and this is because of the increased glucose requirement by the neutrophils at the site to fight the infection. There is a theoretical possibility of utilizing FDG-PET in the future to monitor treatment response, predict recovery and survey the long-term consequences of COVID-19.

Deep vein thrombosis and peripheral thrombosis are common in areas with high COVID-19 prevalence due to an increased risk of hypercoagulability; therefore, the use of compression ultrasonography is expected to increase. CT pulmonary angiography is mainly used to confirm the prognosis of pulmonary embolism (PE) and stratify patients with acute PE. Point of care echocardiography might be useful as the sensitivity of right ventricular dilation in detecting PE using POC echocardiography can be as high as 90%. Echocardiography can also be used to evaluate COVID-19-related acute cardiac injuries as abnormalities in echocardiography are linked to a worse prognosis and more severe disease[13].

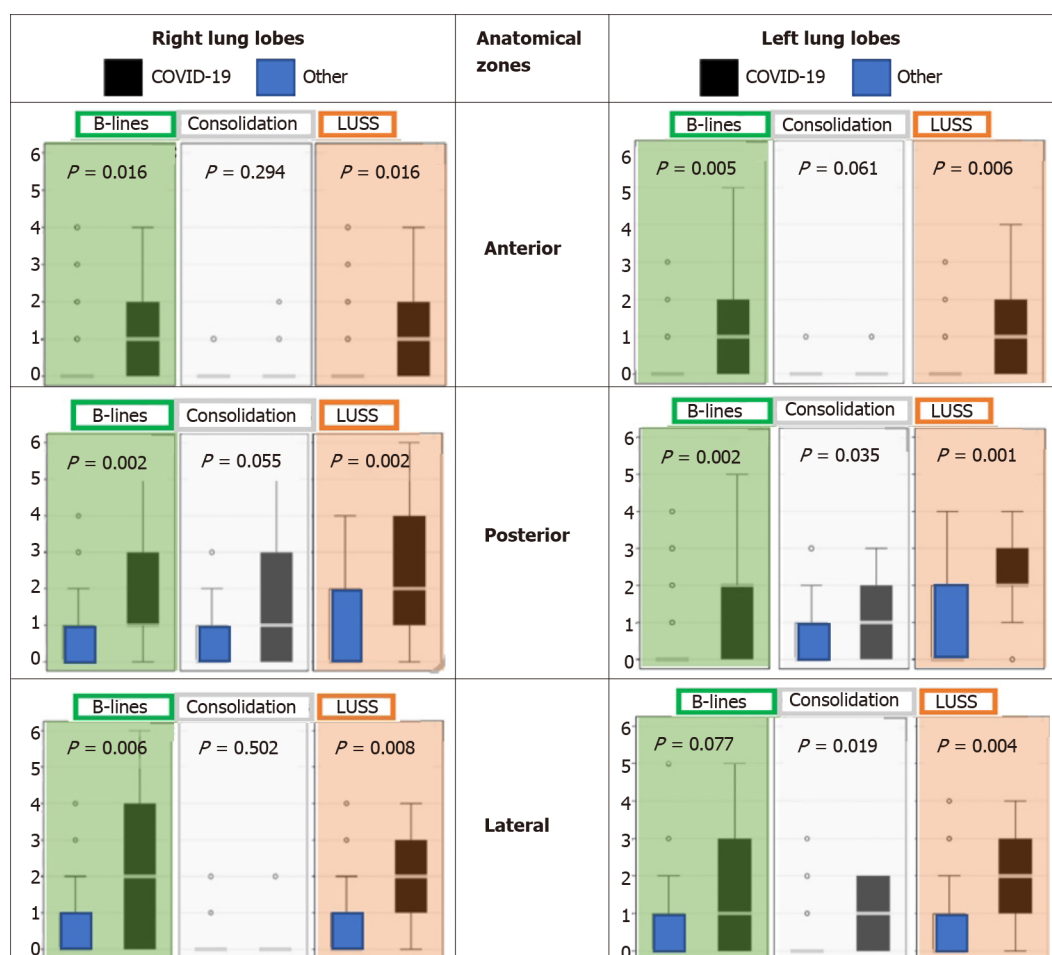


**Figure 11** Lung ultrasonography presentation of B-lines (green panel), subpleural consolidations (white panel), and lung ultrasound scores (orange panel) at different lung zones (anterior, lateral, posterior) in patients with a primary diagnosis of coronavirus disease 2019 ( $n = 11$ ) and without coronavirus disease 2019 (other,  $n = 38$ ). Boxplots around median and interquartile range (IQR), with outliers within 1.5 IQR of the nearest quartile. Other (extrapulmonary infection/inflammation ( $n = 10$ ), pneumonia of other etiology ( $n = 8$ ), exacerbated asthma/ chronic obstructive pulmonary disease ( $n = 7$ ), pulmonary neoplasia ( $n = 4$ ), pulmonary embolism ( $n = 2$ ), congestive heart failure ( $n = 2$ ), and not documented ( $n = 5$ )). Statistically significant outcomes with  $P < 0.05$ . Data utilized from Speidel *et al*[67]. COVID-19: Coronavirus disease 2019; LUSS: Lung ultrasound score.

## CLASSIFICATION SYSTEMS

### CO-RADS classification system

In March 2020, a classification system by the Dutch Association for Radiology was implemented to aid with making the diagnosis of COVID-19. This system was called CO-RADS which stands for COVID-19 reporting and data system and was developed to report CT findings with ease and replicability among other physicians, as prior to this, no system had been developed directly for COVID-19. The system assigns the CT scan a CO-RAD score between 1 to 5 depending on the radiological findings of the chest, and in some cases, a score of 0 and 6 can be used. A score of 0 and 6 is used when the CT is uninterpretable, and a positive RT-PCR test must be present, respectively. Level 1 classification indicates a very low level of suspicion for COVID-19 as these cases do not have any nodules bilaterally and only have normal/benign findings[69]. Infections that can be considered level 1 for COVID-19 include mild or severe emphysema, perifissural nodules, lung tumor indications, and fibrosis[69]. This category is also known as negative for pneumonia. Level 2 is as having a low likelihood of COVID-19, but encompasses infectious diseases such as bronchitis, infectious bronchiolitis, bronchopneumonia, lobar pneumonia, and pulmonary abscesses[69]. CT features include those similar to an atypical pulmonary appearance like tree-in-bud sign, a centrilobular nodular pattern, lobar or segmental consolidation, and lung cavitation. Level 3 is the “middle ground” where the viewer can be unsure of the diagnosis as the features seen are those consistent with COVID-19 but also with viral pneumonia or non-infectious causes[69]. Findings in this level consist of perihilar GGO, homogenous extensive GGO with or without sparing of some secondary



pulmonary lobules, or GGO together with smooth interlobular septal thickening with or without pleural. GGO can also be seen on CT, which is characteristic of COVID-19, but the opacities seen are also compatible with organizing pneumonia. Although levels 4 and 5 have similar findings, the presence of GGO with or without consolidations in lung areas close to the visceral pleura indicates a CO-RADS score of level 5 [69]. A summary of the CO-RADS categories and its criteria outlined by Prokop *et al* are outlined in Table 1.

A study by Bellini *et al* [70] analyzed the diagnostic yield of CO-RADS in identifying lung involvement in patients suspected of COVID-19 ( $n = 572$ , COVID-19 ( $n = 142$ ), not COVID-19 ( $n = 430$ )) by multiple radiologist and physicians at different levels of expertise. Overall, CO-RADS showed promising accuracy for lung involvement with a mean AUC of 72% (95%CI: 67% to 75%)[70]. The receiver operating characteristic (ROC) curve revealed that application of a threshold  $\geq 4$  resulted in a moderate specificity of 81% (95%CI: 76% to 84%) and a low sensitivity of 61% (95%CI: 52% to 69%)[70]. The CO-RADS rating among all readers was moderate as shown by Fleiss' Kappa statistic of 0.43 (95%CI: 0.42 to 0.44) and with a substantial agreement for categories; CO-RADS 1 (Fleiss' K = 0.61 (95%CI: 0.60 to 0.62) and for CO-RADS 5 (Fleiss' K = 0.60 (95%CI: 0.58 to 0.61))[70].

## MULBSTA SCORING SYSTEM

Another scoring system used for COVID-19 is known as the MuLBSTA score, which looks at key components such as multi-lobar infiltration, hypo-lymphocytosis, bacterial coinfection, smoking history, hypertension, and age. Five points are assigned for multi-lobar infiltration, 4 points if the lymphocyte count is less than or equal to  $0.8 \times 10^9/L$ , 4 points for bacterial infiltration that is confirmed by lab results or on CT, 3 points for those who are currently smoking (2 for those who have previously been smokers), 2 points for hypertension, and 1 point for age above 60-years-old. A total score of 12 was used as the cut-off; those with scores between 0 and 11 were considered low risk while those with a score of  $\geq 12$  are considered high-risk patients. Those who are in the high-risk category are more likely to require intensive care unit treatment or were more likely to die due to the infection. This scoring system became useful as it helps to predict the prognosis of patients based on other clinical features and co-morbidities[66]. A retrospective study by Ma *et al* [71] ( $n = 330$ ), showed that the ROC curve analysis on the MuLBSTA early warning scoring system for severe COVID-19 patients has an accuracy of 92.7% (95%CI: 89.2% to 96.3%), sensitivity of 65.1%, and specificity of 95.4%. These outcomes indicate that MuLBSTA is a good early warning system for severe COVID-19 patients.

## RALE CLASSIFICATION

This system aims to associate the course and severity of CXR in COVID-19 with the diagnostic RT-PCR result. The RALE score involves individually assessing each lung and depending on how much of the lung is involved, a score is assigned to it. With no involvement, the score is 0, less than 25% lung involvement is 1, 25% lung involvement is 2, 50% of the lung is 3, and a level 4 classification is given when the lung is involved more than 75%. The overall score is calculated by adding the two scores, indicating the involvement of each lung[66]. The RALE score can be used to predict the outcomes of patients with COVID-19 pneumonia and their need for mechanical ventilation (MV). Interestingly, this scoring system is practical and only one of the few ones that incorporate a prognostic value. This makes it a valuable proxy system to compare against an artificial intelligence (AI) model.

One study by Ebrahimian *et al* [72] evaluated the implementation of AI such as the commercially available AI algorithm (qXR v2.1 c2; Qure.ai Technologies, Mumbai, Maharashtra) has been on the rise. This model was trained on patient data with a positive SARS-CoV-2 RT-PCR assay. The AI score had a strong positive correlation with RALE score for each site of the patient CXR ( $r^2 = 0.79$  to  $0.86$ ;  $P < 0.0001$ )[72]. It also revealed that patients that received MV or deceased had a significantly higher AI or RALE score when compared to those not requiring MV or attained convalescence [72]. This study concluded that instead of comparing the RALE and AI score to the baseline CXRs, combining the RALE and AI score over progressive serial CXRs with clinical and lab data would drastically improve the predictability of both the AI score and the subjective RALE score.

**Table 1 Association between CO-RADS categories and level of suspicion for pulmonary involvement of coronavirus disease 2019**

CO-RADS category	Suspicion level for pulmonary involvement of COVID-19	Summary
0	Not interpretable	Scan insufficient for assigning score
1	Very low	Normal or non-infectious scan
2	Low	Typical for other infection but not COVID-19
3	Ambiguous	Non-specific features of COVID-19
4	High	Increased suspicion of COVID-19
5	Very high	Typical features of COVID-19
6	Proven	Positive RT-PCR test for COVID-19

Table modified from Prokop *et al*[69]. COVID-19: Coronavirus disease 2019.

## BRIXIA SCORE

This score was designed and implemented for serial monitoring by the 'Radiology Unit 2 of ASST Spedali Civili di Brescia' and was later validated for risk stratification on a greater population by Borghesi *et al*[73]. According to this scoring system, the lung is divided into six different zones, three on each of the lungs, in either anteroposterior or posteroanterior views. With regards to the scoring of the zones, the score given can be between and including 0-3 based on the involvement of the lung. A score of 0 is given if there are no abnormalities seen on X-ray, a score of 1 is given when there are interstitial infiltrates. Two is given if there are interstitial and alveolar infiltrates, with the interstitial markings being more prominent. A score of 3 is assigned when there are both interstitial and alveolar infiltrates present, with the latter being more prominent. These scores are given to each of the 6 zones and are then aggregated to get a final score. This type of semiquantitative scoring makes CXR interpreting faster and more streamlined for evaluation[73]. The Brixia score becomes more useful when serial CXRs are performed as this enables documentation of additional sub-scores. The H-score is the highest Brixia score documented during the serial CXRs. Contrastingly, the L-score is the lowest Brixia score documented during the serial CXRs. Additionally, the Brixia score is documented at admission (A-score) and discharge/death (E-score).

One study by Maroldi *et al*[74] retrospectively assessed the clinical value of the Brixia score in 953 COVID-19 patients. In this study, the H-score was significantly higher with a median of 12 and interquartile range (IQR) between 9 to 14 in the deceased cohort compared to the discharged cohort (median: 8, IQR 5 to 11). Similarly, the L-score (7 *vs* 5;  $P < 0.0003$ ), A-score (9 *vs* 8;  $P < 0.039$ ), and E-score (12 *vs* 7;  $P < 0.0001$ ) were all higher in the deceased cohort than the discharged cohort[74]. Overall, logistic regression showed a significant predictive value for H-score of OR 1.25. The ROC curve revealed an AUC of 0.863[74]. Additional Cox proportional hazards regression revealed age has a hazard ratio (HR) of 4.17 ( $P = 0.0001$ ), H-score of  $< 9$  has a HR 0.36 ( $P = 0.0012$ ) and worsening of H-score compared to a score below 3, which has a HR of 1.57 ( $P = 0.0227$ ) and is associated with a worse outcome[74]. These outcomes demonstrate the importance of the Brixia score in the monitoring and assessment of COVID-19 pneumonia and its strong correlation with a patient's prognosis.

## PERMANENT LUNG SCARRING POST COVID-19

Research into the evolution of COVID-19 pneumonia imaging during the follow-up in the later stages of the disease is an interesting area. Zhao *et al*[75] demonstrated that at 3 mo, typical lung features (GGO, interstitial thickening, and crazy paving) were almost resolved, with some fibrosis. High-resolution CT scans of patients ( $n = 55$ ) revealed that 67.27% had GGO ( $n = 37$ ), 27.27% had interstitial thickening ( $n = 15$ ), and 5.45% had crazy-paving patterns ( $n = 3$ )[75]. However, the study only included 55 patients who had non-critical COVID-19 pneumonia. Long-term follow-up studies with a larger sample size are crucial to better understand the trends in recovery. The available literature reports consistent findings of partial healing of GGO and consol-

idation from approximately day 14. In some patients, CT findings also demonstrated signs of fibrosis. In February to March 2020, a case series provided the earliest reports of follow-up CT findings. Partial healing of a mixed pattern of GGO and consolidation occurred from the day 14 onwards according to Duan and Qin[76], and Shi *et al*[77]. Wei *et al*[79], reported lung fibrosis in COVID-19 patients on day 12 which was corroborated by a case presented by Li *et al*[78] which described similar findings on day 14. Pan *et al*[80] presented a retrospective study ( $n = 63$ ) following up COVID-19 patients. These patients were re-examined in intervals of 3-14 d wherein enlarged fibrous stripes and solid white nodules were documented. Pan *et al*[42] reported that after 14 d, 65% had GGO ( $n = 13/20$ ) and 75% had consolidation ( $n = 15/20$ ), but crazy-paving pattern was absent in all 20 patients. Bernheim *et al*[81] found that in 25 patients, after 6-12 d, 88% had GGO ( $n = 22/25$ ) and 60% had consolidation ( $n = 15/25$ ). Crazy-paving pattern was present in 20% of patients ( $n = 5$ ), and 24% had bronchial wall thickening ( $n = 6$ ) but no patients had underlying pulmonary fibrosis [81]. Wang *et al*[82] reported that during days 12-17 there was a notable increase in the mixed pattern, although GGO were still predominant. Xiong *et al*[83] observed that after an average of 11.6 d the follow-up CT showed progressive GGO, consolidation, interstitial thickening, fibrous stripes, and air bronchograms. These findings aid our understanding of the recovery patterns in infected patients. Furthermore, follow-up and management plans will need high-quality evidence to guide clinical decision-making and monitor treatment efficacy with supplemental oxygen and antifibrotic agents.

## AI INTERVENTIONAL SYSTEMS

AI is a broad concept that refers to a set of advanced computational algorithms that utilizes heuristic pattern recognition for a given training dataset and therefore makes predictions on unseen testing datasets. Radiomics utilizes data-characterization algorithms for extracting and evaluating features from radiological medical images and further uses them to creating statistical models with the intent to provide support for diagnosis and management[84]. Radiologic parameters considered for analysis include size, shape and textural features that have useful spatial information on pixel or voxel distribution and patterns[85]. Integration of AI into radiomic datasets has the potential to streamline COVID-19 diagnosis. In early February 2020, Beijing-based AI company *Infervision* launched the “Coronavirus artificial intelligence solution,” an algorithm that utilizes CT imaging data to diagnose COVID-19 on CT[86]. The reports revealed an increased ability to read images in 10 s, drastically improving clinical workflow efficiency, and reducing variable human error, while continuously improving diagnostic accuracy[87].

Another study developed a deep-learning COVID-19 diagnosis system from a dataset including 11356 CT volumes from COVID-19, influenza-A/B, non-viral community-acquired pneumonia and non-pneumonia subjects from China[88]. The basic workflow of the deep-learning-based diagnosis model contains utilization of CT data as the input, the lung is then segmented, COVID-19 diagnosis is made based on the location of infectious slices (Figure 12). This study found that the AI system outperformed very experienced radiologists based on speed. Another study by Harmon *et al*[89] showed that the use of the AI system that can detect COVID-19 pneumonia with 90.8% accuracy, 84% sensitivity, and 93% specificity. A total of 1280 patients from China, Italy, and Japan were used to train the deep-learning algorithms, and the system was tested independently on 1337 patients, with normal controls from oncology, emergency, and pneumonia-related indications. There was a 10% false-positive rate of incorrectly diagnosed COVID-19 related patients. This indicates potential for overlapped diagnosis with other pneumonia etiologies. Another limiting factor in using AI is the need for thousands of high-quality CT studies to train the AI. Overall, AI systems could be trained to be extremely accurate, sensitive, and specific for COVID-19 diagnosis. However, it may be more useful in specific assessment of imaging findings of COVID-19[88,89].

A subsequent study conducted by Yu *et al*[90] investigated various pre-trained deep learning AI models against 246 severe cases and 483 non-severe COVID-19 cases and found that DenseNet-201 with cubic SVM model achieved a high severity classification accuracy of 95.20% and 95.34% for ten-fold cross-validation and leave-one-out validation, respectively. These effective results show that the utility of the proposed pipeline model was able to achieve a rapid and accurate identification of the severity of COVID-19, indicating its potential for use by clinicians in not just diagnosis but also



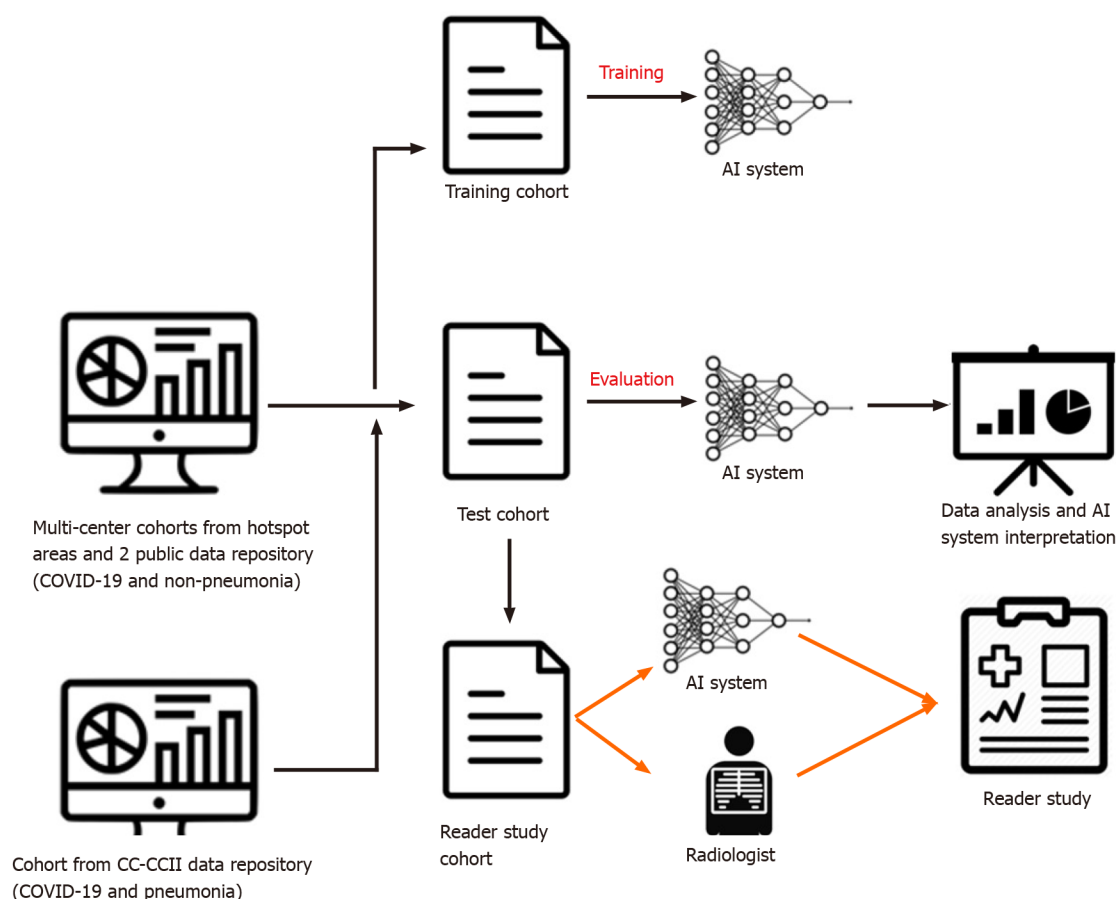


**Figure 12 Basic workflow of the artificial intelligence system.** AI: Artificial intelligence; COVID-19: Coronavirus disease 2019.

decisions relating to severity management and prioritization[90].

In May 2020, radiologist Laghi[91] wrote a correspondence letter in *The Lancet* detailing her concern that the diagnostic value of AI algorithms in CT scans was not supported by scientific evidence. In fact, since the high-resolution CT findings are not pathognomonic of COVID-19 infection and have poor accuracy in screening asymptomatic individuals according to the American College of Radiology, there have been growing concerns over the integration of AI radiology into the screening of this disease[92].

## RADIOLOGY PANEL: FIRST AND SECOND WAVE

### **First wave experience**

The overwhelming nature of COVID-19 has strained global healthcare services and greatly impacted radiology departments. To cope with increasing admissions during peaks, radiologists and radiology trainees have experienced redeployment to areas of clinical need. One hospital saw 21% of their total radiology employees reassigned to other duties[93]. Following official guidelines[94], medical facilities also rescheduled non-urgent elective procedures, and this had a major effect on total imaging volume. While the exact drop varies within institutions, a large New York metropolitan health system reported an 87%, 4%, and 45% reduction in outpatient, inpatient, and emergency imaging respectively, during the pandemic[95].

Moreover, it has become increasingly evident that COVID-19 is not limited to the lungs, rather it can affect other organs too. An early published clinical cohort of COVID-19 displayed acute cardiac injury, shock, and arrhythmia in 7.2%, 8.7%, and 16.7% of patients respectively, with a higher prevalence in patients requiring intensive care[96]. Neurological manifestations have also been recorded; another observational study demonstrated neurological symptoms in 36.4% of hospitalized COVID patients [97]. Alongside observations of kidney involvement and hypercoagulability in patients, this leaves a potentially important role for radiologists when considering

COVID-19 as a multisystem disease[98,99].

Regarding the role of imaging, our understanding has changed with the course of the pandemic. Chest CT was temporarily part of the official diagnostic criteria for COVID-19 due to the nature of the early emergency in China; however, since then, chest CT findings are no longer considered diagnostic. Current guidelines establish that RT-PCR assays are the standard for definitive COVID-19 diagnosis[100,101]. Instead, CXR and chest CT have been the most common imaging modalities specified for presumptive diagnosis, triage and management of patients with suspected or known COVID-19 infection[102]. After the diagnosis is confirmed, the role of imaging may be limited but while waiting for PCR positive it can be very useful for clinicians. Portable CXR is often used as the primary imaging study in suspected patients, chest CT is far more sensitive in detecting lung lesions but has been reserved for more specific cases[4,13].

## FORWARD PREPARATION FOR THE SECOND WAVE

As radiologists get ready for the second wave of COVID-19, it is important to continue developing on lessons learned from the 1<sup>st</sup> wave. With that in mind, a general framework that can be applied to radiology departments when preparing for the second wave and beyond is the concepts of building, sustaining, and adapting[103].

The main idea of the first strategy is to create capacity before it is needed. This can be done by increasing hours of staff, getting more manpower, or by expanding operations into other sites as seen in Singapore General Hospital's (SGH) Emergency Department[103]. When faced with increased local transmission of COVID-19, management of an adjacent Ambulatory Surgery Centre was transferred to the ED, allowing for operations to be ramped up and for portable radiology services to grow [104]. Additional capacity can also be created by increasing portable imaging capability through renting extra units so they can be deployed into operations when needed[105].

Moving on to the second strategy of sustaining, the central idea here is to operate at a pace that is maintainable in the long-term. This would involve preserving supplies such as Personal Protective Equipment, preventing staff burnout, simplifying hastily designed processes, and alternating work times or work sites[103]. In the University of Alabama at Birmingham, home picture archiving and communication system workstations were rapidly deployed in anticipation of a potential COVID-19 crisis [106]. With this measure, the number of people coming on-site could be limited in the long-term while also contributing to social distancing amongst radiologists.

Lastly, the third strategy, adapting, highlights the importance of being flexible. Some ways this can be achieved include rapidly scaling up responses, reconfiguring spaces, improvising, and embracing new roles when faced with increased demands [103]. This is demonstrated at SGH, where in order to monitor changes in the pandemic, a smaller radiology disease outbreak task force was assembled to assess overnight incidents and anticipate changes during the day[4].

## CONCLUSION

The burden of this disease is evident through the rampant rise in fatality, morbidity, and mortality rates across the world. Despite the integration of stringent public health measures, this spread continues and is leaving an everlasting impact on both humanity and the economy. Radiologists have significantly adjusted their practices in accordance with the pandemic and as frontline workers, it is essential for them to identify the classical findings associated with COVID-19 and use their expertise towards engaging in optimal strategies to slow disease progression. Advances in the role of radiology in COVID-19 research have piled up within a short-period, hence it is prudent to remain acquainted with important findings. Some notable findings consist of the early stage of disease producing a classical GGO appearance on majority of the CT scans, and the late stage of disease showing highly specific fibrotic lesions due to scarring of the lung parenchyma. The purpose of identifying these characteristic features and associating them with a time course can be crucial towards the management plan for each patient. Additionally, the role of radiology can further be integrated into the scoring systems discussed in this review for risk stratification and appropriate assessment and treatment strategies for infected cases. Nevertheless, medical imaging has been suggested to have promising value as a rapid adjunctive

tool in patients with COVID-19 through assisting with the diagnosis, evaluating patients with clinical deterioration, and providing the multidisciplinary team with vital examinations that could support the management strategies.

## REFERENCES

- 1 **World Health Organization.** Laboratory testing for 2019 novel coronavirus (2019-nCoV) in suspected human cases 19 March 2020. [cited 22 January 2021]. Available from: <https://www.who.int/publications/i/item/10665-331501>
- 2 **Böger B, Fachi MM, Vilhena RO, Cobre AF, Tonin FS, Pontarolo R.** Systematic review with meta-analysis of the accuracy of diagnostic tests for COVID-19. *Am J Infect Control* 2021; **49**: 21-29 [PMID: 32659413 DOI: 10.1016/j.ajic.2020.07.011]
- 3 **Liotti FM, Menchinelli G, Marchetti S, Posteraro B, Landi F, Sanguinetti M, Cattani P.** Assessment of SARS-CoV-2 RNA Test Results Among Patients Who Recovered From COVID-19 With Prior Negative Results. *JAMA Intern Med* 2021; **181**: 702-704 [PMID: 33180119 DOI: 10.1001/jamainternmed.2020.7570]
- 4 **Mossa-Basha M, Meltzer CC, Kim DC, Tuite MJ, Kolli KP, Tan BS.** Radiology Department Preparedness for COVID-19: Radiology Scientific Expert Review Panel. *Radiology* 2020; **296**: E106-E112 [PMID: 32175814 DOI: 10.1148/radiol.20200988]
- 5 **Younes N, Al-Sadeq DW, Al-Jighefee H, Younes S, Al-Jamal O, Daas HI, Yassine HM, Nasrallah GK.** Challenges in Laboratory Diagnosis of the Novel Coronavirus SARS-CoV-2. *Viruses* 2020; **12**: 582 [PMID: 32466458 DOI: 10.3390/v12060582]
- 6 **Weiss SR, Navas-Martin S.** Coronavirus pathogenesis and the emerging pathogen severe acute respiratory syndrome coronavirus. *Microbiol Mol Biol Rev* 2005; **69**: 635-664 [PMID: 16339739 DOI: 10.1128/MMBR.69.4.635-664.2005]
- 7 **Yuki K, Fujiogi M, Koutsogiannaki S.** COVID-19 pathophysiology: A review. *Clin Immunol* 2020; **215**: 108427 [PMID: 32325252 DOI: 10.1016/j.clim.2020.108427]
- 8 **Corman VM, Muth D, Niemeyer D, Drosten C.** Chapter Eight - Hosts and Sources of Endemic Human Coronaviruses. In: *Advances in Virus Research*. Kielian M, Mettenleiter TC, Roossinck MJ, editors. Elsevier, 2018: 163-188 [DOI: 10.1016/bs.aivir.2018.01.001]
- 9 **Kakodkar P, Kaka N, Baig MN.** A Comprehensive Literature Review on the Clinical Presentation, and Management of the Pandemic Coronavirus Disease 2019 (COVID-19). *Cureus* 2020; **12**: e7560 [PMID: 32269893 DOI: 10.7759/cureus.7560]
- 10 **Kim EA, Lee KS, Primack SL, Yoon HK, Byun HS, Kim TS, Suh GY, Kwon OJ, Han J.** Viral pneumonias in adults: radiologic and pathologic findings. *Radiographics* 2002; **22**: S137-S149 [PMID: 12376607 DOI: 10.1148/radiographics.22.suppl\_1.g02oc15s137]
- 11 **Luks AM, Freer L, Grissom CK, McIntosh SE, Schoene RB, Swenson ER, Hackett PH.** COVID-19 Lung Injury is Not High Altitude Pulmonary Edema. *High Alt Med Biol* 2020; **21**: 192-193 [PMID: 32281877 DOI: 10.1089/ham.2020.0055]
- 12 **Gralinski LE, Baric RS.** Molecular pathology of emerging coronavirus infections. *J Pathol* 2015; **235**: 185-195 [PMID: 25270030 DOI: 10.1002/path.4454]
- 13 **Manna S, Wruble J, Maron SZ, Toussie D, Voutsinas N, Finkelstein M, Cedillo MA, Diamond J, Eber C, Jacobi A, Chung M, Bernheim A.** COVID-19: A Multimodality Review of Radiologic Techniques, Clinical Utility, and Imaging Features. *Radiol Cardiothorac Imaging* 2020; **2**: e200210 [PMID: 33778588 DOI: 10.1148/ryct.20200210]
- 14 **Lev MH, Gonzalez RG.** 17 - CT Angiography and CT Perfusion Imaging. In: *Brain Mapping: The Methods*. 2nd ed. Toga AW, Mazziotta JC, editors. San Diego: Academic Press, 2002: 427-484 [DOI: 10.1016/b978-012088592-3/50076-1]
- 15 **Singh B, Kaur P, Reid RJ, Shamoof F, Bikkina M.** COVID-19 and Influenza Co-Infection: Report of Three Cases. *Cureus* 2020; **12**: e9852 [PMID: 32832306 DOI: 10.7759/cureus.9852]
- 16 **Shi H, Han X, Jiang N, Cao Y, Alwalid O, Gu J, Fan Y, Zheng C.** Radiological findings from 81 patients with COVID-19 pneumonia in Wuhan, China: a descriptive study. *Lancet Infect Dis* 2020; **20**: 425-434 [PMID: 32105637 DOI: 10.1016/S1473-3099(20)30086-4]
- 17 **Pormohammad A, Ghorbani S, Khatami A, Farzi R, Baradaran B, Turner DL, Turner RJ, Bahr NC, Idrovo JP.** Comparison of confirmed COVID-19 with SARS and MERS cases - Clinical characteristics, laboratory findings, radiographic signs and outcomes: A systematic review and meta-analysis. *Rev Med Virol* 2020; **30**: e2112 [PMID: 32502331 DOI: 10.1002/rmv.2112]
- 18 **Carotti M, Salaffi F, Sarzi-Puttini P, Agostini A, Borgheresi A, Minorati D, Galli M, Marotto D, Giovagnoni A.** Chest CT features of coronavirus disease 2019 (COVID-19) pneumonia: key points for radiologists. *Radiol Med* 2020; **125**: 636-646 [PMID: 32500509 DOI: 10.1007/s11547-020-01237-4]
- 19 **Martini K, Blüthgen C, Walter JE, Messerli M, Nguyen-Kim TDL, Frauenfelder T.** Accuracy of Conventional and Machine Learning Enhanced Chest Radiography for the Assessment of COVID-19 Pneumonia: Intra-Individual Comparison with CT. *J Clin Med* 2020; **9**: 3576 [PMID: 33171999 DOI: 10.3390/jcm9113576]
- 20 **Rampa L, Miceli A, Casilli F, Biraghi T, Barbara B, Donatelli F.** Lung complication in COVID-19 convalescence: A spontaneous pneumothorax and pneumatocele case report. *J Respir Dis Med* 2020;

- 2 [DOI: [10.15761/jrdm.1000115](https://doi.org/10.15761/jrdm.1000115)]
- 21 **Kaufman AE**, Naidu S, Ramachandran S, Kaufman DS, Fayad ZA, Mani V. Review of radiographic findings in COVID-19. *World J Radiol* 2020; **12**: 142-155 [PMID: [32913561](https://pubmed.ncbi.nlm.nih.gov/32913561/) DOI: [10.4329/wjr.v12.i8.142](https://doi.org/10.4329/wjr.v12.i8.142)]
- 22 **Yasin R**, Gouda W. Chest X-ray findings monitoring COVID-19 disease course and severity. *Egypt J Radiol Nucl Med* 2020; **51**: 193 [DOI: [10.1186/s43055-020-00296-x](https://doi.org/10.1186/s43055-020-00296-x)]
- 23 **Borakati A**, Perera A, Johnson J, Sood T. Diagnostic accuracy of X-ray versus CT in COVID-19: a propensity-matched database study. *BMJ Open* 2020; **10**: e042946 [PMID: [33158840](https://pubmed.ncbi.nlm.nih.gov/33158840/) DOI: [10.1136/bmjopen-2020-042946](https://doi.org/10.1136/bmjopen-2020-042946)]
- 24 **Ng MY**, Lee EYP, Yang J, Yang F, Li X, Wang H, Lui MM, Lo CS, Leung B, Khong PL, Hui CK, Yuen KY, Kuo MD. Imaging Profile of the COVID-19 Infection: Radiologic Findings and Literature Review. *Radiol Cardiothorac Imaging* 2020; **2**: e200034 [PMID: [33778547](https://pubmed.ncbi.nlm.nih.gov/33778547/) DOI: [10.1148/ryct.2020200034](https://doi.org/10.1148/ryct.2020200034)]
- 25 **Bao C**, Liu X, Zhang H, Li Y, Liu J. Coronavirus Disease 2019 (COVID-19) CT Findings: A Systematic Review and Meta-analysis. *J Am Coll Radiol* 2020; **17**: 701-709 [PMID: [32283052](https://pubmed.ncbi.nlm.nih.gov/32283052/) DOI: [10.1016/j.jacr.2020.03.006](https://doi.org/10.1016/j.jacr.2020.03.006)]
- 26 **Gillespie M**, Flannery P, Schumann JA, Dincher N, Mills R, Can A. Crazy-Paving: A Computed Tomographic Finding of Coronavirus Disease 2019. *Clin Pract Cases Emerg Med* 2020; **4**: 461-463 [PMID: [32926713](https://pubmed.ncbi.nlm.nih.gov/32926713/) DOI: [10.5811/cpcem.2020.5.47998](https://doi.org/10.5811/cpcem.2020.5.47998)]
- 27 **Fu Z**, Tang N, Chen Y, Ma L, Wei Y, Lu Y, Ye K, Liu H, Tang F, Huang G, Yang Y, Xu F. CT features of COVID-19 patients with two consecutive negative RT-PCR tests after treatment. *Sci Rep* 2020; **10**: 11548 [PMID: [32665633](https://pubmed.ncbi.nlm.nih.gov/32665633/) DOI: [10.1038/s41598-020-68509-x](https://doi.org/10.1038/s41598-020-68509-x)]
- 28 **Ali TF**, Tawab MA, ElHariri MA. CT chest of COVID-19 patients: What should a radiologist know? *Egypt J Radiol Nucl Med* 2020; **51**: 120 [DOI: [10.1186/s43055-020-00245-8](https://doi.org/10.1186/s43055-020-00245-8)]
- 29 **Pakdemirli E**, Mandalia U, Monib S. Positive Chest CT Features in Patients With COVID-19 Pneumonia and Negative Real-Time Polymerase Chain Reaction Test. *Cureus* 2020; **12**: e9942 [PMID: [32850265](https://pubmed.ncbi.nlm.nih.gov/32850265/) DOI: [10.7759/cureus.9942](https://doi.org/10.7759/cureus.9942)]
- 30 **Sales AR**, Casagrande EM, Hochegger B, Zanetti G, Marchiori E. The Reversed Halo Sign and COVID-19: Possible Histopathological Mechanisms Related to the Appearance of This Imaging Finding. *Arch Bronconeumol* 2021; **57** Suppl 1: 73-75 [PMID: [32792171](https://pubmed.ncbi.nlm.nih.gov/32792171/) DOI: [10.1016/j.arbres.2020.06.029](https://doi.org/10.1016/j.arbres.2020.06.029)]
- 31 **Ojha V**, Mani A, Pandey NN, Sharma S, Kumar S. CT in coronavirus disease 2019 (COVID-19): a systematic review of chest CT findings in 4410 adult patients. *Eur Radiol* 2020; **30**: 6129-6138 [PMID: [32474632](https://pubmed.ncbi.nlm.nih.gov/32474632/) DOI: [10.1007/s00330-020-06975-7](https://doi.org/10.1007/s00330-020-06975-7)]
- 32 **Kwee TC**, Kwee RM. Chest CT in COVID-19: What the Radiologist Needs to Know. *Radiographics* 2020; **40**: 1848-1865 [PMID: [33095680](https://pubmed.ncbi.nlm.nih.gov/33095680/) DOI: [10.1148/rg.2020200159](https://doi.org/10.1148/rg.2020200159)]
- 33 **Kong W**, Agarwal PP. Chest Imaging Appearance of COVID-19 Infection. *Radiol Cardiothorac Imaging* 2020; **2**: e200028 [PMID: [33778544](https://pubmed.ncbi.nlm.nih.gov/33778544/) DOI: [10.1148/ryct.2020200028](https://doi.org/10.1148/ryct.2020200028)]
- 34 **Meirelles GSP**. COVID-19: a brief update for radiologists. *Radiol Bras* 2020; **53**: 320-328 [PMID: [33071376](https://pubmed.ncbi.nlm.nih.gov/33071376/) DOI: [10.1590/0100-3984.2020.0074](https://doi.org/10.1590/0100-3984.2020.0074)]
- 35 **Zhang Q**, Douglas A, Abideen ZU, Khanal S, Tzarnas S. Novel Coronavirus (2019-nCoV) in Disguise. *Cureus* 2020; **12**: e7521 [PMID: [32377469](https://pubmed.ncbi.nlm.nih.gov/32377469/) DOI: [10.7759/cureus.7521](https://doi.org/10.7759/cureus.7521)]
- 36 **Mughal MS**, Rehman R, Osman R, Kan N, Mirza H, Eng MH. Hilar lymphadenopathy, a novel finding in the setting of coronavirus disease (COVID-19): A case report. *J Med Case Rep* 2020; **14**: 124 [PMID: [32771058](https://pubmed.ncbi.nlm.nih.gov/32771058/) DOI: [10.1186/s13256-020-02452-3](https://doi.org/10.1186/s13256-020-02452-3)]
- 37 **Kovács A**, Palásti P, Veréb D, Bozsik B, Palkó A, Kincses ZT. The sensitivity and specificity of chest CT in the diagnosis of COVID-19. *Eur Radiol* 2021; **31**: 2819-2824 [PMID: [33051732](https://pubmed.ncbi.nlm.nih.gov/33051732/) DOI: [10.1007/s00330-020-07347-x](https://doi.org/10.1007/s00330-020-07347-x)]
- 38 **Souza CA**, Müller NL, Johkoh T, Akira M. Drug-induced eosinophilic pneumonia: high-resolution CT findings in 14 patients. *AJR Am J Roentgenol* 2006; **186**: 368-373 [PMID: [16423940](https://pubmed.ncbi.nlm.nih.gov/16423940/) DOI: [10.2214/AJR.04.1847](https://doi.org/10.2214/AJR.04.1847)]
- 39 **Rossi SE**, Erasmus JJ, McAdams HP, Sporn TA, Goodman PC. Pulmonary drug toxicity: radiologic and pathologic manifestations. *Radiographics* 2000; **20**: 1245-1259 [PMID: [10992015](https://pubmed.ncbi.nlm.nih.gov/10992015/) DOI: [10.1148/radiographics.20.5.g00se081245](https://doi.org/10.1148/radiographics.20.5.g00se081245)]
- 40 **Lin YH**, Hsu HS. Ground glass opacity on chest CT scans from screening to treatment: A literature review. *J Chin Med Assoc* 2020; **83**: 887-890 [PMID: [32675737](https://pubmed.ncbi.nlm.nih.gov/32675737/) DOI: [10.1097/JCMA.000000000000394](https://doi.org/10.1097/JCMA.000000000000394)]
- 41 **Gu J**, Yang L, Li T, Liu Y, Zhang J, Ning K, Su D. Temporal relationship between serial RT-PCR results and serial chest CT imaging, and serial CT changes in coronavirus 2019 (COVID-19) pneumonia: a descriptive study of 155 cases in China. *Eur Radiol* 2021; **31**: 1175-1184 [PMID: [32930834](https://pubmed.ncbi.nlm.nih.gov/32930834/) DOI: [10.1007/s00330-020-07268-9](https://doi.org/10.1007/s00330-020-07268-9)]
- 42 **Pan F**, Ye T, Sun P, Gui S, Liang B, Li L, Zheng D, Wang J, Hesketh RL, Yang L, Zheng C. Time Course of Lung Changes at Chest CT during Recovery from Coronavirus Disease 2019 (COVID-19). *Radiology* 2020; **295**: 715-721 [PMID: [32053470](https://pubmed.ncbi.nlm.nih.gov/32053470/) DOI: [10.1148/radiol.2020200370](https://doi.org/10.1148/radiol.2020200370)]
- 43 **Peng QY**, Wang XT, Zhang LN; Chinese Critical Care Ultrasound Study Group (CCUSG). Findings of lung ultrasonography of novel corona virus pneumonia during the 2019-2020 epidemic. *Intensive Care Med* 2020; **46**: 849-850 [PMID: [32166346](https://pubmed.ncbi.nlm.nih.gov/32166346/) DOI: [10.1007/s00134-020-05996-6](https://doi.org/10.1007/s00134-020-05996-6)]
- 44 **Poggiali E**, Dacrema A, Bastoni D, Tinelli V, Demichele E, Mateo Ramos P, Marciàno T, Silva M, Vercelli A, Magnacavallo A. Can Lung US Help Critical Care Clinicians in the Early Diagnosis of



- Novel Coronavirus (COVID-19) Pneumonia? *Radiology* 2020; **295**: E6 [PMID: [32167853](#) DOI: [10.1148/radiol.202000847](#)]
- 45 **Via G**, Storti E, Gulati G, Neri L, Mojoli F, Braschi A. Lung ultrasound in the ICU: from diagnostic instrument to respiratory monitoring tool. *Minerva Anesthesiol* 2012; **78**: 1282-1296 [PMID: [22858877](#)]
  - 46 **Vetrugno L**, Bove T, Orso D, Barbariol F, Bassi F, Boero E, Ferrari G, Kong R. Our Italian experience using lung ultrasound for identification, grading and serial follow-up of severity of lung involvement for management of patients with COVID-19. *Echocardiography* 2020; **37**: 625-627 [PMID: [32239532](#) DOI: [10.1111/echo.14664](#)]
  - 47 **Testa A**, Soldati G, Copetti R, Giannuzzi R, Portale G, Gentiloni-Silveri N. Early recognition of the 2009 pandemic influenza A (H1N1) pneumonia by chest ultrasound. *Crit Care* 2012; **16**: R30 [PMID: [22340202](#) DOI: [10.1186/cc11201](#)]
  - 48 **Bitar ZI**, Maadarani OS, El-Shably AM, Al-Ajmi MJ. Diagnostic accuracy of chest ultrasound in patients with pneumonia in the intensive care unit: A single-hospital study. *Health Sci Rep* 2019; **2**: e102 [PMID: [30697596](#) DOI: [10.1002/hsr2.102](#)]
  - 49 **Youssef A**, Serra C, Piliu G. Lung ultrasound in the coronavirus disease 2019 pandemic: a practical guide for obstetricians and gynecologists. *Am J Obstet Gynecol* 2020; **223**: 128-131 [PMID: [32437667](#) DOI: [10.1016/j.ajog.2020.05.014](#)]
  - 50 **Moro F**, Buonsenso D, Moruzzi MC, Inchingolo R, Smargiassi A, Demi L, Larici AR, Scambia G, Lanzone A, Testa AC. How to perform lung ultrasound in pregnant women with suspected COVID-19. *Ultrasound Obstet Gynecol* 2020; **55**: 593-598 [PMID: [32207208](#) DOI: [10.1002/uog.22028](#)]
  - 51 **Gargani L**, Sicari R, Raciti M, Serasini L, Passera M, Torino C, Letachowicz K, Ekart R, Fliser D, Covic A, Balafa O, Stavroulopoulos A, Massy ZA, Fiaccadori E, Caiazza A, Bachelet T, Slotki I, Shavit L, Martinez-Castelao A, Coudert-Krier MJ, Rossignol P, Kraemer TD, Hannedouche T, Panichi V, Wiecek A, Pontoriero G, Sarafidis P, Klinger M, Hojs R, Seiler-Mueller S, Lizzi F, Onofriescu M, Zarzoulas F, Tripepi R, Mallamaci F, Tripepi G, Picano E, London GM, Zoccali C. Efficacy of a remote web-based lung ultrasound training for nephrologists and cardiologists: a LUST trial sub-project. *Nephrol Dial Transplant* 2016; **31**: 1982-1988 [PMID: [27672089](#) DOI: [10.1093/ndt/gfw329](#)]
  - 52 **Cardim N**, Dalen H, Voigt JU, Ionescu A, Price S, Neskovic AN, Edvardsen T, Galderisi M, Sicari R, Donal E, Stefanidis A, Delgado V, Zamorano J, Popescu BA. The use of handheld ultrasound devices: a position statement of the European Association of Cardiovascular Imaging (2018 update). *Eur Heart J Cardiovasc Imaging* 2019; **20**: 245-252 [PMID: [30351358](#) DOI: [10.1093/ehjci/jej145](#)]
  - 53 **News BW**. ICN CEO Howard Catton BBC World News interview on COVID-19. In: Who's Who. Bloomsbury Publishing plc, 2018 [DOI: [10.1093/ww/9780199540884.013.u17734](#)]
  - 54 **Buonsenso D**, Piano A, Raffaelli F, Bonadia N, de Gaetano Donati K, Franceschi F. Point-of-Care Lung Ultrasound findings in novel coronavirus disease-19 pneumoniae: a case report and potential applications during COVID-19 outbreak. *Eur Rev Med Pharmacol Sci* 2020; **24**: 2776-2780 [PMID: [32196627](#) DOI: [10.26355/eurrev\\_202003\\_20549](#)]
  - 55 **Lichtenstein DA**, Mezière GA, Lagoueyte JF, Biderman P, Goldstein I, Gepner A. A-lines and B-lines: lung ultrasound as a bedside tool for predicting pulmonary artery occlusion pressure in the critically ill. *Chest* 2009; **136**: 1014-1020 [PMID: [19809049](#) DOI: [10.1378/chest.09-0001](#)]
  - 56 **Volpicelli G**, Lamorte A, Villén T. What's new in lung ultrasound during the COVID-19 pandemic. *Intensive Care Med* 2020; **46**: 1445-1448 [PMID: [32367169](#) DOI: [10.1007/s00134-020-06048-9](#)]
  - 57 **Allinovi M**, Parise A, Giacalone M, Amerio A, Delsante M, Odone A, Franci A, Gigliotti F, Amadasi S, Delmonte D, Parri N, Mangia A. Lung Ultrasound May Support Diagnosis and Monitoring of COVID-19 Pneumonia. *Ultrasound Med Biol* 2020; **46**: 2908-2917 [PMID: [32807570](#) DOI: [10.1016/j.ultrasmedbio.2020.07.018](#)]
  - 58 **Huang Y**, Wang S, Liu Y, Zhang Y, Zheng C, Zheng Y, Zhang C, Min W, Zhou H, Yu M, Hu M. A preliminary study on the ultrasonic manifestations of peripulmonary lesions of non-critical novel coronavirus pneumonia (COVID-19). *SSRN* 2020 [DOI: [10.2139/ssrn.3544750](#)]
  - 59 **Norbedo S**, Blaivas M, Raffaldi I, Caroselli C. Lung Ultrasound Point-of-View in Pediatric and Adult COVID-19 Infection. *J Ultrasound Med* 2021; **40**: 899-908 [PMID: [32894621](#) DOI: [10.1002/jum.15475](#)]
  - 60 **McDermott C**, Daly J, Carley S. Combatting COVID-19: is ultrasound an important piece in the diagnostic puzzle? *Emerg Med J* 2020; **37**: 644-649 [PMID: [32907844](#) DOI: [10.1136/emered-2020-209721](#)]
  - 61 **Zhu F**, Zhao X, Wang T, Wang Z, Guo F, Xue H, Chang P, Liang H, Ni W, Wang Y, Chen L, Jiang B. Ultrasonic Characteristics and Severity Assessment of Lung Ultrasound in COVID-19 Pneumonia in Wuhan, China: A Retrospective, Observational Study. *Engineering* 2020; **7**: 367-375 [DOI: [10.1016/j.eng.2020.09.007](#)]
  - 62 **Soldati G**, Smargiassi A, Inchingolo R, Buonsenso D, Perrone T, Briganti DF, Perlini S, Torri E, Mariani A, Mossolani EE, Tursi F, Mento F, Demi L. Proposal for International Standardization of the Use of Lung Ultrasound for Patients With COVID-19: A Simple, Quantitative, Reproducible Method. *J Ultrasound Med* 2020; **39**: 1413-1419 [PMID: [32227492](#) DOI: [10.1002/jum.15285](#)]
  - 63 **Schmid B**, Feuerstein D, Lang CN, Fink K, Steger R, Rieder M, Duerschmied D, Busch HJ, Damjanovic D. Lung ultrasound in the emergency department - a valuable tool in the management of patients presenting with respiratory symptoms during the SARS-CoV-2 pandemic. *BMC Emerg Med* 2020; **20**: 96 [PMID: [33287732](#) DOI: [10.1186/s12873-020-00389-w](#)]

- 64 **Dargent A**, Chatelain E, Kreitmann L, Quenot JP, Cour M, Argaud L; COVID-LUS study group. Lung ultrasound score to monitor COVID-19 pneumonia progression in patients with ARDS. *PLoS One* 2020; **15**: e0236312 [PMID: 32692769 DOI: 10.1371/journal.pone.0236312]
- 65 **Manivel V**, Lesnewski A, Shamim S, Carbonatto G, Govindan T. CLUE: COVID-19 Lung ultrasound in emergency department. *Emerg Med Australas* 2020; **32**: 694-696 [PMID: 32386264 DOI: 10.1111/1742-6723.13546]
- 66 **Lu X**, Zhang M, Qian A, Tang L, Xu S. Lung ultrasound score in establishing the timing of intubation in COVID-19 interstitial pneumonia: A preliminary retrospective observational study. *PLoS One* 2020; **15**: e0238679 [PMID: 32881950 DOI: 10.1371/journal.pone.0238679]
- 67 **Speidel V**, Conen A, Gisler V, Fux CA, Haubitz S. Lung Assessment with Point-of-Care Ultrasound in Respiratory Coronavirus Disease (COVID-19): A Prospective Cohort Study. *Ultrasound Med Biol* 2021; **47**: 896-901 [PMID: 33487473 DOI: 10.1016/j.ultrasmedbio.2020.12.021]
- 68 **Alfuraih AM**. Point of care lung ultrasound in COVID-19: hype or hope? *BJR Open* 2020; **2**: 20200027 [PMID: 33178984 DOI: 10.1259/bjro.20200027]
- 69 **Prokop M**, van Everdingen W, van Rees Vellinga T, Quarles van Ufford H, Stöger L, Beenen L, Geurts B, Gietema H, Krdzalic J, Schaefer-Prokop C, van Ginneken B, Brink M; COVID-19 Standardized Reporting Working Group of the Dutch Radiological Society. CO-RADS: A Categorical CT Assessment Scheme for Patients Suspected of Having COVID-19-Definition and Evaluation. *Radiology* 2020; **296**: E97-E104 [PMID: 32339082 DOI: 10.1148/radiol.2020201473]
- 70 **Bellini D**, Panvini N, Rengo M, Vicini S, Lichtner M, Tieghi T, Ippoliti D, Giulio F, Orlando E, Iozzino M, Ciolfi MG, Montechiarello S, d'Ambrosio U, d'Adamo E, Gambaretto C, Panno S, Caldon V, Ambrogi C, Carbone I. Diagnostic accuracy and interobserver variability of CO-RADS in patients with suspected coronavirus disease-2019: a multireader validation study. *Eur Radiol* 2021; **31**: 1932-1940 [PMID: 32968883 DOI: 10.1007/s00330-020-07273-y]
- 71 **Ma B**, Gong J, Yang Y, Yao X, Deng X, Chen X. Applicability of MuLBSTA scoring system as diagnostic and prognostic role in early warning of severe COVID-19. *Microb Pathog* 2021; **150**: 104706 [PMID: 33347962 DOI: 10.1016/j.micpath.2020.104706]
- 72 **Ebrahimian S**, Homayounieh F, Rockenbach MABC, Putha P, Raj T, Dayan I, Bizzo BC, Buch V, Wu D, Kim K, Li Q, Digumarthy SR, Kalra MK. Artificial intelligence matches subjective severity assessment of pneumonia for prediction of patient outcome and need for mechanical ventilation: a cohort study. *Sci Rep* 2021; **11**: 858 [PMID: 33441578 DOI: 10.1038/s41598-020-79470-0]
- 73 **Signoroni A**, Savardi M, Benini S, Adami N, Leonardi R, Gibellini P, Vaccher F, Ravanelli M, Borghesi A, Maroldi R, Farina D. BS-Net: Learning COVID-19 pneumonia severity on a large chest X-ray dataset. *Med Image Anal* 2021; **71**: 102046 [PMID: 33862337 DOI: 10.1016/j.media.2021.102046]
- 74 **Maroldi R**, Rondi P, Agazzi GM, Ravanelli M, Borghesi A, Farina D. Which role for chest x-ray score in predicting the outcome in COVID-19 pneumonia? *Eur Radiol* 2021; **31**: 4016-4022 [PMID: 33263159 DOI: 10.1007/s00330-020-07504-2]
- 75 **Zhao YM**, Shang YM, Song WB, Li QQ, Xie H, Xu QF, Jia JL, Li LM, Mao HL, Zhou XM, Luo H, Gao YF, Xu AG. Follow-up study of the pulmonary function and related physiological characteristics of COVID-19 survivors three months after recovery. *EclinicalMedicine* 2020; **25**: 100463 [PMID: 32838236 DOI: 10.1016/j.eclim.2020.100463]
- 76 **Duan YN**, Qin J. Pre- and Posttreatment Chest CT Findings: 2019 Novel Coronavirus (2019-nCoV) Pneumonia. *Radiology* 2020; **295**: 21 [PMID: 32049602 DOI: 10.1148/radiol.2020200323]
- 77 **Shi H**, Han X, Zheng C. Evolution of CT Manifestations in a Patient Recovered from 2019 Novel Coronavirus (2019-nCoV) Pneumonia in Wuhan, China. *Radiology* 2020; **295**: 20 [PMID: 32032497 DOI: 10.1148/radiol.2020200269]
- 78 **Li M**, Lei P, Zeng B, Li Z, Yu P, Fan B, Wang C, Zhou J, Hu S, Liu H. Coronavirus Disease (COVID-19): Spectrum of CT Findings and Temporal Progression of the Disease. *Acad Radiol* 2020; **27**: 603-608 [PMID: 32204987 DOI: 10.1016/j.acra.2020.03.003]
- 79 **Wei J**, Xu H, Xiong J, Shen Q, Fan B, Ye C, Dong W, Hu F. 2019 Novel Coronavirus (COVID-19) Pneumonia: Serial Computed Tomography Findings. *Korean J Radiol* 2020; **21**: 501-504 [PMID: 32100486 DOI: 10.3348/kjr.2020.0112]
- 80 **Pan Y**, Guan H, Zhou S, Wang Y, Li Q, Zhu T, Hu Q, Xia L. Initial CT findings and temporal changes in patients with the novel coronavirus pneumonia (2019-nCoV): a study of 63 patients in Wuhan, China. *Eur Radiol* 2020; **30**: 3306-3309 [PMID: 32055945 DOI: 10.1007/s00330-020-06731-x]
- 81 **Bernheim A**, Mei X, Huang M, Yang Y, Fayad ZA, Zhang N, Diao K, Lin B, Zhu X, Li K, Li S, Shan H, Jacobi A, Chung M. Chest CT Findings in Coronavirus Disease-19 (COVID-19): Relationship to Duration of Infection. *Radiology* 2020; **295**: 200463 [PMID: 32077789 DOI: 10.1148/radiol.2020200463]
- 82 **Wang Y**, Dong C, Hu Y, Li C, Ren Q, Zhang X, Shi H, Zhou M. Temporal Changes of CT Findings in 90 Patients with COVID-19 Pneumonia: A Longitudinal Study. *Radiology* 2020; **296**: E55-E64 [PMID: 32191587 DOI: 10.1148/radiol.2020200843]
- 83 **Xiong Y**, Sun D, Liu Y, Fan Y, Zhao L, Li X, Zhu W. Clinical and High-Resolution CT Features of the COVID-19 Infection: Comparison of the Initial and Follow-up Changes. *Invest Radiol* 2020; **55**: 332-339 [PMID: 32134800 DOI: 10.1097/RLI.0000000000000674]
- 84 **Tan HB**, Xiong F, Jiang YL, Huang WC, Wang Y, Li HH, You T, Fu TT, Lu R, Peng BW. The study of automatic machine learning base on radiomics of non-focus area in the first chest CT of

- different clinical types of COVID-19 pneumonia. *Sci Rep* 2020; **10**: 18926 [PMID: 33144676 DOI: 10.1038/s41598-020-76141-y]
- 85 **Gillies RJ**, Kinahan PE, Hricak H. Radiomics: Images Are More than Pictures, They Are Data. *Radiology* 2016; **278**: 563-577 [PMID: 26579733 DOI: 10.1148/radiol.201511169]
  - 86 **Machine learning in RayStation**. Infervision in the Frontlines Against the Coronavirus 2020. [cited 22 January 2021]. Available from: <https://www.itnonline.com/content/infervision-frontlines-against-coronavirus>
  - 87 **McCall B**. COVID-19 and artificial intelligence: protecting health-care workers and curbing the spread. *Lancet Digit Health* 2020; **2**: e166-e167 [PMID: 32289116 DOI: 10.1016/S2589-7500(20)30054-6]
  - 88 **Jin C**, Chen W, Cao Y, Xu Z, Tan Z, Zhang X, Deng L, Zheng C, Zhou J, Shi H, Feng J. Development and evaluation of an artificial intelligence system for COVID-19 diagnosis. *Nat Commun* 2020; **11**: 5088 [PMID: 33037212 DOI: 10.1038/s41467-020-18685-1]
  - 89 **Harmon SA**, Sanford TH, Xu S, Turkbey EB, Roth H, Xu Z, Yang D, Myronenko A, Anderson V, Amalou A, Blain M, Kassin M, Long D, Varble N, Walker SM, Bagci U, Ierardi AM, Stellato E, Plensich GG, Franceschelli G, Girlando C, Irmici G, Labella D, Hammoud D, Malayeri A, Jones E, Summers RM, Choyke PL, Xu D, Flores M, Tamura K, Obinata H, Mori H, Patella F, Cariati M, Carrafiello G, An P, Wood BJ, Turkbey B. Artificial intelligence for the detection of COVID-19 pneumonia on chest CT using multinational datasets. *Nat Commun* 2020; **11**: 4080 [PMID: 32796848 DOI: 10.1038/s41467-020-17971-2]
  - 90 **Yu Z**, Li X, Sun H, Wang J, Zhao T, Chen H, Ma Y, Zhu S, Xie Z. Rapid identification of COVID-19 severity in CT scans through classification of deep features. *Biomed Eng Online* 2020; **19**: 63 [PMID: 32787937 DOI: 10.1186/s12938-020-00807-x]
  - 91 **Laghi A**. Cautions about radiologic diagnosis of COVID-19 infection driven by artificial intelligence. *Lancet Digit Health* 2020; **2**: e225 [PMID: 32373786 DOI: 10.1016/S2589-7500(20)30079-0]
  - 92 **Bai HX**, Hsieh B, Xiong Z, Halsey K, Choi JW, Tran TML, Pan I, Shi LB, Wang DC, Mei J, Jiang XL, Zeng QH, Eglin TK, Hu PF, Agarwal S, Xie FF, Li S, Healey T, Atalay MK, Liao WH. Performance of Radiologists in Differentiating COVID-19 from Non-COVID-19 Viral Pneumonia at Chest CT. *Radiology* 2020; **296**: E46-E54 [PMID: 32155105 DOI: 10.1148/radiol.20200823]
  - 93 **Shi J**, Giess CS, Martin T, Lemaire KA, Curley PJ, Bay C, Mayo-Smith WW, Boland GW, Khorasani R. Radiology Workload Changes During the COVID-19 Pandemic: Implications for Staff Redeployment. *Acad Radiol* 2021; **28**: 1-7 [PMID: 33036897 DOI: 10.1016/j.acra.2020.09.008]
  - 94 **American College of Radiology**. ACR COVID-19 Clinical Resources for Radiologists. 2020 [cited 22 January 2021]. Available from: <https://www.acr.org/clinical-resources/COVID-19-Radiology-Resources>
  - 95 **Naidich JJ**, Boltyenkov A, Wang JJ, Chusid J, Hughes D, Sanelli PC. Impact of the Coronavirus Disease 2019 (COVID-19) Pandemic on Imaging Case Volumes. *J Am Coll Radiol* 2020; **17**: 865-872 [PMID: 32425710 DOI: 10.1016/j.jacr.2020.05.004]
  - 96 **Wang D**, Hu B, Hu C, Zhu F, Liu X, Zhang J, Wang B, Xiang H, Cheng Z, Xiong Y, Zhao Y, Li Y, Wang X, Peng Z. Clinical Characteristics of 138 Hospitalized Patients With 2019 Novel Coronavirus-Infected Pneumonia in Wuhan, China. *JAMA* 2020; **323**: 1061-1069 [PMID: 32031570 DOI: 10.1001/jama.2020.1585]
  - 97 **Mao L**, Jin H, Wang M, Hu Y, Chen S, He Q, Chang J, Hong C, Zhou Y, Wang D, Miao X, Li Y, Hu B. Neurologic Manifestations of Hospitalized Patients With Coronavirus Disease 2019 in Wuhan, China. *JAMA Neurol* 2020; **77**: 683-690 [PMID: 32275288 DOI: 10.1001/jamaneurol.2020.1127]
  - 98 **Ronco C**, Reis T. Kidney involvement in COVID-19 and rationale for extracorporeal therapies. *Nat Rev Nephrol* 2020; **16**: 308-310 [PMID: 32273593 DOI: 10.1038/s41581-020-0284-7]
  - 99 **Tang N**, Li D, Wang X, Sun Z. Abnormal coagulation parameters are associated with poor prognosis in patients with novel coronavirus pneumonia. *J Thromb Haemost* 2020; **18**: 844-847 [PMID: 32073213 DOI: 10.1111/jth.14768]
  - 100 **American College of Radiology**. ACR Recommendations for the use of Chest Radiography and Computed Tomography (CT) for Suspected COVID-19 Infection. 2020 [cited 22 January 2021]. Available from: <https://www.acr.org/Advocacy-and-Economics/ACR-Position-Statements/Recommendations-for-Chest-Radiography-and-CT-for-Suspected-COVID19-Infection>
  - 101 **Zu ZY**, Jiang MD, Xu PP, Chen W, Ni QQ, Lu GM, Zhang LJ. Coronavirus Disease 2019 (COVID-19): A Perspective from China. *Radiology* 2020; **296**: E15-E25 [PMID: 32083985 DOI: 10.1148/radiol.20200490]
  - 102 **Panayiotou A**, Rafailidis V, Puttick T, Satchithananda K, Gray A, Sidhu PS. Escalation and de-escalation of the radiology response to COVID-19 in a tertiary hospital in South London: The King's College Hospital experience. *Br J Radiol* 2020; **93**: 20201034 [PMID: 33112652 DOI: 10.1259/bjr.20201034]
  - 103 **Jeffrey S**. Klein M, Bien Soo Tan, MBBS, Lionel Tim-Ee Cheng, MBBS, Marta Heilbrun, MD, Dushyant Sahani, MD. RSNA Hosts Second Webinar on Radiology Surge and Second Surge Preparedness. [cited 22 January 2021]. Available from: <https://www.rsna.org/en/news/2020/June/COVID-19-Surge-Preparedness-Part-Two>
  - 104 **Quah LJJ**, Tan BKK, Fua TP, Wee CPJ, Lim CS, Nadarajan G, Zakaria ND, Chan SJ, Wan PW, Teo LT, Chua YY, Wong E, Venkataraman A. Reorganising the emergency department to manage

the COVID-19 outbreak. *Int J Emerg Med* 2020; **13**: 32 [PMID: [32552659](#) DOI: [10.1186/s12245-020-00294-w](#)]

- 105 **Cheng LT**, Chan LP, Tan BH, Chen RC, Tay KH, Ling ML, Tan BS. Déjà Vu or Jamais Vu? *AJR Am J Roentgenol* 2020; **214**: 1206-1210 [PMID: [32130047](#) DOI: [10.2214/AJR.20.22927](#)]
- 106 **Tridandapani S**, Holl G, Canon CL. Rapid Deployment of Home PACS Workstations to Enable Social Distancing in the Coronavirus Disease (COVID-19) Era. *AJR Am J Roentgenol* 2020; **215**: 1351-1353 [PMID: [32432912](#) DOI: [10.2214/AJR.20.23495](#)]



## Role of cardiac magnetic resonance imaging in the diagnosis and management of COVID-19 related myocarditis: Clinical and imaging considerations

Lavannya Atri, Michael Morgan, Sean Harrell, Wael AlJaroudi, Adam E Berman

**ORCID number:** Lavannya Atri 0000-0002-0601-5575; Michael Morgan 0000-0002-4780-5944; Sean Harrell 0000-0002-1381-3049; Wael AlJaroudi 0000-0003-0890-4437; Adam E Berman 0000-0002-9023-1130.

**Author contributions:** Atri L and Morgan M wrote the paper; Harrell S, AlJaroudi W, Berman AE made critical revisions and added content to the manuscript; Berman AE conceived the topic and provided oversight of the writing, editing and submission process.

**Conflict-of-interest statement:** Authors declare no conflict of interest for this article. This manuscript is not under review elsewhere and there is no prior publication of manuscript contents. The views expressed in this article are solely those of the authors.

**Open-Access:** This article is an open-access article that was selected by an in-house editor and fully peer-reviewed by external reviewers. It is distributed in accordance with the Creative Commons Attribution NonCommercial (CC BY-NC 4.0) license, which permits others to distribute, remix, adapt, build upon this work non-commercially, and license their derivative works

**Lavannya Atri, Michael Morgan, Sean Harrell, Wael AlJaroudi, Adam E Berman**, Division of Cardiology, Medical College of Georgia, Augusta University, Augusta, GA 30912, United States

**Adam E Berman**, Division of Health Policy, Medical College of Georgia, Augusta University, Augusta, GA 30912, United States

**Adam E Berman**, Division of Health Economics and Modeling, Medical College of Georgia, Augusta University, Augusta, GA 30912, United States

**Corresponding author:** Lavannya Atri, MS, Division of Cardiology, Medical College of Georgia, Augusta University, 1120 15<sup>th</sup> Street, Augusta, GA 30912, United States. [latri@augusta.edu](mailto:latri@augusta.edu)

### Abstract

There is a growing evidence of cardiovascular complications in coronavirus disease 2019 (COVID-19) patients. As evidence accumulated of COVID-19 mediated inflammatory effects on the myocardium, substantial attention has been directed towards cardiovascular imaging modalities that facilitate this diagnosis. Cardiac magnetic resonance imaging (CMRI) is the gold standard for the detection of structural and functional myocardial alterations and its role in identifying patients with COVID-19 mediated cardiac injury is growing. Despite its utility in the diagnosis of myocardial injury in this population, CMRI's impact on patient management is still evolving. This review provides a framework for the use of CMRI in diagnosis and management of COVID-19 patients from the perspective of a cardiologist. We review the role of CMRI in the management of both the acutely and remotely COVID-19 infected patient. We discuss patient selection for this imaging modality; T1, T2, and late gadolinium enhancement imaging techniques; and previously described CMRI findings in other cardiomyopathies with potential implications in COVID-19 recovered patients.

**Key Words:** Cardiac magnetic resonance imaging; COVID-19; Cardiovascular magnetic resonance; Myocarditis; Coronavirus; Cardiovascular complications

©The Author(s) 2021. Published by Baishideng Publishing Group Inc. All rights reserved.

on different terms, provided the original work is properly cited and the use is non-commercial. See: <http://creativecommons.org/licenses/by-nc/4.0/>

**Manuscript source:** Invited manuscript

**Specialty type:** Cardiac and cardiovascular systems

**Country/Territory of origin:** United States

**Peer-review report's scientific quality classification**

Grade A (Excellent): A  
Grade B (Very good): 0  
Grade C (Good): C  
Grade D (Fair): 0  
Grade E (Poor): 0

**Received:** February 28, 2021

**Peer-review started:** February 28, 2021

**First decision:** May 6, 2021

**Revised:** May 27, 2021

**Accepted:** August 30, 2021

**Article in press:** August 30, 2021

**Published online:** September 28, 2021

**P-Reviewer:** Gaisenok O, Kelle S

**S-Editor:** Wang JL

**L-Editor:** A

**P-Editor:** Liu JH



**Core Tip:** Cardiovascular magnetic resonance imaging (CMRI) is a powerful imaging modality used in defining cardiac tissue characterization. As the prevalence and incidence of coronavirus disease 2019 (COVID-19) continues to rise, the utility of CMRI in defining COVID-19 related myocardial damage is growing. This review discusses the impact of CMRI in diagnosing myocardial involvement in acutely ill and recovered COVID-19 patients as well as its implications for patient management.

**Citation:** Atri L, Morgan M, Harrell S, AlJaroudi W, Berman AE. Role of cardiac magnetic resonance imaging in the diagnosis and management of COVID-19 related myocarditis: Clinical and imaging considerations. *World J Radiol* 2021; 13(9): 283-293

**URL:** <https://www.wjgnet.com/1949-8470/full/v13/i9/283.htm>

**DOI:** <https://dx.doi.org/10.4329/wjr.v13.i9.283>

## INTRODUCTION

Severe acute respiratory syndrome coronavirus 2 (SARS-CoV-2), the novel coronavirus responsible for the coronavirus disease 2019 (COVID-19) pandemic, continues to spread across the United States (US) and globally. As of January 21, 2021, the US reported over 23 million confirmed cases of COVID-19 as well as over 400000 COVID-19 related mortalities[1]. It has been previously reported that COVID-19 patients often have complications involving acute myocardial injury. These injuries are the most frequently reported cardiovascular abnormality in COVID-19, and occur in approximately 8%-12% of all patients[2]. Other cardiovascular effects of COVID-19 include endothelial damage, systolic heart failure, and arrhythmias[3]. Proposed mechanisms for cardiac injury include those mediated by systemic inflammation, direct viral attack on cardiomyocytes, myocardial interstitial fibrosis, overactive cytokine and interferon immune response, coronary plaque destabilization, and hypoxia[4,5].

Myocarditis is an increasingly recognized complication of COVID-19[6]. While endomyocardial biopsy remains the gold standard for tissue diagnosis, this procedure is invasive, characterized by potential serious complications and may be impractical in certain patient populations. Non-invasive imaging modalities, however, provide a safe alternative to aid in the diagnosis and management of myocarditis. While echocardiography possesses distinct advantages including low cost, accessibility, and faster interpretation times that may be beneficial in resource-scarce settings, many patients with early or mild myocarditis may have a normal echocardiogram[7]. Computed tomography (CT) modalities lack high quality myocardial tissue characterization that is essential for the diagnosis of myocarditis while exposing patients to significant amounts of radiation and contrast materials. Nuclear imaging is another potential modality to aid in the diagnosis of myocarditis, but lacks the spatial resolution to distinguish mid or epicardial myocardial perfusion defects (myocarditis) from subendocardial perfusion defects (ischemic) with significant partial volume effect and hence limited diagnostic accuracy[7].

Cardiovascular magnetic resonance imaging (CMRI) techniques remain the preferred modality for assessing patients with suspected myocarditis. CMRI provides detailed anatomical visualization, tissue-level analysis, safety, quantitative accuracy, and inter-observer consistency[7,8]. CMRI techniques are not without their limitations. These include higher cost when compared to echocardiography, longer exam times, and reliance on imaging interpretation by readers specifically trained in this discipline. Despite these limitations, CMRI remains the preferred imaging modality in the assessment of COVID-19 patients suspected of myocarditis and has the potential of playing a pivotal role in early diagnosis COVID-19-related cardiac injury. Finally, CMRI has the unique ability to evaluate subclinical and chronic cardiac involvement following COVID-19 infection.

## CMRI AND CARDIAC TISSUE CHARACTERIZATION

CMRI represents the gold standard for the noninvasive cardiac tissue characterization, detection of acute and chronic myocardial changes, and myocardial viability[9-12].

This volumetric and functional assessment utility has expanded its indications for not only diagnostic purposes, but also treatment guidance and patient follow-up as is currently being investigated in those patients with COVID-19 related acute myocarditis[13]. CMRI is also currently used to risk stratify patients with ischemic heart disease and myocarditis, assess precise ejection fraction, quantify scar tissue, and predict location of re-entrant circuits within the scar to guide catheter ablation[14]. The future of CMRI continues to grow with the incorporation of artificial intelligence, post-processing techniques and development of new MR sequences such as T1 and T2 mapping[13].

### **T1 mapping**

Non-ischemic cardiomyopathies may present with acute edema and diffuse tissue fibrosis that is captured well using T1 mapping[15]. T1 mapping techniques may identify the heterogeneity of damaged cardiac tissue without the use of contrast. The native T1 values increase in areas of edema and fibrosis as seen in acute myocarditis (including the acute phase of COVID-19) and the T1 values decrease in areas of lipid overload as seen in Anderson-Fabry diseases[13,16]. These elevated T1 values can also be seen early amyloid deposition, aortic stenosis, and dilated cardiomyopathy[13].

### **T2 mapping**

T2 mapping technique is similar to T1 imaging as it also identifies areas of inflammation and edema. Being highly sensitive to the water content of myocardial tissue, T2 can reliably identify patients with inflammatory cardiomyopathies and is indicated to detect inflammation associated with viral myocardial damage, myocardial infarction, sarcoidosis, toxicity from chemotherapeutic drugs, transplant rejection as well as detection of iron overload[13,16,17].

### **Late gadolinium enhancement**

Late gadolinium enhancement (LGE) imaging techniques involves the use of gadolinium as a contrast agent to identify heterogeneity within myocardial tissue. LGE imaging represents a cornerstone of CMRI as it is used to define chronic myocardial fibrosis and necrosis caused by ischemia as well as myocardial fibrosis frequently present in non-ischemic dilated cardiomyopathy. Damaged cardiac tissue has a slower gadolinium washout time than healthy tissue, which allows for not only identification of myocardial scarring, but also its quantification[11,12,18]. LGE images of COVID-19 patients suspected of myocardial involvement revealed enhancement at the left ventricular base, suggestive of myocarditis (Figure 1).

Renal function should be assessed prior to the use of LGE as its use is relatively contraindicated for patients with significant renal impairment, although new generation Gadolinium agents seem to be safer to use[14,16,19]. Current guidelines proposed by the European Society of Cardiology, American Heart Association (AHA) and American College of Cardiology indicate the use of CMRI for diagnosis and management of coronary artery disease and cardiomyopathies, with a class I recommendation for suspected infiltrative causes[13,14,20].

Although data regarding CMRI characteristics of COVID-19 myocarditis is limited to case reports and series, a small study did compare 8 patients with COVID-19 myocarditis to 8 patients with non-COVID-19 myocarditis and 12 healthy patients[21]. Patients with suspected acute COVID-19 myocarditis (with elevated troponin and CRP) were found to have a pattern of diffuse myocardial edema detected as diffuse globally higher T1 and T2 myocardial relaxation times. Comparatively, the patients with non-COVID-19 myocarditis had a more focal disease with prolonged T1 and T2 relaxation times and more visible myocardial edema and LGE lesions. It was also noted that skeletal muscle T1 was elevated in COVID-19 myocarditis patients, which impacted the T2 ratio to not be elevated significantly. Severe wall-motion abnormalities due to stress-induced cardiomyopathy and small pericardial effusions were also detected as CMRI enhancements in the COVID-19 myocarditis group[21].

---

## **ROLE OF CMRI IN PATIENTS INFECTED WITH COVID-19**

---

### **A review of the literature**

An increased prevalence of myocardial injury has been reported in patients affected by COVID-19. As described above, these findings may range from evidence of acute myocarditis to fibrosis remote from time of infection. Given these considerations,



**Figure 1** Delayed cardiac magnetic resonance image obtained after Gd administration showing patchy late Gd enhancement in the mid-myocardium of the basal inferolateral and mid anteroseptal walls consistent with prior myocarditis in patient who recovered from coronavirus disease 2019.

CMRI has played an important role (Table 1) in non-invasive cardiac evaluations in COVID-19 populations[16]. Despite this growing understanding of COVID-19 myocardial involvement, cases of COVID-19 myocarditis are likely underreported due to lack of imaging to reduce viral spread[22]. As a result, data at the population level regarding COVID-19 myocarditis is currently lacking. One recent study from Annie *et al*[23] showed the prevalence of COVID-19 myocarditis across a large multi-national registry to be 0.01% (256 patients). Despite this small prevalence, these patients were associated with increased mortality, underscoring the importance of diagnosing patients with myocarditis[23]. Due to the limitation of available large-scale data, however, our literature review is primarily centered around case-control studies. Kariyanna *et al*[24] performed a systematic review of myocarditis in COVID-19. Global case reports and retrospective studies were included in an effort to better describe trends exhibited by COVID-19 patients suspected of having myocarditis. It was determined that absence of troponin elevation was insufficient to exclude myocarditis. The most consistent findings in patients with suspected myocarditis were bilateral ground glass opacities detected on chest CT and late gadolinium enhancement from CMRI, both of which findings were observed in all patients in the study. Myocardial edema was reported in more than half of these patients, and it appears as though tissue characterization through the use of LGE and T1/T2 mapping is more useful at detecting myocardial damage than assessing ventricular function[25,26].

Understanding the complications that follow COVID-19 infection is an evolving area of research. Currently, there are several studies reporting CMRI findings in convalescent COVID-19 patients. In the largest prospective CMRI study performed to date examining 100 recovered COVID-19 positive patients, Puntmann *et al*[25] found that 78% of the patients had abnormal CMRI findings. These findings suggested ongoing cardiac inflammation independent of the severity of initial COVID-19 clinical presentation. Of the 78 patients diagnosed with COVID-19 related myocardial involvement, raised T1 was found in 73, raised T2 in 60, and abnormal LGE findings in 32. The elevated T1 Levels indicated diffuse myocardial fibrosis, while the elevated T2 Levels represented edema. The patients with both T1 and T2 elevated relaxation times reflected active myocardial edema that may have resulted from virus-mediated acute cardiac injury or dysregulation of an innate inflammatory immune response, whereas the patients with increased T1 but normal T2 Levels were felt to demonstrate healed residual diffuse myocardial injury[25,27]. These values were confirmed with the use of histological findings in severe cases. Furthermore, the abnormal pericardial LGE reflected cardiac tissue injury due to myocardial inflammation that was further supported by the pericardial effusion and active pericarditis[25]. It was also found that left and right ventricular ejection fraction represents a suboptimal marker of early disease detection and outcomes prediction as compared to direct tissue characterization by CMRI.



**Table 1 Summary of existing data surrounding the use of cardiac magnetic resonance imaging use in coronavirus disease 2019 patients**

Ref.	Study design	Sample size	CMRI findings	Other diagnostic findings
Kariyanna <i>et al</i> [24], 2020	Systematic review of 9 case reports and 2 retrospective studies	11 COVID-19 patients with reported myocardial inflammation or myocarditis	LGE highlighted in 100% of the patients	Elevated cardiac markers (Troponin, CK-MB, BNP) in 9 cases. Bilateral ground glass opacities seen in all patients with CT (6 cases). ECG abnormalities (ST-elevation and T-wave inversion) in 7 cases, and decreased LVEF in 6 cases. Active inflammation reported in the all biopsies performed (2 cases) and cardiomegaly reported in 7 cases
Puntmann <i>et al</i> [25], 2020	Prospective observational cohort study	100 recovered COVID-19 patients	Raised T1 in 73% of patients, raised T2 in 60%, LGE findings in 32%, and pericardial enhancement in 22%	Elevated troponin in 71% of patients, and significantly elevated Troponin in 5%. Endomyocardial biopsy revealed active lymphocytic inflammation. Lower LVEF and RVEF noted
Huang <i>et al</i> [26], 2020	Retrospective study	26 recovered COVID-19 patients who reported cardiac symptoms and underwent CMRI	Elevated T2 and/or LGE in 58% (15 patients) with 14 patients having myocardial edema and 8 LGE +. Global T1, T2, and extracellular volume were elevated in patients with abnormal CMRIs	Decreased RVEF, cardiac index, and stroke volume found in patients with positive CMRI findings
Clark <i>et al</i> [27], 2020	Retrospective cohort analysis	22 collegiate athletes with prior COVID-19 infection	LGE found in 9% (2 athletes)	All patients had normal Troponin, normal ECG, normal LVEF. LV mass was higher and RVEF was lower in athletes compared to control group
Li <i>et al</i> [28], 2021	Prospective observational cohort study	40 COVID-19 patients with moderate to severe pneumonia and no cardiovascular medical history	LGE findings in 3% (1 patient), elevated extracellular volume values in 60% (24 patients)	Normal LV and RV size and function. 70% (24 patients) had lower LV 2D-global longitudinal strain with subclinical changes of myocardial dysfunction

CMRI: Cardiac magnetic resonance imaging; COVID-19: Coronavirus disease 2019; LGE: Late gadolinium enhancement; CK-MB: Creatine kinase-MB; BNP: B-type natriuretic peptide; CT: Computed tomography; ECG: Electrocardiogram; LVEF: Left ventricular ejection fraction; RVEF: Right ventricular ejection fraction LV: Left ventricular; RV: Right ventricular.

This study highlights the considerable potential for cardiac involvement even in COVID-19 patients who had a milder presentation or those without cardiovascular comorbidities. The persistence of myocardial damage beyond the acute phase of infection was illustrated, but the extent of this potentially chronic injury is yet to be determined and requires further investigation.

Huang *et al*[26] reported a single-center retrospective study from China and found that out of 26 patients who reported cardiac symptoms during COVID-19 recovery, 15 of them had evidence of myocardial abnormalities on CMRI evaluation. Major findings included myocardial edema, fibrosis, and right ventricular impairment through the use of T1, T2, and LGE imaging. Of note, all patients had no previous history of myocardial injury. This, taken with the fact that the median length of time between symptom onset and CMRI scan was 50 days, suggests persistent COVID-19 cardiac involvement in a majority of this patient cohort. Further follow-up of patients with CMR abnormalities is necessary to confirm long-lasting myocardial involvement following resolution of COVID-19 infection.

While the detection of abnormal CMRI findings in patients with presenting true cardiac symptoms may seem intuitive, the necessity of excluding cardiac involvement in asymptomatic or minimally symptomatic represents an evolving concept amongst the global cardiovascular community. Subclinical myocardial involvement remains a common finding among COVID-19 patients who had a CMRI performed[25,28]. Indeed, Li *et al*[28] identified 28 out of 40 COVID-19 patients with myocardial dysfunction based upon reduced left ventricular 2D-global longitudinal strain when compared to healthy controls. In addition, 24 of the 40 patients showed elevated extracellular volume fraction compared to healthy controls indicating diffuse interstitial fibrosis in a majority of these patients. Interestingly, only one patient in this study demonstrated the presence of LGE. This reduced percentage of patients with LGE compared to findings from other studies could be a result of differing inclusion and exclusion criteria. Regardless, these findings indicate the appreciable prevalence of subclinical cardiac abnormalities recognized by CMRI months after COVID-19 recovery.

Owing to concern for the potential development of ventricular arrhythmias and sudden cardiac death (SCD) secondary to myocarditis in general, and expected similarly with COVID-19 myocarditis specifically, it is important to assess the extent of myocardial damage[29-32]. The first sign of underlying cardiac disease is oftentimes SCD in patients with ventricular arrhythmias[31]. This is especially true of patient populations that are at increased risk for arrhythmia development such as competitive athletes[30,32]. In light of the still unknown prevalence of COVID-19 related chronic cardiovascular sequelae, the question may be raised as to when a clinician should screen patients using CMRI. Phelan *et al*[30] provide recommendations on how to manage high risk recovering COVID-19 athletes. Initial restriction from play for 3 to 6 mo is recommended to allow for resolution of active inflammation[30]. Athletics can be resumed upon normalization of left ventricular function and cardiac biomarkers and absence of arrhythmias[30].

CMRI can reproducibly and accurately localize tissue injury, and thus has the ability to play an important role in fatal arrhythmia risk stratification along with prediction of reentrant circuits to guide ablation procedures[14]. LGE in particular has been shown to be the best predictor of all-cause mortality in biopsy-proven viral myocarditis, emphasizing the utility of CMR in COVID-19 patients[31,33].

While myocarditis appears to be the main form of cardiac involvement in COVID-19 patients, other forms of myocardial injury have also been observed to a smaller extent. These include but are not limited to myocardial infarction, pulmonary embolism, and Takotsubo cardiomyopathy[34-37]. These cardiovascular conditions may present similarly with chest pain, dyspnea, and positive troponin; however, they may be distinguished with CMRI[38], which further emphasizes the utility of CMRI in COVID-19 patients with signs of cardiac involvement.

---

## MANAGEMENT RECOMMENDATIONS/GUIDELINES

---

Although the role of CMRI in the diagnosis of COVID-19 related cardiac injury is accepted, its practical utilization in both the inpatient and outpatient venues faces challenges in this continuously expanding patient population. In an effort to address these concerns, the Society of Cardiovascular Magnetic Resonance (SCMR) created specific guidelines treating the use of CMRI in COVID-19 patients[39,40]. These treatment guidelines cover a variety of imaging settings, including the acutely ill patient suspected of having acute COVID-19 related myocardial injury. In these instances, the SCMR recommends a short imaging protocol of 10-15 minutes for patients with active COVID-19 infection and a poor functional status[16]. CMRI can be performed on ventilated patients through special guidelines but is highly discouraged unless absolutely clinically necessary[39]. A holistic approach is recommended with the safety of patients and healthcare workers in mind and the use of clinical judgement to suspect acute myocardial injury[39]. If used in an inpatient setting, a dedicated CMRI scanner should be established when possible to limit the spread of COVID-19 [16]. In most circumstances, CMRI should be postponed until after resolution of the patient's contagious state and performed in an outpatient setting[27,39]. Once completed, further cardiovascular recommendations may be made based upon imaging findings. Given the breadth of patients affected by COVID-19, it is possible to detect preexisting and undiagnosed cardiac abnormalities and/or true COVID-19 related injury. Consequently, cardiovascular specialists must adopt a tailored approach to the treatment of these patients in light of their clinical circumstances. For example, patients with cardiomyopathy detected on CMRI may be candidates for consultation by a dedicated congestive heart failure treatment team[41].

---

## APPROACHES TO THE ROLE OF CMRI IN THE COVID-19 ERA

---

Due to the novelty of the COVID-19 pandemic, there is a lack of consensus on how to manage the long-term cardiac effects of COVID-19. The high prevalence and disease burden of the COVID-19 pandemic and the constraints it's placed on healthcare resources make the determination of CMRI guidelines a difficult healthcare decision with ethical dimensions. Our center recommends using a risk stratification method to determine if a CMRI is needed for each individual patient (Table 2). High risk individuals include patients who have an abnormal echocardiogram, abnormal electrocardiogram (EKG), positive troponin levels, or history of myocarditis, myocardial infarction, or non-obstructive coronary artery disease. These patients should

**Table 2 Proposed indications for cardiac magnetic resonance imaging in coronavirus disease 2019 patients**

CMRI is indicated	CMRI not indicated
High risk patients with 2 or more of the following criteria	Low risk patients with all of the following criteria
Symptomatic	Asymptomatic
Elevated troponin	Negative troponin
Abnormal echocardiogram	Normal echocardiogram
Abnormal EKG	
High risk for ventricular arrhythmia or sudden death	
Myocardial infarction	
Clinical suspicion for myocardial injury	

CMRI: Cardiac magnetic resonance imaging; EKG: Echocardiogram.

receive a CMRI if available.

While suspicion of myocarditis can be determined based on biomarkers, EKG, and echocardiography, these tests may not be sufficient to determine the true etiology of cardiac involvement. EKG manifestations of myocarditis vary considerably and most commonly involve sinus tachycardia and nonspecific T wave and ST segment changes [42]. Echocardiography may demonstrate increased wall thickness and hyperechogenicity but more often than not provide inconclusive findings[43]. These tests provide little use in differentiating myocarditis from similarly presenting processes such as myocardial infarction or pulmonary embolus. If the aforementioned workup does not point towards a definitive diagnosis of myocarditis, CMRI may be indicated to provide direct tissue characterization, assess cardiac function indirectly based on the degree of inflammation present, and produce the confidence necessary to establish the diagnosis of myocarditis[42,44,45]. In addition, contrast-enhanced MRI may be a useful, noninvasive tool for long-term follow-up of patients with acute myocarditis and provide more accurate data on predicting outcome. A small study of 16 patients with myocarditis found that contrast enhancement ratio at 4 wk after disease onset was predictive of long-term outcomes[12].

Patients who are asymptomatic or have negative labs or normal echocardiogram findings are low priority for receiving CMRI. While post-COVID-19 asymptomatic myocardial involvement has been documented in the literature as mentioned above, this group of individuals with no symptoms should forgo CMRI at this time unless symptoms arise due to constraints on healthcare resources amidst the pandemic.

There is, however, a large gray area between these patient extremes. Athletes, for example, are a unique patient population as they are at higher risk of sudden cardiac death if they resume vigorous exercise with signs of myocarditis[32]. While there is disagreement in the approach of these patients, we believe clinicians should defer to the 2015 AHA Return to Play guidelines[32]. If there are any abnormalities on imaging, athletes should sit out from play with repeat imaging likely warranted in three to six months[32]. Reintroduction to play can take place gradually if biomarkers and EKG findings normalize and imaging shows no active inflammation[32]. At this time, it is unclear if resolution of myocarditis-related LGE is necessary for athletes to resume competition, so physicians should continue to use clinical judgment in their assessment of these patients. The Big Ten Athletics organization has taken the lead on evaluating their collegiate athletes following COVID-19 infection by creating a Big Ten Cardiac Registry[46]. Every student-athlete who tests positive undergoes cardiac testing involving EKG, biomarkers, echocardiogram, and CMRI to thoroughly evaluate cardiac structure and function[46]. This cautious approach is ideal but may not be practical for resource-scarce areas across the country, highlighting the importance of center-specific guidelines. It should be emphasized that determining appropriate imaging guidelines is an ongoing process that should utilize new findings as they are brought forward.

While athletes make up a unique subset of patients, the general public also stands to benefit from CMR imaging as indicated in Table 2.

## LIMITATIONS OF THE USE CMRI IN PATIENTS WITH COVID-19

There are significant practical limitations regarding the use of CMRI in COVID-19 patients. In addition to limited availability at the global scale, CMRI represents a more expensive and time-consuming imaging modality when compared to conventional alternatives such as echocardiography. Additionally, consistent interpretation of CMRI images is vital to the widespread applicability of CMRI prognostic data[30]. This may be difficult to achieve considering many medical providers do not have access to the imaging modality itself or to cardiac imaging specialists who can accurately interpret the acquired images[47]. The lack of easy access to CMRI imaging creates the potential for selection bias in studies reporting CMRI results. These limitations must be taken into consideration during the creation of imaging guidelines of COVID-19 patients worldwide. Actively contagious COVID-19 patients with suspected cardiac involvement pose a unique challenge to clinicians. In order to reduce COVID-19 spread, CMR imaging may not be appropriate in COVID-19 patients who are actively contagious, thus placing a limitation on CMRI use in the early stage of COVID-19 infection[16]. Finally, it should also be noted that the CMRI studies conducted on COVID-19 patients discussed above all lack a pre-infection CMRI for comparison. Therefore, although unlikely, it is feasible that some included patients may have had preexisting changes detectable by CMRI following an unrelated COVID-19 infection. The lack of internal control limits the applicability of these research findings; nevertheless, the reported prevalence of myocardial abnormalities detected in these studies appears higher than that encountered both in clinical practice and the literature and thus deserves consideration.

## FUTURE DIRECTION

The COVID-19 pandemic has created an unprecedented quest to obtain and synthesize data in a brief amount of time. A major topic, and one that is of particular concern, is the cardiovascular effects seen both acutely and in the chronic setting. Myocardial injury secondary to COVID-19 and the use of CMRI is an evolving subject. A systematic review of the literature, while limited, yields important insights into the use of CMRI.

In regards to active COVID-19 infection with concern for acute myocardial injury, CMRI has a more limited role. CMRI should be used in the acute setting when the findings will alter management and treatment strategies. Additionally, CMRI is able to aid in the diagnosis of myocardial infarction, RV strain in pulmonary embolism, and Takatsubo cardiomyopathy[34]. Given the infectious nature of the coronavirus, the risk of exposure and transmission of COVID-19 to healthcare workers should be kept in mind. CMRI should be performed cautiously or postponed unless they alter the treatment and management of patients in a time-critical manner.

Although CMRI usage will be constricted the general population vastly due to cost and availability limitations, we suspect a major use of CMRI moving forward will be in athletes who have recovered from COVID-19. This is due to the increased risk of adverse events including sudden cardiac death for this specific population. As demonstrated by Phelan *et al*[30], CMRI is recommended in athletes if clinical concern is elevated, despite normal or unremarkable biomarkers and/or Echocardiogram and EKG. Additionally, Rink *et al*[46] has created an athlete registry and will be performing CMRI on every student athlete that has recovered from COVID-19. As high school, collegiate, and professional sports begin their seasons, much consideration and caution will be present in those athletes who have recovered from COVID-19. Given what we know about evidence of LGE and associated ventricular events, indications for withholding athletes from competitive sport may certainly arise.

## CONCLUSION

As a relatively new imaging modality with ongoing research, guidelines regarding CMRI use continue to evolve as new techniques and advances emerge. The role of CMRI in the diagnosis of COVID-19 related illness is evolving as well. Small studies have demonstrated the presence of cardiac injury even in minimally or asymptomatic COVID-19 patients. While the long-term sequelae of COVID-19 mediated cardiac disease is unknown, the diagnostic yield of CMRI places it squarely in the forefront of imaging strategies for this growing patient population. While factors such as



availability and cost may limit the widespread adoption of CMRI, its use in selected populations such as competitive athletes remain important. Further studies examining the prognostic utility of CMRI findings in the recovered COVID-19 population appears warranted.

## REFERENCES

- 1 **Center for Disease Control and Prevention.** CDC COVID Data Tracker, 2021. Available from: [https://covid.cdc.gov/covid-data-tracker/#cases\\_casesper100klast7days](https://covid.cdc.gov/covid-data-tracker/#cases_casesper100klast7days)
- 2 **Paramasivam A, Priyadharsini JV, Raghunandhakumar S, Elumalai P.** A novel COVID-19 and its effects on cardiovascular disease. *Hypertens Res* 2020; **43**: 729-730 [PMID: [32355222](#) DOI: [10.1038/s41440-020-0461-x](#)]
- 3 **Madjid M, Safavi-Naeini P, Solomon SD, Vardeny O.** Potential Effects of Coronaviruses on the Cardiovascular System: A Review. *JAMA Cardiol* 2020; **5**: 831-840 [PMID: [32219363](#) DOI: [10.1001/jamacardio.2020.1286](#)]
- 4 **Bansal M.** Cardiovascular disease and COVID-19. *Diabetes Metab Syndr* 2020; **14**: 247-250 [PMID: [32247212](#) DOI: [10.1016/j.dsx.2020.03.013](#)]
- 5 **Babapoor-Farrokhran S, Gill D, Walker J, Rasekhi RT, Bozorgnia B, Amanullah A.** Myocardial injury and COVID-19: Possible mechanisms. *Life Sci* 2020; **253**: 117723 [PMID: [32360126](#) DOI: [10.1016/j.lfs.2020.117723](#)]
- 6 **Shi S, Qin M, Shen B, Cai Y, Liu T, Yang F, Gong W, Liu X, Liang J, Zhao Q, Huang H, Yang B, Huang C.** Association of Cardiac Injury With Mortality in Hospitalized Patients With COVID-19 in Wuhan, China. *JAMA Cardiol* 2020; **5**: 802-810 [PMID: [32211816](#) DOI: [10.1001/jamacardio.2020.0950](#)]
- 7 **Friedrich MG, Sechtem U, Schulz-Menger J, Holmvang G, Alakija P, Cooper LT, White JA, Abdel-Aty H, Gutberlet M, Prasad S, Aletras A, Laissy JP, Paterson I, Filipchuk NG, Kumar A, Pauschinger M, Liu P; International Consensus Group on Cardiovascular Magnetic Resonance in Myocarditis.** Cardiovascular magnetic resonance in myocarditis: A JACC White Paper. *J Am Coll Cardiol* 2009; **53**: 1475-1487 [PMID: [19389557](#) DOI: [10.1016/j.jacc.2009.02.007](#)]
- 8 **Agdamag ACC, Edmiston JB, Charpentier V, Chowdhury M, Fraser M, Maharaj VR, Francis GS, Alexy T.** Update on COVID-19 Myocarditis. *Medicina (Kaunas)* 2020; **56** [PMID: [33317101](#) DOI: [10.3390/medicina56120678](#)]
- 9 **Ferreira VM, Piechnik SK, Robson MD, Neubauer S, Karamitsos TD.** Myocardial tissue characterization by magnetic resonance imaging: novel applications of T1 and T2 mapping. *J Thorac Imaging* 2014; **29**: 147-154 [PMID: [24576837](#) DOI: [10.1097/RTI.0000000000000077](#)]
- 10 **Mather AN, Fairbairn TA, Artis NJ, Greenwood JP, Plein S.** Timing of cardiovascular MR imaging after acute myocardial infarction: effect on estimates of infarct characteristics and prediction of late ventricular remodeling. *Radiology* 2011; **261**: 116-126 [PMID: [21828188](#) DOI: [10.1148/radiol.11110228](#)]
- 11 **Kim RJ, Wu E, Rafael A, Chen EL, Parker MA, Simonetti O, Klocke FJ, Bonow RO, Judd RM.** The use of contrast-enhanced magnetic resonance imaging to identify reversible myocardial dysfunction. *N Engl J Med* 2000; **343**: 1445-1453 [PMID: [11078769](#) DOI: [10.1056/NEJM200011163432003](#)]
- 12 **Wagner A, Mahrholdt H, Holly TA, Elliott MD, Regenfus M, Parker M, Klocke FJ, Bonow RO, Kim RJ, Judd RM.** Contrast-enhanced MRI and routine single photon emission computed tomography (SPECT) perfusion imaging for detection of subendocardial myocardial infarcts: an imaging study. *Lancet* 2003; **361**: 374-379 [PMID: [12573373](#) DOI: [10.1016/S0140-6736\(03\)12389-6](#)]
- 13 **Busse A, Rajagopal R, Yücel S, Beller E, Öner A, Streckenbach F, Cantré D, Ince H, Weber MA, Meinel FG.** Cardiac MRI-Update 2020. *Radiologe* 2020; **60**: 33-40 [PMID: [32385547](#) DOI: [10.1007/s00117-020-00687-1](#)]
- 14 **Nelson T, Garg P, Clayton RH, Lee J.** The Role of Cardiac MRI in the Management of Ventricular Arrhythmias in Ischaemic and Non-ischaemic Dilated Cardiomyopathy. *Arrhythm Electrophysiol Rev* 2019; **8**: 191-201 [PMID: [31463057](#) DOI: [10.15420/aer.2019.5.1](#)]
- 15 **Nakamori S, Bui AH, Jang J, El-Rewaidy HA, Kato S, Ngo LH, Josephson ME, Manning WJ, Nezafat R.** Increased myocardial native T<sub>1</sub> relaxation time in patients with nonischemic dilated cardiomyopathy with complex ventricular arrhythmia. *J Magn Reson Imaging* 2018; **47**: 779-786 [PMID: [28737018](#) DOI: [10.1002/jmri.25811](#)]
- 16 **Kelle S, Bucciarelli-Ducci C, Judd RM, Kwong RY, Simonetti O, Plein S, Raimondi F, Weinsaft JW, Wong TC, Carr J.** Society for Cardiovascular Magnetic Resonance (SCMR) recommended CMR protocols for scanning patients with active or convalescent phase COVID-19 infection. *J Cardiovasc Magn Reson* 2020; **22**: 61 [PMID: [32878639](#) DOI: [10.1186/s12968-020-00656-6](#)]
- 17 **Whean P, Armstrong R, Daly CA.** Recent Advances in T1 and T2 Mapping in the Assessment of Fulminant Myocarditis by Cardiac Magnetic Resonance. *Curr Cardiol Rep* 2020; **22**: 47 [PMID: [32472218](#) DOI: [10.1007/s11886-020-01295-0](#)]
- 18 **Neilan TG, Coelho-Filho OR, Danik SB, Shah RV, Dodson JA, Verdini DJ, Tokuda M, Daly CA, Tedrow UB, Stevenson WG, Jerosch-Herold M, Ghoshhajra BB, Kwong RY.** CMR quantification of myocardial scar provides additive prognostic information in nonischemic cardiomyopathy. *JACC Cardiovasc Imaging* 2013; **6**: 944-954 [PMID: [23932642](#) DOI: [10.1016/j.jcmg.2013.05.013](#)]

- 19 **Schieda N**, Blaichman JI, Costa AF, Glikstein R, Hurrell C, James M, Jabehdar Maralani P, Shabana W, Tang A, Tsampalieros A, van der Pol CB, Hiremath S. Gadolinium-Based Contrast Agents in Kidney Disease: A Comprehensive Review and Clinical Practice Guideline Issued by the Canadian Association of Radiologists. *Can J Kidney Health Dis* 2018; **5**: 2054358118778573 [PMID: [29977584](#) DOI: [10.1177/2054358118778573](#)]
- 20 **von Knobelsdorff-Brenkenhoff F**, Pilz G, Schulz-Menger J. Representation of cardiovascular magnetic resonance in the AHA / ACC guidelines. *J Cardiovasc Magn Reson* 2017; **19**: 70 [PMID: [28942735](#) DOI: [10.1186/s12968-017-0385-z](#)]
- 21 **Luetkens JA**, Isaak A, Öztürk C, Mesrobian N, Monin M, Schlabe S, Reinert M, Faron A, Heine A, Velten M, Dabir D, Boesecke C, Strassburg CP, Attenberger U, Zimmer S, Duerr GD, Nattermann J. Cardiac MRI in Suspected Acute COVID-19 Myocarditis. *Radiol Cardiothorac Imaging* 2021; **3**: e200628 [PMID: [33969316](#) DOI: [10.1148/ryct.2021200628](#)]
- 22 **Panchal A**, Kyveritakis A, Mikolich JR, Biederman RWW. Contemporary use of cardiac imaging for COVID-19 patients: a three center experience defining a potential role for cardiac MRI. *Int J Cardiovasc Imaging* 2021; **37**: 1721-1733 [PMID: [33559800](#) DOI: [10.1007/s10554-020-02139-2](#)]
- 23 **Annie FH**, Embrey S, Alkhaimy H, Elashery AR, Nanjundappa A. association between myocarditis and mortality in COVID-19 patients in a large registry. *J Am Coll Cardiol* 2021; **77**: 3037 [DOI: [10.1016/S0735-1097\(21\)04392-8](#)]
- 24 **Kariyanna PT**, Sutarjono B, Grewal E, Singh KP, Aurora L, Smith L, Chandrakumar HP, Jayarangaiah A, Goldman SA, Salifu MO, McFarlane IM. A Systematic Review of COVID-19 and Myocarditis. *Am J Med Case Rep* 2020; **8**: 299-305 [PMID: [32747875](#)]
- 25 **Puntmann VO**, Carerj ML, Wieters I, Fahim M, Arendt C, Hoffmann J, Shchendrygina A, Escher F, Vasa-Nicotera M, Zeiher AM, Vahreschild M, Nagel E. Outcomes of Cardiovascular Magnetic Resonance Imaging in Patients Recently Recovered From Coronavirus Disease 2019 (COVID-19). *JAMA Cardiol* 2020; **5**: 1265-1273 [PMID: [32730619](#) DOI: [10.1001/jamacardio.2020.3557](#)]
- 26 **Huang L**, Zhao P, Tang D, Zhu T, Han R, Zhan C, Liu W, Zeng H, Tao Q, Xia L. Cardiac Involvement in Patients Recovered From COVID-2019 Identified Using Magnetic Resonance Imaging. *JACC Cardiovasc Imaging* 2020; **13**: 2330-2339 [PMID: [32763118](#) DOI: [10.1016/j.jcmg.2020.05.004](#)]
- 27 **Clark DE**, Parikh A, Dendy JM, Diamond AB, George-Durrett K, Fish FA, Fitch W, Hughes SG, Soslow JH. COVID-19 Myocardial Pathology Evaluated Through screening Cardiac Magnetic Resonance (COMPETE CMR). *medRxiv* 2020 [PMID: [32908996](#) DOI: [10.1101/2020.08.31.20185140](#)]
- 28 **Li X**, Wang H, Zhao R, Wang T, Zhu Y, Qian Y, Liu B, Yu Y, Han Y. Elevated Extracellular Volume Fraction and Reduced Global Longitudinal Strains in Participants Recovered from COVID-19 without Clinical Cardiac Findings. *Radiology* 2021; **299**: E230-E240 [PMID: [33434112](#) DOI: [10.1148/radiol.2021203998](#)]
- 29 **Schumm J**, Greulich S, Wagner A, Grün S, Ong P, Bentz K, Klingel K, Kandolf R, Bruder O, Schneider S, Sechtem U, Mahrholdt H. Cardiovascular magnetic resonance risk stratification in patients with clinically suspected myocarditis. *J Cardiovasc Magn Reson* 2014; **16**: 14 [PMID: [24461053](#) DOI: [10.1186/1532-429X-16-14](#)]
- 30 **Phelan D**, Kim JH, Elliott MD, Wasfy MM, Cremer P, Johri AM, Emery MS, Sengupta PP, Sharma S, Martinez MW, La Gerche A. Screening of Potential Cardiac Involvement in Competitive Athletes Recovering From COVID-19: An Expert Consensus Statement. *JACC Cardiovasc Imaging* 2020; **13**: 2635-2652 [PMID: [33303102](#) DOI: [10.1016/j.jcmg.2020.10.005](#)]
- 31 **Mavrogeni S**, Petrou E, Kolovou G, Theodorakis G, Iliodromitis E. Prediction of ventricular arrhythmias using cardiovascular magnetic resonance. *Eur Heart J Cardiovasc Imaging* 2013; **14**: 518-525 [PMID: [23324829](#) DOI: [10.1093/ehjci/jes302](#)]
- 32 **Maron BJ**, Udelson JE, Bonow RO, Nishimura RA, Ackerman MJ, Estes NA 3rd, Cooper LT Jr, Link MS, Maron MS; American Heart Association Electrocardiography and Arrhythmias Committee of Council on Clinical Cardiology, Council on Cardiovascular Disease in Young, Council on Cardiovascular and Stroke Nursing, Council on Functional Genomics and Translational Biology, and American College of Cardiology. Eligibility and Disqualification Recommendations for Competitive Athletes With Cardiovascular Abnormalities: Task Force 3: Hypertrophic Cardiomyopathy, Arrhythmogenic Right Ventricular Cardiomyopathy and Other Cardiomyopathies, and Myocarditis: A Scientific Statement From the American Heart Association and American College of Cardiology. *Circulation* 2015; **132**: e273-e280 [PMID: [26621644](#) DOI: [10.1161/CIR.0000000000000239](#)]
- 33 **Grün S**, Schumm J, Greulich S, Wagner A, Schneider S, Bruder O, Kispert EM, Hill S, Ong P, Klingel K, Kandolf R, Sechtem U, Mahrholdt H. Long-term follow-up of biopsy-proven viral myocarditis: predictors of mortality and incomplete recovery. *J Am Coll Cardiol* 2012; **59**: 1604-1615 [PMID: [22365425](#) DOI: [10.1016/j.jacc.2012.01.007](#)]
- 34 **Giustino G**, Croft LB, Oates CP, Rahman K, Lerakis S, Reddy VY, Goldman M. Takotsubo Cardiomyopathy in COVID-19. *J Am Coll Cardiol* 2020; **76**: 628-629 [PMID: [32517962](#) DOI: [10.1016/j.jacc.2020.05.068](#)]
- 35 **Modin D**, Claggett B, Sindet-Pedersen C, Lassen MCH, Skaarup KG, Jensen JUS, Fralick M, Schou M, Lamberts M, Gerdts T, Fosbøl EL, Phelps M, Kragholm KH, Andersen MP, Køber L, Torp-Pedersen C, Solomon SD, Gislason G, Biering-Sørensen T. Acute COVID-19 and the Incidence of Ischemic Stroke and Acute Myocardial Infarction. *Circulation* 2020; **142**: 2080-2082 [PMID: [33054349](#) DOI: [10.1161/CIRCULATIONAHA.120.050809](#)]

- 36 **Bilaloglu S**, Aphinyanaphongs Y, Jones S, Iturrate E, Hochman J, Berger JS. Thrombosis in Hospitalized Patients With COVID-19 in a New York City Health System. *JAMA* 2020; **324**: 799-801 [PMID: 32702090 DOI: 10.1001/jama.2020.13372]
- 37 **Poissy J**, Goutay J, Caplan M, Parmentier E, Duburcq T, Lassalle F, Jeanpierre E, Rauch A, Labreuche J, Susen S; Lille ICU Haemostasis COVID-19 Group. Pulmonary Embolism in Patients With COVID-19: Awareness of an Increased Prevalence. *Circulation* 2020; **142**: 184-186 [PMID: 32330083 DOI: 10.1161/CIRCULATIONAHA.120.047430]
- 38 **Doltra A**, Amundsen BH, Gebker R, Fleck E, Kelle S. Emerging concepts for myocardial late gadolinium enhancement MRI. *Curr Cardiol Rev* 2013; **9**: 185-190 [PMID: 23909638 DOI: 10.2174/1573403x113099990030]
- 39 **Han Y**, Chen T, Bryant J, Bucciarelli-Ducci C, Dyke C, Elliott MD, Ferrari VA, Friedrich MG, Lawton C, Manning WJ, Ordovas K, Plein S, Powell AJ, Raman SV, Carr J. Society for Cardiovascular Magnetic Resonance (SCMR) guidance for the practice of cardiovascular magnetic resonance during the COVID-19 pandemic. *J Cardiovasc Magn Reson* 2020; **22**: 26 [PMID: 32340614 DOI: 10.1186/s12968-020-00628-w]
- 40 **Allen BD**, Wong TC, Bucciarelli-Ducci C, Bryant J, Chen T, Dall'Armellina E, Finn JP, Fontana M, Francone M, Han Y, Hays AG, Jacob R, Lawton C, Manning WJ, Ordovas K, Parwani P, Plein S, Powell AJ, Raman SV, Salerno M, Carr JC. Society for Cardiovascular Magnetic Resonance (SCMR) guidance for re-activation of cardiovascular magnetic resonance practice after peak phase of the COVID-19 pandemic. *J Cardiovasc Magn Reson* 2020; **22**: 58 [PMID: 32772930 DOI: 10.1186/s12968-020-00654-8]
- 41 **Friedrich MG**. Cardiac MR in Times of COVID. 2020 Mar 24. In: JCMR Journal Club. Available from: [https://scmr.org/resource/dynamic/blogs/20200414\\_133132\\_16845.pdf](https://scmr.org/resource/dynamic/blogs/20200414_133132_16845.pdf)
- 42 **Basman C**, Agrawal PR, McRee C, Saravolatz L, Chen-Scarabelli C, Scarabelli TM. Diagnostic Approach to Myocarditis Mimicking Myocardial Infarction at Initial Presentation. *Cardiol Res* 2016; **7**: 209-213 [PMID: 28197294 DOI: 10.14740/cr485w]
- 43 **Friedrich MG**, Marcotte F. Cardiac magnetic resonance assessment of myocarditis. *Circ Cardiovasc Imaging* 2013; **6**: 833-839 [PMID: 24046380 DOI: 10.1161/CIRCIMAGING.113.000416]
- 44 **Puntmann VO**, Valbuena S, Hinojar R, Petersen SE, Greenwood JP, Kramer CM, Kwong RY, McCann GP, Berry C, Nagel E; SCMR Clinical Trial Writing Group. Society for Cardiovascular Magnetic Resonance (SCMR) expert consensus for CMR imaging endpoints in clinical research: part I - analytical validation and clinical qualification. *J Cardiovasc Magn Reson* 2018; **20**: 67 [PMID: 30231886 DOI: 10.1186/s12968-018-0484-5]
- 45 **Olimulder MA**, van Es J, Galjee MA. The importance of cardiac MRI as a diagnostic tool in viral myocarditis-induced cardiomyopathy. *Neth Heart J* 2009; **17**: 481-486 [PMID: 20087452 DOI: 10.1007/BF03086308]
- 46 **Big Ten Cardiac Registry Steering Committee**, Rink LD, Daniels CJ, Boersma D, Borchers J, Busch J, Kovan J, Kratochvil CJ, Rifat S, Rosenthal G, Chung EH. Competitive Sports, the Coronavirus Disease 2019 Pandemic, and Big Ten Athletics. *Circ Cardiovasc Qual Outcomes* 2020; **13**: e007608 [PMID: 33125280 DOI: 10.1161/CIRCOUTCOMES.120.007608]
- 47 **Pfeiffer MP**, Biederman RW. Cardiac MRI: A General Overview with Emphasis on Current Use and Indications. *Med Clin North Am* 2015; **99**: 849-861 [PMID: 26042886 DOI: 10.1016/j.mcna.2015.02.011]

## Review on radiological evolution of COVID-19 pneumonia using computed tomography

Chiara Casartelli, Fabiana Perrone, Maurizio Balbi, Veronica Alfieri, Gianluca Milanese, Sebastiano Buti, Mario Silva, Nicola Sverzellati, Melissa Bersanelli

**ORCID number:** Chiara Casartelli 0000-0002-7638-5299; Fabiana Perrone 0000-0001-8090-770X; Maurizio Balbi 0000-0002-8436-3655; Veronica Alfieri 0000-0003-0456-069X; Gianluca Milanese 0000-0003-1974-4854; Sebastiano Buti 0000-0003-0876-0226; Mario Silva 0000-0002-2538-7032; Nicola Sverzellati 0000-0002-4820-3785; Melissa Bersanelli 0000-0002-6527-6281.

**Author contributions:** Bersanelli M, Perrone F and Casartelli C designed the work, planned the literature review according to PRISMA methods and identified the areas of interests to discuss; Perrone F and Casartelli C collected the data; Casartelli C, Balbi M and Alfieri V wrote the first draft of the manuscript; Bersanelli M revised the manuscript for relevant scientific content and copyediting; Buti S, Milanese G, Silva M and Sverzellati N revised the manuscript for relevant scientific content; All authors have read and approved the final version of the manuscript.

**Conflict-of-interest statement:** Bersanelli M received honoraria as a speaker at scientific events by Bristol-Myers Squibb (BMS), Novartis, Astra Zeneca, Pierre Fabre, and Pfizer and as a consultant for advisory role by

Chiara Casartelli, Fabiana Perrone, Sebastiano Buti, Melissa Bersanelli, Medical Oncology Unit, University Hospital of Parma, Parma 43126, Italy

Chiara Casartelli, Fabiana Perrone, Nicola Sverzellati, Melissa Bersanelli, Department of Medicine and Surgery, University of Parma, Parma 43126, Italy

Maurizio Balbi, Gianluca Milanese, Mario Silva, Nicola Sverzellati, Division of Radiology, University of Parma, Parma 43126, Italy

Veronica Alfieri, Department of Medicine and Surgery, Respiratory Disease and Lung Function Unit, University of Parma, Parma 43126, Italy

**Corresponding author:** Fabiana Perrone, MD, Doctor, Medical Oncology Unit, University Hospital of Parma, Via A. Gramsci, 14, Parma 43126, Italy. [fabiana.perrone89@libero.it](mailto:fabiana.perrone89@libero.it)

### Abstract

#### BACKGROUND

Pneumonia is the main manifestation of coronavirus disease 2019 (COVID-19) infection. Chest computed tomography is recommended for the initial evaluation of the disease; this technique can also be helpful to monitor the disease progression and evaluate the therapeutic efficacy.

#### AIM

To review the currently available literature regarding the radiological follow-up of COVID-19-related lung alterations using the computed tomography scan, to describe the evidence about the dynamic evolution of COVID-19 pneumonia and verify the potential usefulness of the radiological follow-up.

#### METHODS

We used pertinent keywords on PubMed to select relevant studies; the articles we considered were published until October 30, 2020. Through this selection, 69 studies were identified, and 16 were finally included in the review.

#### RESULTS

Summarizing the included works' findings, we identified well-defined stages in the short follow-up time frame. A radiographic deterioration reaching a peak roughly within the first 2 wk; after the peak, an absorption process and repairing signs are observed. At later radiological follow-up, with the limitation of little

Novartis, BMS, IPSEN, and Pfizer; she also received fees for copyright transfer by Sciclone Pharmaceuticals and research funding by Roche S.p.A., Seqirus UK, Pfizer, Novartis, BMS, AstraZeneca, and Sanofi Genzyme. Buti S received honoraria as a speaker at scientific events and advisory role by Bristol-Myers Squibb (BMS), Pfizer, MSD, Ipsen, Roche, Eli-Lilly, AstraZeneca and Novartis; he also received research funding from Novartis. All the other authors declare they have no conflicts of interest to disclose.

#### PRISMA 2009 Checklist statement:

The authors have read the PRISMA 2009 Checklist, and the manuscript was prepared and revised according to the PRISMA 2009 Checklist.

**Open-Access:** This article is an open-access article that was selected by an in-house editor and fully peer-reviewed by external reviewers. It is distributed in accordance with the Creative Commons Attribution NonCommercial (CC BY-NC 4.0) license, which permits others to distribute, remix, adapt, build upon this work non-commercially, and license their derivative works on different terms, provided the original work is properly cited and the use is non-commercial. See: <http://creativecommons.org/licenses/by-nc/4.0/>

**Manuscript source:** Invited manuscript

**Specialty type:** Radiology, nuclear medicine and medical imaging

**Country/Territory of origin:** Italy

#### Peer-review report's scientific quality classification

Grade A (Excellent): 0  
Grade B (Very good): B  
Grade C (Good): 0  
Grade D (Fair): 0  
Grade E (Poor): 0

**Received:** February 26, 2021

**Peer-review started:** February 26, 2021

**First decision:** July 18, 2021

evidence available, the lesions usually did not recover completely.

#### CONCLUSION

Following computed tomography scan evolution over time could help physicians better understand the clinical impact of COVID-19 pneumonia and manage the possible sequelae; a longer follow-up is advisable to verify the complete resolution or the presence of long-term damage.

**Key Words:** COVID-19; Computed tomography; Pneumonia; Radiological evolution; Follow-up; Long-term consequences; Lung damage; SARS-CoV-2

©The Author(s) 2021. Published by Baishideng Publishing Group Inc. All rights reserved.

**Core Tip:** Given the recent discovery and study of severe acute respiratory syndrome coronavirus 2 infection, the evolution of coronavirus disease 2019 pneumonia has not been entirely defined yet. Chest computed tomography is an effective method to identify and follow coronavirus disease 2019 pneumonia over time. In this review, we considered the radiological changes on computed tomography scan and described the possible clinical pulmonary sequelae in order to understand the long-term outcome of coronavirus disease 2019 pneumonia better.

**Citation:** Casartelli C, Perrone F, Balbi M, Alfieri V, Milanese G, Buti S, Silva M, Sverzellati N, Bersanelli M. Review on radiological evolution of COVID-19 pneumonia using computed tomography. *World J Radiol* 2021; 13(9): 294-306

**URL:** <https://www.wjgnet.com/1949-8470/full/v13/i9/294.htm>

**DOI:** <https://dx.doi.org/10.4329/wjr.v13.i9.294>

#### INTRODUCTION

SARS-CoV-2, which stands for severe acute respiratory syndrome coronavirus 2, was first identified in December 2019 in Wuhan, China. The coronavirus disease 2019 (COVID-19) caused by SARS-CoV-2 has rapidly spread from China to all around the world within a few months, leading the World Health Organization to declare it a pandemic on March 11, 2020[1].

The transmission of SARS-CoV-2 happens through direct, indirect or close contact with infected people through infected secretions, such as saliva and respiratory secretions or their respiratory droplets. The main organ affected is the lung, with pneumonia being the major manifestation of the infection[2].

The gold standard for SARS-CoV-2 diagnosis is real-time reverse transcription-polymerase chain reaction. However, computed tomography (CT) is recommended for initial evaluation and diagnosis, and it is also useful in monitoring the disease progression and evaluating the therapeutic efficacy[3,4].

Until now, many reports have focused on CT scan features at diagnosis[5-7]. On the other hand, there are relatively few studies evaluating serial temporal changes in patients who underwent repeated CT examinations and, particularly, in the late follow-up.

Our aim is to review the literature currently available on the radiological follow-up of COVID-19-related lung alterations using the CT scan to describe the evidence about the dynamic evolution of COVID-19 pneumonia.

#### MATERIALS AND METHODS

We conducted this systematic review according to the Preferred Reporting Items guidelines for Systematic Reviews and Meta-Analysis (PRISMA) Statement[8]. The primary aim was to collect, describe and discuss the dynamic radiological evolution of COVID-19 pneumonia.



**Revised:** July 28, 2021**Accepted:** August 13, 2021**Article in press:** August 13, 2021**Published online:** September 28, 2021**P-Reviewer:** Braga MB**S-Editor:** Gao CC**L-Editor:** Filipodia**P-Editor:** Liu JH

### Search strategy

Two authors (Casartelli C and Perrone F) carried out a comprehensive systematic search for published articles on the MEDLINE/PubMed library until October 31, 2020. Given the absence of articles on this topic before December 2019, when the first COVID-19 outbreak started, no upper limit for the search was chosen.

The following search keywords were used: “COVID-19” [all fields] AND “computed tomography” [all fields] AND “evolution” [all fields]. The reference lists of the included articles and reviews/meta-analyses on our research topic were also reviewed to identify additional relevant papers.

### Study selection and eligibility criteria

Retrospective studies, prospective studies and case reports describing the evolution of COVID-19 pneumonia on CT scan were included. Only English language articles were considered eligible. Studies with insufficient radiological data were excluded. We planned qualitative analysis only, forecasting a high heterogeneity between the eligible studies, likely preventing quantitative analyses.

### Data extraction and synthesis

The study characteristics (first author, year of publication, type of study, number of patients included, CT scan follow-up, dynamic evolution and main CT manifestations) were extracted from the included articles by a single author (Casartelli C). Two reviewers (Perrone F and Casartelli C) initially performed the data extraction, and then it was independently reviewed by an additional reviewer (Bersanelli M).

Any doubt or disagreement was discussed with a fourth investigator (Buti S) and resolved with all investigators’ consensus.

## RESULTS

### General description

The study selection led to the inclusion of 16 reports: 13 retrospective studies[9-21], 1 prospective study[22] and 2 case series[23,24]. The outline of the search is reported in Figure 1.

These reports (more specifically, 15 from China[9-23], 1 from Italy[24]) have analyzed several cases of pneumonia caused by SARS-CoV-2 diagnosed through CT without contrast (Table 1).

Most of the reports have considered moderate/common pneumonia; if pneumonia was not explicitly classified, most of the articles included patients with a good and defined prognosis, who were ultimately discharged from the hospital, while patients with severe/critical pneumonia were generally excluded.

Four studies have also included a minority group of patients showing severe/critical pneumonia[10,14,17,20]; the 11 patients described by Sun Q *et al*[23] case series had severe pneumonia[23].

### Scoring system

The most common score used to evaluate dynamic CT evolution was a semi-quantitative scoring system, which considered the total area of involvement of the lesions. The nature of the semi-quantitative scoring system was similar in the studies considered, even with some adjustments and discrepancies among them.

For example, Liang *et al*[11] assigned a 0-4 score based on the percentage of each lung lobe involvement; in agreement with this, the overall lung total severity score was reached by summing up the five lobe scores, with a possible range from 0 to 20.

Zhou *et al*[12] divided each lung into six zones, and the total score, given by the sum of the different lung regions, could reach a maximum of 48.

Zhang *et al*[15] used yet another adaptation of the system based on the lung segments involved, assigning a score based on the percentage of ground glass opacities (GGOs) and consolidation, with a possible range from 0 to 36.

The study from Liu *et al*[17], analyzing the CT of discharged patients, focused the score on non-GGO lesions since extended GGO areas were defined as a basic manifestation of convalescence, which could lead to an overestimation of the CT score.

Other authors, considering the limited accuracy and sensitivity of the semi-quantitative score based mainly on visual evaluation, proposed evaluating dynamic evolution by quantitative techniques.

**Table 1 Characteristics and findings of the studies included in the systematic review**

Ref.	Type of study	Patients included	Mean age in yr, range	CT scan follow-up	CT evaluation, scoring system
Han <i>et al</i> [9], 2020	Retrospective	17 surviving and discharged patients with COVID-19 pneumonia	40 ± 6	4 wk (4 weekly CT scan during hospitalization)	Semi-quantitative
Wang <i>et al</i> [10], 2020	Retrospective	63 patients with asymptomatic/mild, 378 with moderate, 43 with severe/critically COVID-19 pneumonia	47 (33-57)	From symptoms onset to beyond day 15	Quantitative
Liang <i>et al</i> [11], 2020	Retrospective	88 patients with mild COVID-19 pneumonia	42.7 (4-82)	3 wk after disease onset	Semi-quantitative
Sun <i>et al</i> [23], 2021	Case series	11 patients with severe COVID-19 pneumonia	52 (33-75)	CT scan during hospitalization (not well defined, at least 3 wk during hospitalization)	Qualitative
Zhou <i>et al</i> [12], 2020	Retrospective	100 patients with COVID-19 pneumonia (without ARDS)	52.3 ± 13.1 (27-80)	CT during hospitalization (from symptoms onset to beyond day 21)	Semi-quantitative
Wang <i>et al</i> [13], 2020	Retrospective	126 patients with COVID-19 pneumonia, (severe and critical cases excluded)	41.2 ± 10.8	CT scan during hospitalization (mean days of hospitalization 22 ± 5 d (12-40))	Qualitative
Wang <i>et al</i> [14], 2020	Retrospective	79 patients with non-severe (mild/common) COVID-19 pneumonia, 27 with severe pneumonia	48.0 ± 15.4	CT scan during hospitalization (mean days of hospitalization 25) + CT scan at 2-4 wk after discharge	Semi-quantitative
Zhang <i>et al</i> [15], 2020	Retrospective	33 patients with moderate COVID-19 pneumonia	49.0 ± 15.5	CT scan during hospitalization (mean days of hospitalization 20.8, range 18-37)	Semi-quantitative
Feng <i>et al</i> [16], 2020	Retrospective	19 patients with COVID-19 pneumonia	43.6 ± 15.5 (10-67)	0-34 d after symptoms onset	Quantitative
Liu <i>et al</i> [17], 2020	Retrospective	149 discharged patients with COVID-19 pneumonia (142 pneumonia, 7 severe pneumonia, no critical patients included)	43 (36-56)	Basal CT scan at discharge and at 1 <sup>st</sup> , 2 <sup>nd</sup> and 3 <sup>rd</sup> week after discharge	Semi-quantitative
Pan <i>et al</i> [18], 2020	Retrospective	105 patients with COVID-19 pneumonia (severe pneumonia excluded)	48.6 ± 13.1 (23-72)	1-47 d after symptoms onset	Semi-quantitative
Zhuang <i>et al</i> [19], 2021	Retrospective	22 patients with COVID-19 pneumonia with solitary pulmonary lesion	40.7 ± 10.3 (23-54)	CT scan during hospitalization (mean days of hospitalization 19 d, range: 11-44) + first CT scan after discharge	Semi-quantitative
Urciuoli and Guerriero [24], 2020	Case series	6 patients with mild COVID-19 pneumonia	59.5	First CT on admission and 4 mo after symptoms onset	Qualitative
Zhang <i>et al</i> [20], 2020	Retrospective	53 patients with common COVID-19 pneumonia, 20 patients with severe COVID-19 pneumonia	45 ± 14 common pneumonia, 50 ± 15 severe pneumonia	0-30 d after symptoms onset	Quantitative
Pan <i>et al</i> [21], 2020	Retrospective	21 patients with COVID-19 pneumonia (severe pneumonia excluded)	40 ± 9 (25-63)	0-26 d after symptoms onset	Semi-quantitative
Wang <i>et al</i> [22], 2020	Prospective	90 patients with COVID-19 pneumonia	45 ± 14 (5-43)	0-24 d after symptoms onset	Semi-quantitative

ARDS: Acute respiratory distress syndrome; COVID-19: Coronavirus disease 2019; CT: Computed tomography.

For example, Feng *et al*[16] measured the total volume ( $V_T$ ) and mean CT value (CT), and from these, they calculated the mass (m):  $V_T \times (CT + 1000)$ [16].

In the report from Wang *et al*[10], quantitative CT measurements of pulmonary opacities, including volume, density and location, were extracted through deep learning algorithms.

In another report, quantitative CT features were automatically calculated using intelligent artificial algorithms, giving back the percentage of GGO volume, consolidation volume and total lesion volume[15].

Other reports described the evolution of lung lesions qualitatively[13,23,24].

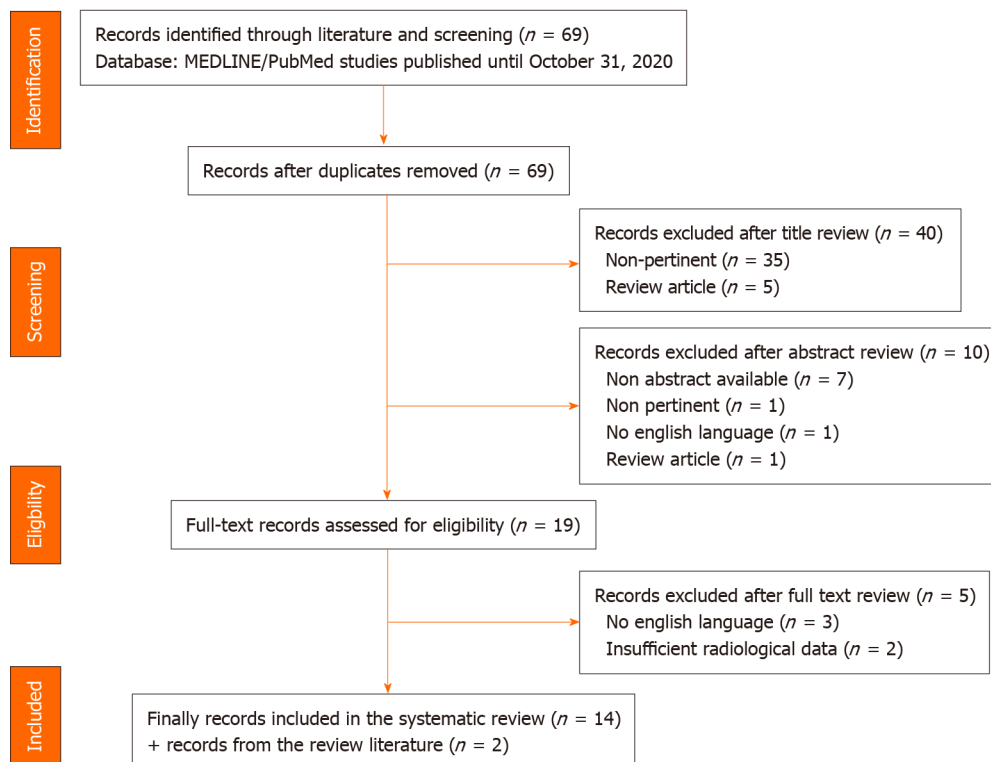


Figure 1 PRISMA flow diagram.

### Radiological dynamic evolution: Severity and timing

Almost all the reports present a short-term radiological follow-up, focusing on the first few weeks from the symptoms appearance and studying serial CT scan approximately in the first 4 wk during hospitalization (Table 1).

It has been observed that the initial CT features and dynamic evolution of COVID-19 pneumonia have specific characteristics and regularity.

Several reports identify well-defined stages, from the onset of the symptoms to radiological recovery.

The most common pattern of radiographic evolution found is as follows. First, there is a progressive rapid radiographic deterioration, during which the lesions keep growing until they reach a peak; once this peak is reached, the lesions stop growing and are gradually reabsorbed and repairing signs appear. Almost all the studies found that the peak was reached roughly within 2 wk after the symptoms appearance, and after that lung abnormalities started to decrease.

There are some exceptions. Zhang *et al*[15] found an earlier peak, 8 d after symptoms onset, and lung lesions improved after 11 d. Wang *et al*[22] discovered a similar peak at around 6-11 d; in this case, though, a significant extent of lung lesions was found for longer times after the peak, showing a slower recovery.

Specific patterns of temporal evolution and relative peaks are shown in Table 2.

When severe pneumonia was considered separately, the disease seemed to have a slightly longer evolution, showing the peak later than for moderate pneumonia cases.

In the report from Zhang *et al*[20], severe pneumonia exhibited a peak approximately 17 d after symptoms onset (compared to moderate pneumonia, which peaked at 12 d in the same study). In the report from Wang *et al*[10], the opacity volume kept increasing even after 15 d in the severe/critical group. Four reports had taken into account a longer CT follow-up, considering CT scan after discharge[14,17,19,24].

Zhuang *et al*[19] considered both CT during hospitalization and the first CT after discharge (22-51 d after symptoms onset). During the latter phase, further absorption of the lung lesions compared with the previous radiological exam was observed, but not all patients showed a complete resolution.

Liu *et al*[17] studied the radiological evolution during the first few weeks after discharge, in particular 1, 2 and 3 wk after discharge. The aim was to determine the cumulative percentage of complete radiological resolution at each time point. They discovered that lung lesions could be entirely absorbed with no sequelae, and they suggested that the optimal time point for an early radiological estimation might be 2

Table 2 Computed tomography scan features of lung lesions according to the follow-up timing of coronavirus disease 2019 pneumonia

Ref.	Short-term follow-up, dynamic evolution during hospitalization period: Severity and timing	Main CT features at short-term follow-up	Late follow-up, dynamic evolution after hospital discharge	Main CT features at late follow-up
Han <i>et al</i> [9], 2020	Initial deterioration to a peak at the 2 <sup>nd</sup> week followed by improvement in the 3 <sup>rd</sup> and 4 <sup>th</sup> week	GGO decreased from 1 <sup>st</sup> week to 2 <sup>nd</sup> week, then increased in 3 and 4. Consolidation and a mixed pattern noted in 2 wk. Crazy paving pattern had the highest frequency in 2 <sup>nd</sup> week	N/A	N/A
Wang <i>et al</i> [10], 2020	Severe/critically ill group: Opacity volume continued to increase beyond 15 d. Moderate group: Peak on days 13-15 (the opacity density began to drop from day 10 to day 12). Asymptomatic/mild group: Highest opacity volume on days 1-3 and almost resolved after 15 d	GGO in the early stages, followed by appearance of consolidations. In the severe/critically ill group: Decreasing trend of GGO, increasing trend of consolidation over time	N/A	N/A
Liang <i>et al</i> [11], 2020	Total severity score showed an increasing trend in the first 2 wk, followed by a slight decrease in the 3 <sup>rd</sup> week	GGO was the most common finding over time, consolidation decreased 2 wk after symptom onset. Reticulations and linear opacities and fibrosis became increasing prevalent later in the disease course	N/A	N/A
Sun <i>et al</i> [23], 2021	Improvement in the first 3 wk after hospitalization	Decrease in consolidation and GGO overtime and appearance of fibrous-like stripes	N/A	N/A
Zhou <i>et al</i> [12], 2020	3 stages: Early rapid progressive stage (1-7 d from symptom onset); > advanced stage with peak levels of abnormalities on CT at 8-14 d; > improvement after 14 d (particularly, after 21 d the absorption was more obvious)	GGO, GGO + reticular pattern/consolidation in the rapid progressive stage. ↑ GGO + reticular pattern and consolidation in the advanced stage. ↓ GGO + reticular pattern and consolidation and ↑ subpleural line, bronchus distortion, and fibrotic strips in the absorption stage	N/A	N/A
Wang <i>et al</i> [13], 2020	3 stages: Progression process; > absorption process; > stage of discharge	↑ GGO with consolidation (↑ crazy paving pattern, ↑ vascular thickening sign ↑ air bronchogram sign) in the progression process. Absorption of consolidation displayed as inhomogeneous partial GGOs with fibrosis shadows, occurrence of the fishing net on trees sign, ↑ fibrosis sign, ↑ subpleural line sign in the absorption process. Further absorption of GGOs, consolidation and fibrosis shadows and no appearance of new lesions in the stage of discharge	N/A	N/A
Wang <i>et al</i> [14], 2020	Radiological aggravation (< 2 wk) and improvement (> 2 wk)	GGO decreased while mixed GGO and consolidation increased from 1 wk to 2 wk after onset; linear opacity increased from 2 wk to 3 wk after onset	1-2 mo after symptom onset (median day 38): In 1/3 of cases complete absorption of lesions. Patients with more severe lesions at day 8-14 (> consolidations, CT score > 4, > 3 lobes involved) were more prone to have pulmonary residuals	Mainly linear opacities
Zhang <i>et al</i> [15], 2020	4 stages: Early stage (0-5 d); > peak stage (6-10 d); > absorption stage (11-15 d); > recovery stage (≥ 16 d)	Mainly GGO, (vascular thickening, bronchial wall thickening, and consolidation were also noted) in the early stage. ↑ GGO, vascular and bronchial thickening, and consolidation (mean peak at 8 d) in the peak stage. GGO and consolidation were predominantly present, with ↑ bronchial wall thickening and vascular thickening in the absorption stage. GGO and consolidation were partially absorbed, and bronchial wall thickening and vascular thickening ↓ (residual GGO and subpleural parenchymal bands) in the recovery stage	N/A	N/A
Feng <i>et al</i> [16], 2020	3 stages: Progressive stage (0-5 d); > peak stage (5-15 d). The greatest severity showed	GGO and interlobular/intralobular septal thickening were the most frequent CT manifestation	N/A	N/A

	approximately 7-8 d from onset; > absorption stage (15-30 d)			
Liu <i>et al</i> [17], 2020	N/A	N/A	At 3 wk follow up CT scan: Complete absorption of lesions in more than half of the patients	Gradually decrease of GGO and fibrous stripe (GGO during the first and fibrous stripe the 3 <sup>rd</sup> week after discharge). "Tinted" sign and bronchovascular bundle distortion
Pan <i>et al</i> [18], 2020	5 stages: 0-3, 4-7, 8-14, 15-21, and > 21 d from symptoms onset (stages A-E, respectively). The total CT score of lung involvement was significantly higher in Stage C. The lung lesions in most patients improved after 14 d since initial symptom onset	Proportion of GGO was similar in each stage, consolidation gradually ↑ from Stage A to C and gradually ↓ from Stage C to E	N/A	N/A
Zhuang <i>et al</i> [19], 2021	Lung involvement peak at approximately 11 d, then lung lesions improved significantly	Mainly GGO in the first scan (0-4 d), crazy-paving pattern and consolidation in scan-2 (4-22 d), lesions were gradually absorbed and tended to be stable and linear opacities were noted in the scan-3 (before discharge, 6-41 d)	1 <sup>st</sup> CT scan after discharge (22-51 d): Further absorption of lung lesions	Various presentations: negative CT scan, GGO, consolidation, linear opacities
Urciuoli and Guerriero [24], 2020	N/A	N/A	Persistence of lung abnormalities in 5/6 cases even if all the patients completely asymptomatic	Various presentations: 1 negative CT scan; in 2 patients, persistence of mixed pattern (GGO and fibrous streaks); in 1 patient fibrotic stripes, in 1 patient mixed pattern (interlobular septal thickening and patchy GGO); in 1 patient fibrotic pattern
Zhang <i>et al</i> [20], 2020	5 stages: Stage 1 (0-3 d), stage 2 (4-7 d), stage 3 (8-14 d), stage 4 (15-21 d), and stage 5 (22-30 d). PTV peaks at 12 d in common pneumonia, at 17 d in severe pneumonia	Common pneumonia: No significant differences in the PTV, PGV and PCV between stages 1-4 (percent of lesions was reduced in stage 5 compared with stage 4). Severe pneumonia PTV, PGV and PCV ↑ from stage 2 to stage 4 and ↓ in stage 5	N/A	N/A
Pan <i>et al</i> [21], 2020	4 stages: Early stage (0-4 d); progressive stage (5-8 d); peak stage (10-13 d); and absorption stage (≥ 14 d). Peak at 10 d after symptoms onset. CT signs improvement at approximately 14 d	GGO in the early stage, ↑ crazy-paving pattern and consolidation in the progressive stage, consolidation in the peak stage, progressive resolution of consolidation in the absorption stage	N/A	N/A
Wang <i>et al</i> [22], 2020	Lung abnormalities increased quickly after the onset of symptoms, peaked around 6-11 d, and were followed by persistence of high levels in extent for a long duration (slow absorption of the lesions)	GGOs trend: "first falling then rising". Consolidation was the second most common feature seen in the first 11 d. Mixed pattern: The second most predominant pattern since illness days 12-17	N/A	N/A

CT: Computer tomography; GGO: Ground glass opacity; N/A: Not applicable; PCV: Percentage of consolidation volume; PGV: Percentage of ground glass opacity volume; PTV: Percentage of total lesion volume.

wk after discharge. In their analysis, the cumulative percentage of the complete radiological resolution was 8%, 42%, 50% and 53% at discharge and during the 1<sup>st</sup>, 2<sup>nd</sup> and 3<sup>rd</sup> week after discharge, respectively[17].

Wang *et al*[14] conducted a study including both common and severe pneumonia, showing that approximately 1/3 of cases had complete absorption of lesions in the first 1-2 mo after symptom onset (median day 38). In their study, patients with more severe lung involvement at days 8-14 (peak) were more prone to have pulmonary residuals.

Urciuoli and Guerriero[24] considered a longer follow-up, with the study of CT up to 4 mo after the onset of the symptoms; the sample of this report was relatively small, as it considered only 6 patients with mild pneumonia. Interestingly, the follow-up CT scan revealed the persistence of lung abnormalities in 5 cases out of 6, even if all patients were completely asymptomatic at that point[24].



### CT scan features of lung lesions at follow-up

The main features of lung lesions in the retrieved reports were multiple, bilateral, with a peripheral subpleural distribution.

In the short-term follow-up some features recurred. Consolidations and GGOs were always described, and often a mixed pattern was noted. Consolidations were more frequent during the peak, sometimes with accompanying signs such as a “crazy paving pattern” or “vascular thickening sign;” after the peak, they were gradually absorbed.

GGOs were described mainly in the early phase, but they could be observed also in later stages. In fact, in the report from Pan *et al*[18] the proportion of GGOs was similar in each stage. In those from Wang *et al*[22], the observed trend of GGOs was described as “first falling then rising” as they were present both in the first phase and in the last CT scan.

After the peak, besides GGOs, repairing CT signs, such as linear opacities, fibrous stripes, subpleural line sign and fibrosis shadows, were noted. Wang *et al*[13] proposed, in the absorption process, a particular sign called “fishing net on trees.” This sign “indicated that the pulmonary lesions were in the stage of obvious absorption but not complete absorption. CT showed that the large area of consolidation was reduced, the density was reduced, the edge had shrunk, and there were significantly more bands and incomplete absorption of fibrosis shadows. The area was similar to a fishing net hanging on a branch that was not fully spread under the background of the increased bronchovascular bundle”[13].

In the longer-term follow-up, CT scans showed various presentations. Zhuang *et al* [19] observed in the first CT scan after discharge further absorption of the lung lesions. Also, GGOs, consolidations and linear opacities were still found in some patients. In the case series of Urciuoli and Guerriero[24], 2 patients presented persistence of a mixed pattern with GGO and fibrous streaks, 1 patient fibrotic stripes, 1 patient a mixed pattern with interlobular septal thickening and patchy GGOs and 1 patient fibrotic pattern[24].

Wang *et al*[22], who followed the CT scan until 4 wk after discharge, found mainly linear opacities. Liu *et al*[17] still observed in some patients GGOs and fibrous stripes even at the 3 wk radiological follow-up, even with a decreasing trend (GGO during the 1<sup>st</sup> week and fibrous stripes during the 3<sup>rd</sup> wk). Two additional signs were found during the evolution: “tinted” sign and bronchovascular bundle distortion. The “tinted” sign was demonstrated to coincide with an extension of the GGO area and a decrease in its density. According to the authors, the appearance of this pattern probably implied the gradual resolution of inflammation with re-expansion of alveoli. The bronchovascular bundle may be caused by inflammatory distraction or subsegmental atelectasis[17].

## DISCUSSION

Current evidence of the temporal evolution of COVID-19 pneumonia derives from studies evaluating a relatively short follow-up period, and data about long-term radiological (and clinical) sequelae are still awaited[17,22,25,26]. The hallmark of early COVID-19 pneumonia includes bilateral, peripheral GGOs and consolidation often showing features resembling organizing pneumonia, such as a perilobular distribution and “reversed halo” sign (*i.e.* a focal, rounded area of ground-glass surrounded by a ring or arc of denser consolidation)[27,28]. These findings are non-specific and variably comprise foci of edema, organization and diffuse alveolar damage that are not too far removed from patients with other acute injuries, even noninfectious[29,30]. Notably, up to 56% of patients have been reported to demonstrate no abnormalities in the first 3 d after onset of symptoms, while conversely patients with no symptoms may show abnormal CT findings[31]. Moreover, still in the initial phase of the disease, pulmonary opacities may be unilateral and lack the characteristic peripheral distribution, possibly reducing diagnostic confidence in differentiating COVID-19 from potential mimickers such as heart failure and other infections[21,32].

The severity of acute COVID-19 manifestations is likely to peak within 2 wk from the disease onset, though reported temporal evolution varies depending on the studied population[12,13,18,21,31]. In this phase, patients may show an increasing extent of pulmonary consolidation, which parallels lung injury evolution. With the awareness of the heterogeneous studies included in the present analysis and intrinsic individual variation of the disease course, patients have been found to enter the so-called absorption stage roughly 14 d from the disease onset[12,13,18,21]. During this

period, consolidation tends to wane, while other findings such as linear opacities, parenchymal bands and reticulation possibly emerge, sometimes leading to a “fibrotic-like” appearance[26]. Even in this last case, it remains unclear whether residual abnormalities truly represent irreversible disease or will solve over time as no studies with a follow-up period greater than 6 mo have been performed so far[26,33]. Remarkably, most studies examined CT patterns in isolation at various time points rather than temporal changes of each pulmonary finding, providing valuable information about the overall disease evolution but missing the opportunity to examine regional linkages between patterns. Future studies are needed to explore how underlying pathogenetic pathways such as diffuse alveolar damage and an auto-inflammatory response would determine imaging features of COVID-19. In this regard, the role of baseline risk factors such as vascular thrombosis and interstitial lung abnormalities remains poorly investigated.

Besides providing clues to assess COVID-19 morphological changes, CT has been used to enrich clinical and laboratory findings to quantify disease severity in the acute setting and longitudinal evolution[12,18,21]. Various methods have been employed to assess CT lung involvement in COVID-19, including qualitative, semi-quantitative and software-based quantitative scoring systems[12,18,21,34-37]. In the included works, most CT scores were based on semi-quantitative methods, while only two studies used artificial intelligence techniques. Several parameters such as symptoms, oxygenation status and laboratory measures of infection and inflammation have been found to correlate with parenchymal involvement at CT, highlighting the potential role of imaging in predicting the clinical course of COVID-19 and optimizing patient care[38-40]. However, further evidence is needed to demonstrate CT scoring usefulness to manage COVID-19 and its actual impact on clinical decision-making in the acute and follow-up setting.

### **Clinical compendium: Pulmonary sequelae of COVID-19**

The clinical counterpart of long-term radiological outcomes of COVID-19 pneumonia is a topic of growing interest. After the first wave of COVID-19, the awareness of patients suffering from residual symptoms, persistent beyond the acute phase of the disease, became very common, leading to the description of a post-COVID syndrome or Long-COVID[41]. However, the type and severity of respiratory impairment or functional sequelae are still unknown.

The current knowledge gained from the previous coronavirus outbreaks (SARS-CoV-1 in 2002-2004 and Middle East respiratory syndrome coronavirus in 2012) and the general understanding about outcomes in the acute distress respiratory syndrome suggest that some COVID-19 survivors might experience impaired lung function and exercise limitation, and some of them develop interstitial lung disease in the mid-long term[42-44].

Up until recently, only a few retrospective studies, including small samples, showed that patients might experience a reduction of forced vital capacity (13 patients at 6 wk) [45] and of forced vital capacity, forced expiratory volume in the first second, total lung capacity (TLC) and diffusion lung carbon monoxide (DLCO) (55 patients at 3 mo) [46].

In one of the largest cohorts studied to date describing the medium-term consequences of the infection (767 patients, follow-up at median time of 81 d after discharge), 51.4% of the patients reported being still symptomatic, with fatigue (55.0%), exertional dyspnea (45.8%) and post-traumatic psychological consequences (30.5%) as the most reported symptoms. Impaired lung function was found in 19% of the patients (reduced DLCO with or without restrictive pattern)[47].

Anastasio *et al*[48] recently published a study on 379 patients evaluated 4 mo after the diagnosis of COVID-19. Almost 69% of the patients reported almost one residual symptom. Patients who had pneumonia showed lower SpO<sub>2</sub> at rest and during the six-minute walking test and TLC compared with patients without prior pneumonia. Furthermore, the authors found an association between SpO<sub>2</sub>/FiO<sub>2</sub> ratio and the pneumonia severity index during the acute phase, and mid-term alteration in SpO<sub>2</sub> at rest and during six-minute walking test, TLC, residual volume and forced vital capacity[48].

In an Italian study with 238 patients enrolled, DLCO was reduced less than 80% of the predicted value in more than half of the patients at 4 mo follow-up, and in 15.5% of the cases were less than 60%. More than 50% of the patients showed functional impairment assessed with Short Physical Performance Battery and 2-minute walk test [49].

In another large cohort of 647 patients evaluated at 3 mo follow-up, patients reported ongoing symptoms, in particularly fatigue (13%), palpitation (10%) and

dyspnea (9%). Those symptoms were significantly higher in patients who experienced severe COVID-19 compared to non-severe patients. In this cohort, only 81 patients were assessed with lung function test. More than half of the patients showed reduced DLCO. Similarly to symptoms, an impaired DLCO was more frequently associated with severe cases than non-severe (68% *vs* 42%). On a multivariate analysis, a CT total severity score > 10.5 and acute distress respiratory syndrome were significantly associated with impaired DLCO[50].

Similar results were found in a smaller cohort of 22 patients at 3 mo follow-up. Furthermore, on multivariate analysis, low TLC was associated with the need for mechanical ventilation and low forced expiratory volume in the first second with a high APACHE II score[51].

In a cohort of 119 patients who survived severe COVID-19 evaluated at 2 mo after discharge, respiratory symptoms (breathlessness 32%, cough 7%) were less frequent than persistent fatigue (68%), sleep disturbance (57%), anxiety and depression (22% and 18%, respectively) and post-traumatic stress disorder (25%). Despite radiological resolution in 87% of the patients, 41% reported persistent limitations in everyday life, and 44% had a Modified British Medical Research Council Questionnaire grade above the pre-COVID19 baseline[52]. A similar study on 134 patients found breathlessness as the most commonly reported symptoms (68%) followed by myalgia (51.5%), extreme fatigue (39.6%), low mood (37.3%) and sleep disturbance (35.1%)[53].

Long-term follow-up will help understand the impact of COVID-19 pneumonia on lung pathophysiology. Therefore, it is advisable to schedule serial follow-up in patients that still present lung function impairment or exercise limitation.

## CONCLUSION

At present, the available literature focus on the acute phase of radiological follow-up of COVID-19 pneumonia and describes well-defined stages in the first few weeks after the onset of the symptoms.

The most common finding seems to be a peak of lung involvement reached roughly within the first 2 wk, characterized mainly by the growth of GGOs and consolidations. After that peak, these manifestations are gradually absorbed, and repairing signs, such as linear opacities, fibrous stripes, subpleural line sign and fibrosis shadows, tend to appear.

When considering later follow-up, up to 4 mo, lesions are usually not completely absorbed. A longer follow-up is definitely needed, especially to check whether the later signs are reversible and how they affect patients' conditions. Following CT scan evolution over time could help physicians better understand the clinical impact of COVID-19 pneumonia and manage the possible sequelae.

## ARTICLE HIGHLIGHTS

### Research background

Pneumonia is the main manifestation of severe acute respiratory syndrome coronavirus 2 infection. Chest computed tomography is an effective way to detect and keep track of coronavirus disease 2019 pneumonia cases over time.

### Research motivation

As of now, few studies evaluated serial computed tomography scan temporal changes during the course of severe acute respiratory syndrome coronavirus 2 pneumonia.

### Research objectives

This systematic review describes the dynamic evolution of coronavirus disease 2019 pneumonia, considering the available literature on this topic.

### Research methods

A systematic review according to PRISMA guidelines was performed. Pertinent keywords on PubMed were used.

### Research results

Different and well-defined stages characterized the first few weeks after the onset of

the symptoms.

### Research conclusions

A peak of lung involvement within the first 2 wk, followed by the gradual absorption of the lesions and the advent of repairing signs was observed. Later follow-up showed that lesions were usually not completely absorbed, at least up to 4 mo.

### Research perspectives

Longer follow-up is needed to check whether the later signs are reversible and how they affect patients' conditions.

## REFERENCES

- 1 **World Health Organization.** WHO Director-General's remarks at the media briefing on 2019-nCoV on 11 February 2020. [cited 11 February 2020] In: World Health Organization [Internet]. Available from: <https://www.who.int/dg/speeches/detail/who-director-general-s-remarks-at-the-media-briefing-on-2019-ncov-on-11-february-2020>
- 2 **World Health Organization.** Transmission of SARS-CoV-2: implications for infection prevention precautions. [cited 11 February 2020] In: World Health Organization [Internet]. Available from: <https://www.who.int/news-room/commentaries/detail/transmission-of-sars-cov-2-implications-for-infection-prevention-precautions>
- 3 **World Health Organization.** Report of the WHO-China Joint Mission on Coronavirus Disease 2019 (COVID-19). [cited 11 February 2020] In: World Health Organization [Internet]. Available from: <https://www.who.int/docs/default-source/coronaviruse/who-china-joint-mission-on-covid-19-final-report.pdf>
- 4 **Qiu T, Liang S, Dabbous M, Wang Y, Han R, Toumi M.** Chinese guidelines related to novel coronavirus pneumonia. *J Mark Access Health Policy* 2020; **8**: 1818446 [PMID: 33133431 DOI: 10.1080/20016689.2020.1818446]
- 5 **Shi H, Han X, Jiang N, Cao Y, Alwalid O, Gu J, Fan Y, Zheng C.** Radiological findings from 81 patients with COVID-19 pneumonia in Wuhan, China: a descriptive study. *Lancet Infect Dis* 2020; **20**: 425-434 [PMID: 32105637 DOI: 10.1016/S1473-3099(20)30086-4]
- 6 **Xu X, Yu C, Qu J, Zhang L, Jiang S, Huang D, Chen B, Zhang Z, Guan W, Ling Z, Jiang R, Hu T, Ding Y, Lin L, Gan Q, Luo L, Tang X, Liu J.** Imaging and clinical features of patients with 2019 novel coronavirus SARS-CoV-2. *Eur J Nucl Med Mol Imaging* 2020; **47**: 1275-1280 [PMID: 32107577 DOI: 10.1007/s00259-020-04735-9]
- 7 **Li K, Wu J, Wu F, Guo D, Chen L, Fang Z, Li C.** The Clinical and Chest CT Features Associated With Severe and Critical COVID-19 Pneumonia. *Invest Radiol* 2020; **55**: 327-331 [PMID: 32118615 DOI: 10.1097/RLI.0000000000000672]
- 8 **Kristjansson M, Bieluch VM, Byeff PD.** Mycobacterium haemophilum infection in immunocompromised patients: case report and review of the literature. *Rev Infect Dis* 1991; **13**: 906-910 [PMID: 1962107 DOI: 10.1093/clinids/13.5.906]
- 9 **Han X, Cao Y, Jiang N, Chen Y, Alwalid O, Zhang X, Gu J, Dai M, Liu J, Zhu W, Zheng C, Shi H.** Novel Coronavirus Disease 2019 (COVID-19) Pneumonia Progression Course in 17 Discharged Patients: Comparison of Clinical and Thin-Section Computed Tomography Features During Recovery. *Clin Infect Dis* 2020; **71**: 723-731 [PMID: 32227091 DOI: 10.1093/cid/ciaa271]
- 10 **Wang YC, Luo H, Liu S, Huang S, Zhou Z, Yu Q, Zhang S, Zhao Z, Yu Y, Yang Y, Wang D, Ju S.** Dynamic evolution of COVID-19 on chest computed tomography: experience from Jiangsu Province of China. *Eur Radiol* 2020; **30**: 6194-6203 [PMID: 32524223 DOI: 10.1007/s00330-020-06976-6]
- 11 **Liang T, Liu Z, Wu CC, Jin C, Zhao H, Wang Y, Wang Z, Li F, Zhou J, Cai S, Liang Y, Zhou H, Wang X, Ren Z, Yang J.** Evolution of CT findings in patients with mild COVID-19 pneumonia. *Eur Radiol* 2020; **30**: 4865-4873 [PMID: 32291502 DOI: 10.1007/s00330-020-06823-8]
- 12 **Zhou S, Zhu T, Wang Y, Xia L.** Imaging features and evolution on CT in 100 COVID-19 pneumonia patients in Wuhan, China. *Eur Radiol* 2020; **30**: 5446-5454 [PMID: 32367418 DOI: 10.1007/s00330-020-06879-6]
- 13 **Wang C, Shi B, Wei C, Ding H, Gu J, Dong J.** Initial CT features and dynamic evolution of early-stage patients with COVID-19. *Radiol Infect Dis* 2020; **7**: 195-203 [PMID: 32864406 DOI: 10.1016/j.jrid.2020.08.002]
- 14 **Wang Y, Jin C, Wu CC, Zhao H, Liang T, Liu Z, Jian Z, Li R, Wang Z, Li F, Zhou J, Cai S, Liu Y, Li H, Liang Y, Tian C, Yang J.** Organizing pneumonia of COVID-19: Time-dependent evolution and outcome in CT findings. *PLoS One* 2020; **15**: e0240347 [PMID: 33175876 DOI: 10.1371/journal.pone.0240347]
- 15 **Zhang H, Liu X, Yu P, Cheng M, Wang W, Sun Y, Zeng B, Fan B.** Dynamic CT assessment of disease change and prognosis of patients with moderate COVID-19 pneumonia. *J Xray Sci Technol* 2020; **28**: 851-861 [PMID: 32741802 DOI: 10.3233/XST-200711]
- 16 **Feng X, Ding X, Zhang F.** Dynamic evolution of lung abnormalities evaluated by quantitative CT techniques in patients with COVID-19 infection. *Epidemiol Infect* 2020; **148**: e136 [PMID: 32624074]



- DOI: [10.1017/S0950268820001508](https://doi.org/10.1017/S0950268820001508)]
- 17 **Liu D**, Zhang W, Pan F, Li L, Yang L, Zheng D, Wang J, Liang B. The pulmonary sequelae in discharged patients with COVID-19: a short-term observational study. *Respir Res* 2020; **21**: 125 [PMID: [32448391](https://pubmed.ncbi.nlm.nih.gov/32448391/) DOI: [10.1186/s12931-020-01385-1](https://doi.org/10.1186/s12931-020-01385-1)]
  - 18 **Pan Y**, Xia L, Wang Y, Guan H. Dynamic changes in computed tomography manifestations of 105 patients with novel coronavirus pneumonia in Wuhan, China. *J Int Med Res* 2020; **48**: 300060520972913 [PMID: [33213239](https://pubmed.ncbi.nlm.nih.gov/33213239/) DOI: [10.1177/0300060520972913](https://doi.org/10.1177/0300060520972913)]
  - 19 **Zhuang Y**, Lin L, Xu X, Xia T, Yu H, Fu G, Yang Y, Wang M, Sun H. Dynamic changes on chest CT of COVID-19 patients with solitary pulmonary lesion in initial CT. *Jpn J Radiol* 2021; **39**: 32-39 [PMID: [32886292](https://pubmed.ncbi.nlm.nih.gov/32886292/) DOI: [10.1007/s11604-020-01037-w](https://doi.org/10.1007/s11604-020-01037-w)]
  - 20 **Zhang Y**, Liu Y, Gong H, Wu L. Quantitative lung lesion features and temporal changes on chest CT in patients with common and severe SARS-CoV-2 pneumonia. *PLoS One* 2020; **15**: e0236858 [PMID: [32706819](https://pubmed.ncbi.nlm.nih.gov/32706819/) DOI: [10.1371/journal.pone.0236858](https://doi.org/10.1371/journal.pone.0236858)]
  - 21 **Pan F**, Ye T, Sun P, Gui S, Liang B, Li L, Zheng D, Wang J, Hesketh RL, Yang L, Zheng C. Time Course of Lung Changes at Chest CT during Recovery from Coronavirus Disease 2019 (COVID-19). *Radiology* 2020; **295**: 715-721 [PMID: [32053470](https://pubmed.ncbi.nlm.nih.gov/32053470/) DOI: [10.1148/radiol.2020200370](https://doi.org/10.1148/radiol.2020200370)]
  - 22 **Wang Y**, Dong C, Hu Y, Li C, Ren Q, Zhang X, Shi H, Zhou M. Temporal Changes of CT Findings in 90 Patients with COVID-19 Pneumonia: A Longitudinal Study. *Radiology* 2020; **296**: E55-E64 [PMID: [32191587](https://pubmed.ncbi.nlm.nih.gov/32191587/) DOI: [10.1148/radiol.2020200843](https://doi.org/10.1148/radiol.2020200843)]
  - 23 **Sun Q**, Li Q, Gao F, Li J, Xu X, Huang X. Evolution of computed tomography manifestations of eleven patients with severe coronavirus disease 2019 (COVID-19) pneumonia. *Int J Clin Pract* 2021; **75**: e13654 [PMID: [32770797](https://pubmed.ncbi.nlm.nih.gov/32770797/) DOI: [10.1111/ijcp.13654](https://doi.org/10.1111/ijcp.13654)]
  - 24 **Urciuoli L**, Guerriero E. Chest CT Findings after 4 Months from the Onset of COVID-19 Pneumonia: A Case Series. *Diagnostics (Basel)* 2020; **10** [PMID: [33152991](https://pubmed.ncbi.nlm.nih.gov/33152991/) DOI: [10.3390/diagnostics10110899](https://doi.org/10.3390/diagnostics10110899)]
  - 25 **Guler SA**, Ebner L, Aubry-Beigelman C, Bridevaux PO, Brutsche M, Clarenbach C, Garzoni C, Geiser TK, Lenoir A, Mancinetti M, Naccini B, Ott SR, Piquilloud L, Prella M, Que YA, Soccal PM, von Garnier C, Funke-Chambour M. Pulmonary function and radiological features 4 mo after COVID-19: first results from the national prospective observational Swiss COVID-19 Lung study. *Eur Respir J* 2021; **57** [PMID: [33419891](https://pubmed.ncbi.nlm.nih.gov/33419891/) DOI: [10.1183/13993003.03690-2020](https://doi.org/10.1183/13993003.03690-2020)]
  - 26 **Han X**, Fan Y, Alwalid O, Li N, Jia X, Yuan M, Li Y, Cao Y, Gu J, Wu H, Shi H. Six-month Follow-up Chest CT Findings after Severe COVID-19 Pneumonia. *Radiology* 2021; **299**: E177-E186 [PMID: [33497317](https://pubmed.ncbi.nlm.nih.gov/33497317/) DOI: [10.1148/radiol.2021203153](https://doi.org/10.1148/radiol.2021203153)]
  - 27 **Chung M**, Bernheim A, Mei X, Zhang N, Huang M, Zeng X, Cui J, Xu W, Yang Y, Fayad ZA, Jacobi A, Li K, Li S, Shan H. CT Imaging Features of 2019 Novel Coronavirus (2019-nCoV). *Radiology* 2020; **295**: 202-207 [PMID: [32017661](https://pubmed.ncbi.nlm.nih.gov/32017661/) DOI: [10.1148/radiol.2020200230](https://doi.org/10.1148/radiol.2020200230)]
  - 28 **Simpson S**, Kay FU, Abbara S, Bhalla S, Chung JH, Chung M, Henry TS, Kanne JP, Kligerman S, Ko JP, Litt H. Radiological Society of North America Expert Consensus Statement on Reporting Chest CT Findings Related to COVID-19. Endorsed by the Society of Thoracic Radiology, the American College of Radiology, and RSNA - Secondary Publication. *J Thorac Imaging* 2020; **35**: 219-227 [PMID: [32324653](https://pubmed.ncbi.nlm.nih.gov/32324653/) DOI: [10.1097/RTI.0000000000000524](https://doi.org/10.1097/RTI.0000000000000524)]
  - 29 **Carsana L**, Sonzogni A, Nasr A, Rossi RS, Pellegrinelli A, Zerbi P, Rech R, Colombo R, Antinori S, Corbellino M, Galli M, Catena E, Tosoni A, Gianatti A, Nebuloni M. Pulmonary post-mortem findings in a series of COVID-19 cases from northern Italy: a two-centre descriptive study. *Lancet Infect Dis* 2020; **20**: 1135-1140 [PMID: [32526193](https://pubmed.ncbi.nlm.nih.gov/32526193/) DOI: [10.1016/S1473-3099\(20\)30434-5](https://doi.org/10.1016/S1473-3099(20)30434-5)]
  - 30 **Vasquez-Bonilla WO**, Orozco R, Argueta V, Sierra M, Zambrano LI, Muñoz-Lara F, López-Molina DS, Arteaga-Livias K, Grimes Z, Bryce C, Paniz-Mondolfi A, Rodríguez-Morales AJ. A review of the main histopathological findings in coronavirus disease 2019. *Hum Pathol* 2020; **105**: 74-83 [PMID: [32750378](https://pubmed.ncbi.nlm.nih.gov/32750378/) DOI: [10.1016/j.humpath.2020.07.023](https://doi.org/10.1016/j.humpath.2020.07.023)]
  - 31 **Bernheim A**, Mei X, Huang M, Yang Y, Fayad ZA, Zhang N, Diao K, Lin B, Zhu X, Li K, Li S, Shan H, Jacobi A, Chung M. Chest CT Findings in Coronavirus Disease-19 (COVID-19): Relationship to Duration of Infection. *Radiology* 2020; **295**: 200463 [PMID: [32077789](https://pubmed.ncbi.nlm.nih.gov/32077789/) DOI: [10.1148/radiol.2020200463](https://doi.org/10.1148/radiol.2020200463)]
  - 32 **Parekh M**, Donuru A, Balasubramanya R, Kapur S. Review of the Chest CT Differential Diagnosis of Ground-Glass Opacities in the COVID Era. *Radiology* 2020; **297**: E289-E302 [PMID: [32633678](https://pubmed.ncbi.nlm.nih.gov/32633678/) DOI: [10.1148/radiol.2020202504](https://doi.org/10.1148/radiol.2020202504)]
  - 33 **Wells AU**, Devaraj A, Desai SR. Interstitial Lung Disease after COVID-19 Infection: A Catalog of Uncertainties. *Radiology* 2021; **299**: E216-E218 [PMID: [33502279](https://pubmed.ncbi.nlm.nih.gov/33502279/) DOI: [10.1148/radiol.2021204482](https://doi.org/10.1148/radiol.2021204482)]
  - 34 **Li K**, Fang Y, Li W, Pan C, Qin P, Zhong Y, Liu X, Huang M, Liao Y, Li S. CT image visual quantitative evaluation and clinical classification of coronavirus disease (COVID-19). *Eur Radiol* 2020; **30**: 4407-4416 [PMID: [32215691](https://pubmed.ncbi.nlm.nih.gov/32215691/) DOI: [10.1007/s00330-020-06817-6](https://doi.org/10.1007/s00330-020-06817-6)]
  - 35 **Yin X**, Min X, Nan Y, Feng Z, Li B, Cai W, Xi X, Wang L. Assessment of the Severity of Coronavirus Disease: Quantitative Computed Tomography Parameters vs Semiquantitative Visual Score. *Korean J Radiol* 2020; **21**: 998-1006 [PMID: [32677384](https://pubmed.ncbi.nlm.nih.gov/32677384/) DOI: [10.3348/kjr.2020.0423](https://doi.org/10.3348/kjr.2020.0423)]
  - 36 **Pu J**, Leader JK, Bandos A, Ke S, Wang J, Shi J, Du P, Guo Y, Wenzel SE, Fuhrman CR, Wilson DO, Sciurba FC, Jin C. Automated quantification of COVID-19 severity and progression using chest CT images. *Eur Radiol* 2021; **31**: 436-446 [PMID: [32789756](https://pubmed.ncbi.nlm.nih.gov/32789756/) DOI: [10.1007/s00330-020-07156-2](https://doi.org/10.1007/s00330-020-07156-2)]
  - 37 **Lassau N**, Ammari S, Chouzenoux E, Gortais H, Herent P, Devilder M, Soliman S, Meyrignac O, Talabard MP, Lamarque JP, Dubois R, Loiseau N, Trichelair P, Bendjebbar E, Garcia G, Balleyguier



- C, Merad M, Stoclin A, Jegou S, Griscelli F, Tetelboum N, Li Y, Verma S, Terris M, Dardouri T, Gupta K, Neacsu A, Chemouni F, Sefta M, Jehanno P, Bousaid I, Boursin Y, Planchet E, Azoulay M, Dachary J, Brulport F, Gonzalez A, Dehaene O, Schiratti JB, Schutte K, Pesquet JC, Talbot H, Pronier E, Wainrib G, Clozel T, Barlesi F, Bellin MF, Blum MGB. Integrating deep learning CT-scan model, biological and clinical variables to predict severity of COVID-19 patients. *Nat Commun* 2021; **12**: 634 [PMID: [33504775](#) DOI: [10.1038/s41467-020-20657-4](#)]
- 38 **Zhao W**, Zhong Z, Xie X, Yu Q, Liu J. Relation Between Chest CT Findings and Clinical Conditions of Coronavirus Disease (COVID-19) Pneumonia: A Multicenter Study. *AJR Am J Roentgenol* 2020; **214**: 1072-1077 [PMID: [32125873](#) DOI: [10.2214/AJR.20.22976](#)]
- 39 **Leonardi A**, Scipione R, Alfieri G, Petrillo R, Dolciami M, Ciccarelli F, Perotti S, Cartocci G, Scala A, Imperiale C, Iafrate F, Francone M, Catalano C, Ricci P. Role of computed tomography in predicting critical disease in patients with covid-19 pneumonia: A retrospective study using a semiautomatic quantitative method. *Eur J Radiol* 2020; **130**: 109202 [PMID: [32745895](#) DOI: [10.1016/j.ejrad.2020.109202](#)]
- 40 **Lanza E**, Muglia R, Bolengo I, Santonocito OG, Lisi C, Angelotti G, Morandini P, Savevski V, Politi LS, Balzarini L. Quantitative chest CT analysis in COVID-19 to predict the need for oxygenation support and intubation. *Eur Radiol* 2020; **30**: 6770-6778 [PMID: [32591888](#) DOI: [10.1007/s00330-020-07013-2](#)]
- 41 **Mahase E**. Covid-19: What do we know about "long covid"? *BMJ* 2020; **370**: m2815 [PMID: [32665317](#) DOI: [10.1136/bmj.m2815](#)]
- 42 **Hui DS**, Joynt GM, Wong KT, Gomersall CD, Li TS, Antonio G, Ko FW, Chan MC, Chan DP, Tong MW, Rainer TH, Ahuja AT, Cockram CS, Sung JJ. Impact of severe acute respiratory syndrome (SARS) on pulmonary function, functional capacity and quality of life in a cohort of survivors. *Thorax* 2005; **60**: 401-409 [PMID: [15860716](#) DOI: [10.1136/thx.2004.030205](#)]
- 43 **Antonio GE**, Wong KT, Hui DS, Wu A, Lee N, Yuen EH, Leung CB, Rainer TH, Cameron P, Chung SS, Sung JJ, Ahuja AT. Thin-section CT in patients with severe acute respiratory syndrome following hospital discharge: preliminary experience. *Radiology* 2003; **228**: 810-815 [PMID: [12805557](#) DOI: [10.1148/radiol.2283030726](#)]
- 44 **Herridge MS**, Tansey CM, Matté A, Tomlinson G, Diaz-Granados N, Cooper A, Guest CB, Mazer CD, Mehta S, Stewart TE, Kudlow P, Cook D, Slutsky AS, Cheung AM; Canadian Critical Care Trials Group. Functional disability 5 years after acute respiratory distress syndrome. *N Engl J Med* 2011; **364**: 1293-1304 [PMID: [21470008](#) DOI: [10.1056/NEJMoa1011802](#)]
- 45 **Fumagalli A**, Misuraca C, Bianchi A, Borsa N, Limonta S, Maggiolini S, Bonardi DR, Corsonello A, Di Rosa M, Soraci L, Lattanzio F, Colombo D. Pulmonary function in patients surviving to COVID-19 pneumonia. *Infection* 2021; **49**: 153-157 [PMID: [32725597](#) DOI: [10.1007/s15010-020-01474-9](#)]
- 46 **Zhao YM**, Shang YM, Song WB, Li QQ, Xie H, Xu QF, Jia JL, Li LM, Mao HL, Zhou XM, Luo H, Gao YF, Xu AG. Follow-up study of the pulmonary function and related physiological characteristics of COVID-19 survivors three months after recovery. *EclinicalMedicine* 2020; **25**: 100463 [PMID: [32838236](#) DOI: [10.1016/j.eclinm.2020.100463](#)]
- 47 **Venturelli S**, Benatti SV, Casati M, Binda F, Zuglian G, Imeri G, Conti C, Biffi AM, Spada MS, Bondi E, Camera G, Severgnini R, Giammarresi A, Marinaro C, Rossini A, Bonaffini PA, Guerra G, Bellasi A, Cesa S, Rizzi M. Surviving COVID-19 in Bergamo province: a post-acute outpatient re-evaluation. *Epidemiol Infect* 2021; **149**: e32 [PMID: [33461632](#) DOI: [10.1017/S0950268821000145](#)]
- 48 **Anastasio F**, Barbuto S, Scarnecchia E, Cosma P, Fugagnoli A, Rossi G, Parravicini M, Parravicini P. Medium-term impact of COVID-19 on pulmonary function, functional capacity and quality of life. *Eur Respir J* 2021 [PMID: [33574080](#) DOI: [10.1183/13993003.04015-2020](#)]
- 49 **Bellan M**, Soddu D, Balbo PE, Baricich A, Zeppegno P, Avanzi GC, Baldon G, Bartolomei G, Battaglia M, Battistini S, Binda V, Borg M, Cantaluppi V, Castello LM, Clivati E, Cisari C, Costanzo M, Croce A, Cuneo D, De Benedittis C, De Vecchi S, Feggi A, Gai M, Gambaro E, Gattoni E, Gramaglia C, Grisafi L, Guerriero C, Hayden E, Jona A, Invernizzi M, Lorenzini L, Loreti L, Martelli M, Marzullo P, Martino E, Panero A, Parachini E, Patrucco F, Patti G, Pirovano A, Prosperini P, Quaglino R, Rigamonti C, Sainaghi PP, Vecchi C, Zecca E, Pirisi M. Respiratory and Psychophysical Sequelae Among Patients With COVID-19 Four Months After Hospital Discharge. *JAMA Netw Open* 2021; **4**: e2036142 [PMID: [33502487](#) DOI: [10.1001/jamanetworkopen.2020.36142](#)]
- 50 **Qin W**, Chen S, Zhang Y, Dong F, Zhang Z, Hu B, Zhu Z, Li F, Wang X, Wang Y, Zhen K, Wang J, Wan Y, Li H, Elalamy I, Li C, Zhai Z, Wang C. Diffusion capacity abnormalities for carbon monoxide in patients with COVID-19 at 3-month follow-up. *Eur Respir J* 2021; **58** [PMID: [33574077](#) DOI: [10.1183/13993003.03677-2020](#)]
- 51 **Truffaut L**, Demey L, Bruyneel AV, Roman A, Alard S, De Vos N, Bruyneel M. Post-discharge critical COVID-19 Lung function related to severity of radiologic lung involvement at admission. *Respir Res* 2021; **22**: 29 [PMID: [33478527](#) DOI: [10.1186/s12931-021-01625-y](#)]
- 52 **D'Cruz RF**, Waller MD, Perrin F, Periselnieris J, Norton S, Smith LJ, Patrick T, Walder D, Heitmann A, Lee K, Madula R, McNulty W, Macedo P, Lyall R, Warwick G, Galloway JB, Birring SS, Patel A, Patel I, Jolley CJ. Chest radiography is a poor predictor of respiratory symptoms and functional impairment in survivors of severe COVID-19 pneumonia. *ERJ Open Res* 2021; **7** [PMID: [33575312](#) DOI: [10.1183/23120541.00655-2020](#)]
- 53 **Sykes DL**, Holdsworth L, Jawad N, Gunasekera P, Morice AH, Crooks MG. Post-COVID-19 Symptom Burden: What is Long-COVID and How Should We Manage It? *Lung* 2021; **199**: 113-119 [PMID: [33569660](#) DOI: [10.1007/s00408-021-00423-z](#)]

# Neonatal infratentorial subdural hematoma contributing to obstructive hydrocephalus in the setting of therapeutic cooling: A case report

Lee K Rousslang, Elizabeth A Rooks, Jaren T Meldrum, Kristopher G Hooten, Jonathan R Wood

**ORCID number:** Lee K Rousslang 0000-0003-0875-1952; Elizabeth A Rooks 0000-0001-6763-4081; Jaren T Meldrum 0000-0001-7072-2621; Kristopher G Hooten 0000-0001-5471-1658; Jonathan R Wood 0000-0002-0295-6079.

**Author contributions:** Rousslang LK is the primary author; Rooks EA assisted by performing research background for the case and contributing portions of the writing; Meldrum JT assisted by providing primary edits and the initial radiological read; Hooten KG was the primary surgeon, and provided surgical insights into the case; Wood JR is the senior author who contributed final edits and portions of the unedited manuscript.

**Informed consent statement:** Informed written consent was obtained.

**Conflict-of-interest statement:** The authors have no financial, personal, or other vested interests in the information contained within this document.

**CARE Checklist (2016) statement:** The manuscript was checked according to the CARE Checklist (2016) statement.

**Lee K Rousslang, Jonathan R Wood,** Department of Radiology, Tripler Army Medical Center, Medical Center, HI 96859, United States

**Elizabeth A Rooks,** Department of Neuroscience, Duke University, Durham, NC 27708, United States

**Jaren T Meldrum,** Department of Radiology, Alaska Native Medical Center, Anchorage, AK 99508, United States

**Kristopher G Hooten,** Department of Neurosurgery, Tripler Army Medical Center, Medical Center, HI 96859, United States

**Corresponding author:** Lee K Rousslang, MD, Doctor, Department of Radiology, Tripler Army Medical Center, 1 Jarrett White Rd, Medical Center, HI 96859, United States.  
[lee.k.rousslang.civ@mail.mil](mailto:lee.k.rousslang.civ@mail.mil)

## Abstract

### BACKGROUND

Symptomatic neonatal subdural hematomas usually result from head trauma incurred during vaginal delivery, most commonly during instrument assistance. Symptomatic subdural hematomas are rare in C-section deliveries that were not preceded by assisted delivery techniques. Although the literature is inconclusive, another possible cause of subdural hematomas is therapeutic hypothermia.

### CASE SUMMARY

We present a case of a term neonate who underwent therapeutic whole-body cooling for hypoxic ischemic encephalopathy following an emergent C-section delivery for prolonged decelerations. Head ultrasound on day of life 3 demonstrated a rounded mass in the posterior fossa. A follow-up brain magnetic resonance imaging confirmed hypoxic ischemic encephalopathy and clarified the subdural hematomas in the posterior fossa causing mass effect and obstructive hydrocephalus.

### CONCLUSION

The aim of this report is to highlight the rarity and importance of mass-like subdural hematomas causing obstructive hydrocephalus, particularly in the setting of hypoxic ischemic encephalopathy and therapeutic whole-body cooling.

**Open-Access:** This article is an open-access article that was selected by an in-house editor and fully peer-reviewed by external reviewers. It is distributed in accordance with the Creative Commons Attribution NonCommercial (CC BY-NC 4.0) license, which permits others to distribute, remix, adapt, build upon this work non-commercially, and license their derivative works on different terms, provided the original work is properly cited and the use is non-commercial. See: <http://creativecommons.org/licenses/by-nc/4.0/>

**Manuscript source:** Unsolicited manuscript

**Specialty type:** Radiology, Nuclear Medicine and Medical Imaging

**Country/Territory of origin:** United States

**Peer-review report's scientific quality classification**

Grade A (Excellent): 0  
Grade B (Very good): 0  
Grade C (Good): 0  
Grade D (Fair): 0  
Grade E (Poor): 0

**Received:** March 30, 2021

**Peer-review started:** March 30, 2021

**First decision:** June 7, 2021

**Revised:** June 22, 2021

**Accepted:** September 8, 2021

**Article in press:** September 8, 2021

**Published online:** September 28, 2021

**P-Reviewer:** Cazorla E

**S-Editor:** Wang JL

**L-Editor:** A

**P-Editor:** Liu JH



**Key Words:** Hypoxic ischemic encephalopathy; Neonatal subdural hematoma; Therapeutic hypothermia; Case report

©The Author(s) 2021. Published by Baishideng Publishing Group Inc. All rights reserved.

**Core Tip:** Screening head ultrasound during hypothermia protocols for hypoxic ischemic encephalopathy (HIE) warrant scrutiny for hemorrhage in unexpected locations. Symptomatic subdural hematomas warrant a high degree of clinical suspicion, particularly due to their rarity in children delivered by C-section. This report highlights the emerging association of HIE, therapeutic hypothermia, and perinatal intracranial hemorrhage. Prompt imaging and neurosurgical intervention may relieve hemorrhage induced obstructive hydrocephalus during therapeutic cooling with good neurological outcomes, preventing need for permanent cerebrospinal fluid diversion. Familiarity with the key imaging characteristics and clinical exam features of mass-like subdural hematomas can help the treatment team consider the diagnosis, and potentially enable a prompt recovery.

**Citation:** Rousslang LK, Rooks EA, Meldrum JT, Hooten KG, Wood JR. Neonatal infratentorial subdural hematoma contributing to obstructive hydrocephalus in the setting of therapeutic cooling: A case report. *World J Radiol* 2021; 13(9): 307-313

**URL:** <https://www.wjgnet.com/1949-8470/full/v13/i9/307.htm>

**DOI:** <https://dx.doi.org/10.4329/wjr.v13.i9.307>

## INTRODUCTION

Perinatal symptomatic subdural hematomas (SDH) are rare. They most commonly occur in the posterior fossa and are classically thought to result from venous disruption caused by birth trauma[1,2]. Although there are case reports of neonatal SDH after spontaneous vaginal delivery, or in-utero, it is still rare to observe a symptomatic SDH following an atraumatic C-section[3,4]. Hypoxic ischemic encephalopathy (HIE) has recently emerged as a potential cause of SDH, but the evidence is unclear and debated, with much of it based on autopsy[5-8]. Therapeutic hypothermia also appears to contribute to SDH, and whole-body cooling has been shown to impair hemostasis *in vivo*[9]. Additionally, Wang *et al*[10] recently reported a case of therapeutic cooling that is thought to have led to a massive SDH.

To the best of our knowledge, this is the first case in the literature to date of a neonate who developed a mass-like subdural hemorrhage of the posterior fossa while undergoing whole-body cooling causing obstructive hydrocephalus, following a non-traumatic C-section delivery.

## CASE PRESENTATION

### Personal and family history

A boy was born at 38 wk and 5 d to a gravida 3, aborta 2 mother *via* emergent C-section for prolonged decelerations and arrest of descent which was thought to be related to maternal difficulty in coordinating pushing efforts with contractions while receiving epidural anesthesia. The decelerations did not respond to changes in maternal positioning, or administration of supplemental oxygen and intravenous fluids. The mother had no pre-existing conditions, and was up to date with all vaccinations. His prenatal course was completely normal, including a 20-wk anatomy scan demonstrating normal brain imaging. Thick meconium was present at delivery, which was otherwise uncomplicated.

### Physical examination

His birth weight was 4.0 kg, with APGAR scores of 1<sup>1</sup>, 3<sup>5</sup>, 4<sup>10</sup>, and 6<sup>15</sup>. At birth he was apneic, with a heart rate < 60, requiring chest compressions and intubation. Shortly after intubation he developed pulmonary hemorrhage and acute hypoxemic

respiratory failure that responded well to endotracheal epinephrine. His respiratory issues were thought to be caused by the aspiration of the thick meconium.

### Laboratory examinations

Immediately after birth, his international normalized ratio (INR) was 2.3, with prothrombin time of 25.6 s, activated partial thromboplastin time of 65 s, and platelets of  $81 \times 10^3$  platelets/uL. To correct his coagulopathy, he was given platelets, cryoprecipitate, and fresh frozen plasma for hemostasis, with downtrend in INR to 1.0 and uptrend in platelets to normal levels ( $> 150 \times 10^3$  platelets/uL) over the next four days.

### Imaging examinations

Head ultrasound (HUS) on the first day of life (DOL) demonstrated left grade 1 germinal matrix hemorrhage, but no other intra-cranial hemorrhage. The patient was then started on whole-body cooling for HIE.

On his fourth day of whole-body cooling, the patient was found to have an increasing head circumference, increasing fontanelle size and fullness, and apneic events, suggestive of obstructive hydrocephalus. His exam further revealed a poor gag reflex and diminished response to stimuli with decreased spontaneous movement. Head ultrasound demonstrated a newly visualized mass in the infratentorial region, thought to represent a cerebellar or tentorial hemorrhage (Figure 1) and the patient was re-warmed.

## FINAL DIAGNOSIS

A same-day brain magnetic resonance imaging (MRI) was performed, revealing a 2.5 cm hematoma in the posterior fossa causing extensive mass effect on the cerebellum, and effacement of the fourth ventricle leading to an obstructive hydrocephalus. There was also widespread hypoxic ischemic injury (Figure 2 and Figure 3). A ventricular access device was placed that day for intermittent cerebrospinal fluid (CSF) diversion.

On DOL 20, due to an increase in apneic and bradycardic episodes, and increasing hydrocephalus on HUS, a repeat MRI was performed, and demonstrated acute on chronic bleeding into the subdural space (Figure 4).

## TREATMENT

Later on DOL 20, the patient underwent successful supratentorial burr-hole evacuation of the subdural hematoma as well as a sub-occipital craniectomy with an infratentorial, supracerebellar evacuation of the thrombus.

## OUTCOME AND FOLLOW-UP

Post-operative imaging demonstrated near complete resolution of the subdural hematoma (Figure 5). MRI at 15 mo of age (Figure 6) demonstrated improved hydrocephalus. At the time of submission, the patient is 29 mo old, and suffers from right spastic hemiplegic cerebral palsy, an expressive aphasia, and strabismus.

## DISCUSSION

While asymptomatic SDH are commonplace after delivery, symptomatic SDH are rare in neonates, with an incidence of approximately 3.8-5.2 of 10000 Live births[11-13]. SDH typically occur in the posterior fossa and are thought to arise from head trauma during vaginal delivery[1,2]. Infratentorial SDH most commonly results from falx or tentorial tears with bridging vein disruption and are worrisome because of their propensity to cause obstructive hydrocephalus, even with small volume bleeds[2]. Elective C-section deliveries are rarely associated with symptomatic SDH, likely due to lower rates of birth trauma.

Many researchers have conjectured that SDH can be secondary to cerebral ischemia [5-8]. The prevailing theory is that ischemia leads to damage of immature blood



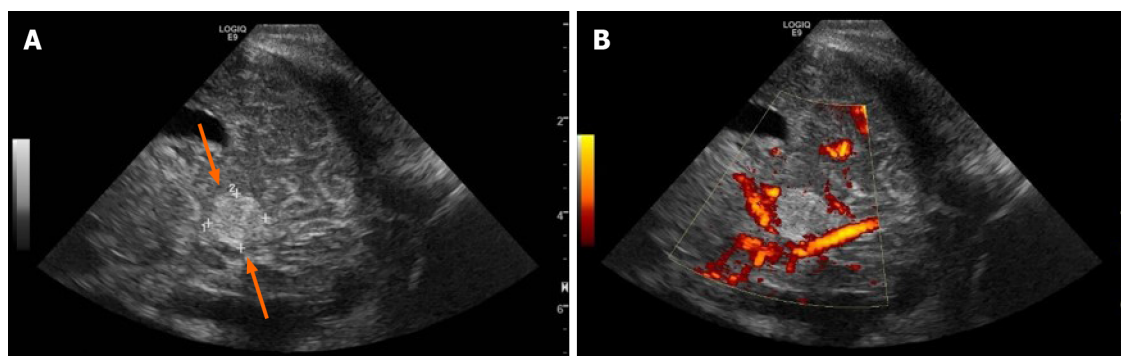


**Figure 1** Head ultrasound through an oblique posterior parietal approach on 3<sup>rd</sup> day of life. The figure demonstrates an echogenic mass (arrows) in the posterior fossa, inferior to the tentorium, measuring 1.2 cm in its greatest dimension (A) with flow in the straight sinus and lack of flow on power Doppler within the mass (B).

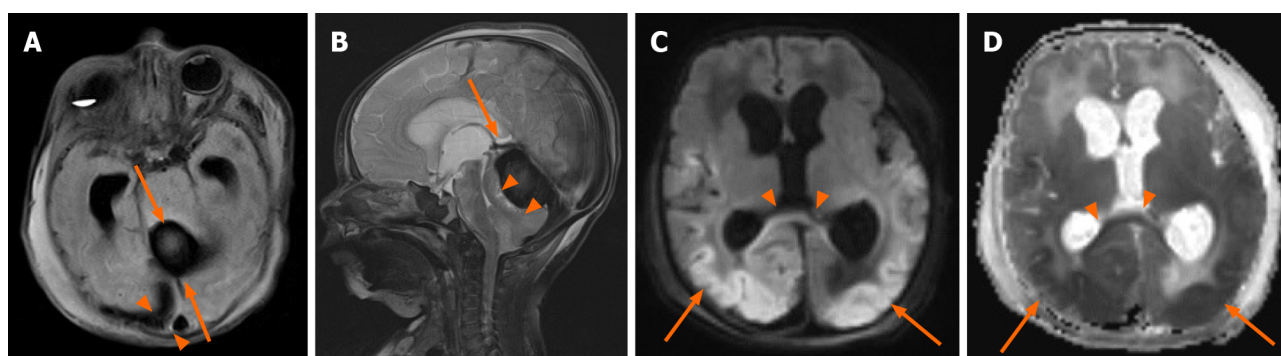


**Figure 2** Axial T2 fluid-attenuated inversion recovery on 4<sup>th</sup> day of life. A: A 2.3 cm × 1.7 cm × 2.5 cm rounded thrombus (arrows) and subdural hemorrhage (arrowheads) as well as transverse sinus thrombosis; B: Sagittal T2 demonstrates thrombus (arrow) in posterior fossa superior to cerebellum causing downward mass effect on the cerebellum and fourth ventricle (arrowheads); C, D: Axial diffusion weighted imaging (C) and corresponding ADC map (D) demonstrate diffusion restriction in the corpus callosum (arrowheads), posterior parietal, temporal, and occipital lobes. Other scattered areas of diffusion restriction were noted throughout the brain and brainstem including the pons, cerebellum and posterior frontal lobes (not shown).

vessels, especially those of the richly vascularized falx cerebri, causing microvascular permeability that leads to intradural hemorrhage (IDH), which is then exacerbated by increased venous pressure[8]. IDH then leads to damage of the weak cell layer between the arachnoid and the dura, causing SDH[8]. However, other smaller studies still debate this theory[14].

The delayed presentation of the SDH in the setting of therapeutic cooling and HIE is what makes this case unique. Our patient's HIE was likely due to meconium aspiration and pulmonary hemorrhage resulting in asphyxia and acute hypoxemic respiratory failure requiring intubation at birth. The presence of the germinal matrix hemorrhage on initial head ultrasound did not preclude the whole-body cooling protocol from being initiated. Although initial therapeutic hypothermia is not known to cause spontaneous SDH, in-vivo studies have shown that hypothermia can impair hemostasis[15]. Furthermore, many of the studies involved in evaluating whole-body cooling were not powered to assess for harm[10]. Given this case involved a C-section with no significant birth trauma, and a delay in the clinical and radiographic presentation of the hemorrhage, it is likely in this case as Cohen *et al*[8] suggests that the SDH occurred as a result of cerebral ischemia, and hypothermia exacerbated the condition.

Successful treatment of neonatal posterior fossa subdural hematomas has been reported in the literature as early as 1940. In the largest reported clinical series of 15 infants, Perrin *et al*[4] demonstrated that successful surgical evacuation of posterior fossa hemorrhages can relieve obstructive hydrocephalus and prevent the need for permanent CSF diversion with good neurologic outcomes. Generally, conservative management is recommended initially but in the presence of hydrocephalus, a worsening clinical exam, or an enlarging hematoma, surgical evacuation should be considered.



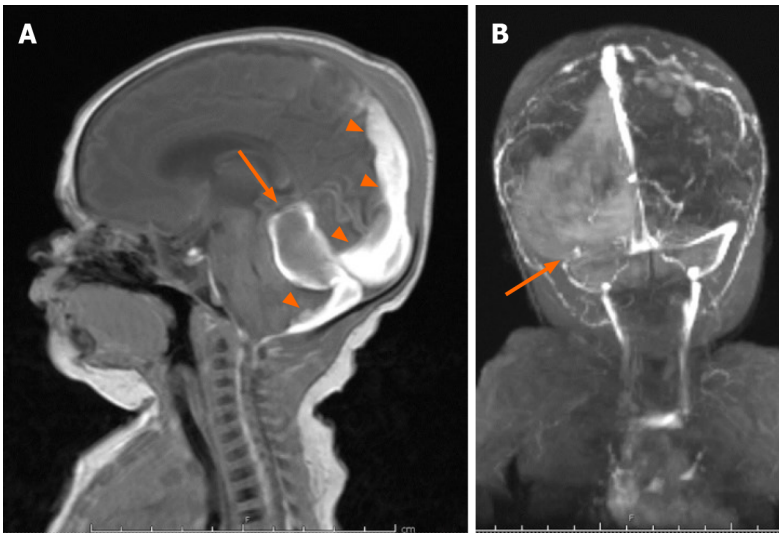


**Figure 3 Brain magnetic resonance imaging on 10<sup>th</sup> day of life.** A: Follow-up brain magnetic resonance imaging on 10<sup>th</sup> day of life re-demonstrates the posterior fossa mass (arrow), with interval high signal on sagittal T1 consistent with evolving blood products, as well as persistent subdural hematoma (arrowheads); B: PA coronal MRI venography demonstrates absent flow in the transverse sinus consistent with transverse sinus thrombosis.

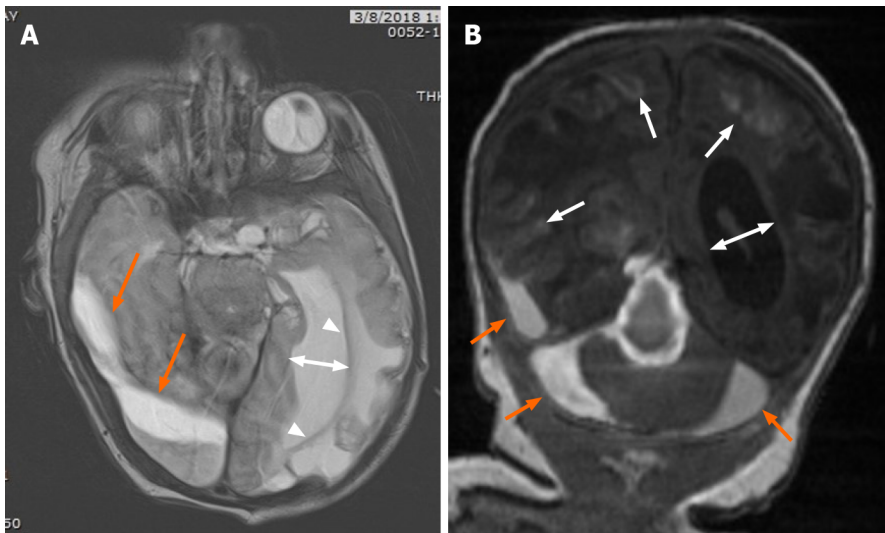


**Figure 4 Follow-up magnetic resonance imaging on 20<sup>th</sup> day of life.** A: Follow-up magnetic resonance imaging on 20<sup>th</sup> day of life revealed evolving blood products (orange arrows) in the subdural space on axial T2, with interval left greater than right cystic encephalomalacia in the parietal and occipital lobes and left greater than right ex-vacuo dilatation of the lateral ventricles (two direction arrow); B: Coronal T1 demonstrates degrading blood product in the right temporal lobe subdural space, and central and peripheral infratentorial subdural spaces (orange arrows) with cortical laminar necrosis (arrows) and increasing obstructive hydrocephalus (two-direction arrow).

## CONCLUSION

Screening HUS during hypothermia protocols for HIE warrant scrutiny for hemorrhage in unexpected locations. Symptomatic subdural hematomas warrant a high degree of clinical suspicion, particularly due to their rarity in children delivered by C-section. This report highlights the emerging association of HIE, therapeutic hypothermia, and perinatal intracranial hemorrhage. Prompt imaging and neurosurgical intervention may relieve hemorrhage induced obstructive hydrocephalus during therapeutic cooling with good neurological outcomes, preventing need for permanent CSF diversion. Familiarity with the key imaging characteristics and clinical exam features of mass-like SDH can help the treatment team consider the diagnosis, and potentially enable a prompt recovery.



**Figure 5** A sagittal T1 magnetic resonance imaging done immediately after subdural hematomas evacuation demonstrates near complete resolution of the subdural hematomas (arrow) and resolution of the obstructive hydrocephalus.

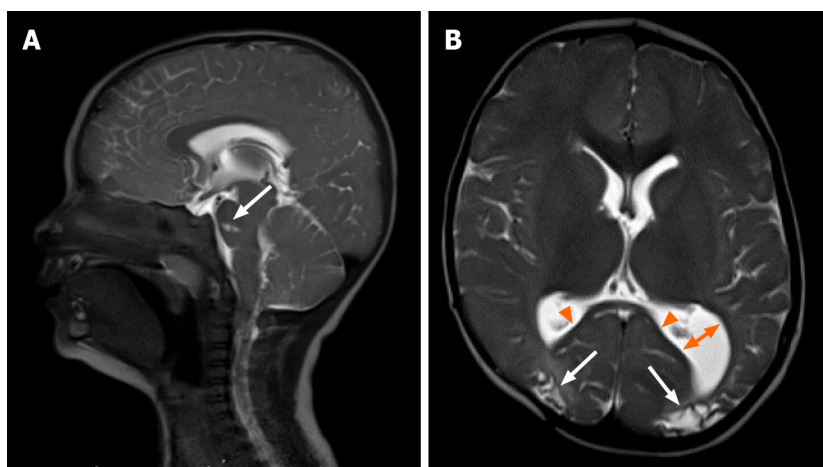


**Figure 6** Follow-up magnetic resonance imaging at 15 mo. A: Follow-up magnetic resonance imaging at 15 mo demonstrates continued resolution of the subdural hematomas and obstructive hydrocephalus on sagittal T2. Note the focal encephalomalacia at the pons (arrow); B: Axial T2 demonstrates encephalomalacic change manifested by thinning of the posterior corpus callosum (arrowheads), decreased gray and white matter of the posterior occipital regions bilaterally (arrows), and colpocephaly of the left lateral ventricle (two direction arrow).

## ACKNOWLEDGEMENTS

The views expressed in this manuscript are those of the authors, and do not reflect the official policy or position of the Department of the Army, Department of Defense, or the United States Government.

## REFERENCES

- 1 Menezes AH, Smith DE, Bell WE. Posterior fossa hemorrhage in the term neonate. *Neurosurgery* 1983; **13**: 452-456 [PMID: 6633841 DOI: 10.1227/00006123-198310000-00021]
- 2 Perlman JM. Brain injury in the term infant. *Semin Perinatol* 2004; **28**: 415-424 [PMID: 15693398 DOI: 10.1053/j.semperi.2004.10.003]
- 3 Gunn TR, Mok PM, Becroft DM. Subdural hemorrhage in utero. *Pediatrics* 1985; **76**: 605-610 [PMID: 3900908]
- 4 Perrin RG, Rutka JT, Drake JM, Meltzer H, Hellman J, Jay V, Hoffman HJ, Humphreys RP. Management and outcomes of posterior fossa subdural hematomas in neonates. *Neurosurgery* 1997; **40**: 1190-9; discussion 1199 [PMID: 9179892 DOI: 10.1097/00006123-199706000-00016]
- 5 Steinbok P, Haw CS, Cochrane DD, Kestle JR. Acute subdural hematoma associated with cerebral

- infarction in the full-term neonate. *Pediatr Neurosurg* 1995; **23**: 206-215 [PMID: [8835211](#) DOI: [10.1159/000120960](#)]
- 6 **McCubbin K**, Thoma L, Mena H, Gill JR. Subdural Hemorrhage and Hypoxia in Children Less than Two Years Old. *Acad Forensic Pathol* 2013; **3**: 213-221 [DOI: [10.23907/2013.027](#)]
- 7 **Henzi BC**, Wagner B, Verma RK, Bigi S. Perinatal intratentorial haemorrhage: a rare but possibly life-threatening condition. *BMJ Case Rep* 2017; **2017** [PMID: [29196306](#) DOI: [10.1136/bcr-2017-221144](#)]
- 8 **Cohen MC**, Scheimberg I. Evidence of occurrence of intradural and subdural hemorrhage in the perinatal and neonatal period in the context of hypoxic Ischemic encephalopathy: an observational study from two referral institutions in the United Kingdom. *Pediatr Dev Pathol* 2009; **12**: 169-176 [PMID: [19007301](#) DOI: [10.2350/08-08-0509.1](#)]
- 9 **Rohrer MJ**, Natale AM. Effect of hypothermia on the coagulation cascade. *Crit Care Med* 1992; **20**: 1402-1405 [PMID: [1395660](#) DOI: [10.1097/00003246-199210000-00007](#)]
- 10 **Wang D**, McMillan H, Bariciak E. Subdural haemorrhage and severe coagulopathy resulting in transtentorial uncal herniation in a neonate undergoing therapeutic hypothermia. *BMJ Case Rep* 2014; **2014** [PMID: [25100805](#) DOI: [10.1136/bcr-2013-203080](#)]
- 11 **Chamnanvanakij S**, Rollins N, Perlman JM. Subdural hematoma in term infants. *Pediatr Neurol* 2002; **26**: 301-304 [PMID: [11992759](#) DOI: [10.1016/s0887-8994\(01\)00420-9](#)]
- 12 **Gupta SN**, Kechli AM, Kanamalla US. Intracranial hemorrhage in term newborns: management and outcomes. *Pediatr Neurol* 2009; **40**: 1-12 [PMID: [19068247](#) DOI: [10.1016/j.pediatrneurol.2008.09.019](#)]
- 13 **Rooks VJ**, Eaton JP, Ruess L, Petermann GW, Keck-Wherley J, Pedersen RC. Prevalence and evolution of intracranial hemorrhage in asymptomatic term infants. *AJNR Am J Neuroradiol* 2008; **29**: 1082-1089 [PMID: [18388219](#) DOI: [10.3174/ajnr.A1004](#)]
- 14 **Byard RW**, Blumbergs P, Rutty G, Sperhake J, Banner J, Krous HF. Lack of evidence for a causal relationship between hypoxic-ischemic encephalopathy and subdural hemorrhage in fetal life, infancy, and early childhood. *Pediatr Dev Pathol* 2007; **10**: 348-350 [PMID: [17929988](#) DOI: [10.2350/06-08-0154.1](#)]
- 15 **Wang CH**, Chen NC, Tsai MS, Yu PH, Wang AY, Chang WT, Huang CH, Chen WJ. Therapeutic Hypothermia and the Risk of Hemorrhage: A Systematic Review and Meta-Analysis of Randomized Controlled Trials. *Medicine (Baltimore)* 2015; **94**: e2152 [PMID: [26632746](#) DOI: [10.1097/MD.0000000000002152](#)]



Published by **Baishideng Publishing Group Inc**  
7041 Koll Center Parkway, Suite 160, Pleasanton, CA 94566, USA

**Telephone:** +1-925-3991568

**E-mail:** [bpgoffice@wjgnet.com](mailto:bpgoffice@wjgnet.com)

**Help Desk:** <https://www.f6publishing.com/helpdesk>

<https://www.wjgnet.com>

